Memorandum 2050 (October 2015). ISSN 1874-4850. Available from: http://www.math.utwente.nl/publications
Department of Applied Mathematics, University of Twente, Enschede, The Netherlands

Newton flows for elliptic functions

G.F. Helminck,
Korteweg-de Vries Institute
University of Amsterdam
P.O. Box 94248
1090 GE Amsterdam
The Netherlands
e-mail: g.f.helminck@uva.nl
F. Twilt,
Department of Applied Mathematics
University of Twente
P.O. Box 217, 7500 AE Enschede
The Netherlands
e-mail: f.twilt@kpnmail.nl

October 16, 2015

Abstract

Newton flows are *dynamical systems* generated by a continuous, desingularized Newton method for mappings from a Euclidean space to itself. We focus on the special case of meromorphic functions on the complex plane. Inspired by the analogy between the rational (complex) and the elliptic (i.e., doubly periodic meromorphic) functions, a theory on the class of so-called *Elliptic Newton flows* is developed.

With respect to an appropriate topology on the set of all elliptic functions f of fixed order $r(\geqslant 2)$ we prove: For *almost all* functions f, the corresponding Newton flows are *structurally stable* i.e., topologically invariant under small perturbations of the zeros and poles for f [*genericity*].

The phase portrait of a structurally stable elliptic Newton flow generates a connected, cellularly embedded, graph $\mathcal{G}(f)$ on T with r vertices, $2r$ edges and r faces that fulfil certain combinatorial properties (*Euler, Hall*) on some of its subgraphs. The graph $\mathcal{G}(f)$ determines the conjugacy class of the flow [*characterization*].

A connected, cellularly embedded toroidal graph $\mathcal{G}$ with the above *Euler* and *Hall* properties, is called a *Newton graph*. Any Newton graph $\mathcal{G}$ can be realized as the graph $\mathcal{G}(f)$ of the structurally stable Newton flow for some function f [*classification*].

This leads to: up till conjugacy between flows and (topological) equivalency between graphs, there is a 1-1 correspondence between the structurally stable Newton flows and Newton graphs, both with respect to the same order r of the underlying functions f [*representation*].

In particular, it follows that in case $r = 2$, there is only one (up to conjugacy) structurally stabe elliptic Newton flow, whereas in case $r = 3$, we find a list of *nine* graphs, determining all possibilities.

Moreover, we pay attention to the so-called *nuclear Newton flows* of order r, and indicate how - by a bifurcation procedure - any structurally stable elliptic Newton flow of order r can be obtained from such a nuclear flow.

Finally, we show that the detection of elliptic Newton flows is possible in polynomial time.

The proofs of the above results rely on Peixoto's characterization/classification theorems for structurally stable dynamical systems on compact 2-dimensional manifolds, Stiemke's theorem of the alternatives, Hall's theorem of distinct representatives, the Heffter-Edmonds-Ringer rotation principle for embedded graphs, an existence theorem on gradient dynamical systems by Smale, and an interpretation of Newton flows as steady streams.

Subject classification: 05C45, 05C75, 30C15, 30D30, 30F99, 33E15, 34D30, 37C15, 37C20, 37C70, 49M15, 68Q25.

Keywords: Dynamical system (gradient-), Newton flow (rational-, elliptic-; desingularized), structural stability, elliptic function (Jacobian, Weierstrass), phase portrait, Newton graph (elliptic-, nuclear-, pseudo-; rational-), cellularly embedded toroidal (distinguished) graph, face traversal procedure, steady stream, complexity.

1 Meromorphic Newton flows

In this section we briefly explain the concept of meromorphic Newton flow. For details and historical notes, see [3], [4], [8], [21], [22]. In the sequel, let f stand for a non-constant meromorphic function on the complex plane. So, $f(z)$ is complex analytic for all z in $\mathbb{C}$ with the possible exception of (countably many) isolated singularities: the *poles* for f.

The (damped) Newton method for finding zeros of f (with starting point z^0) is given by

$$z_{n+1} - z_n = -t_n \frac{f(z_n)}{f'(z_n)},\ t_n \neq 0,\ n = 0, 1, \ldots, z_0 = z^0. \tag{1}$$

Dividing both sides of (1) by the "damping factor" t_n and choosing t_n smaller and smaller, yields an "infinitesimal version" of (1), namely

$$\frac{dz}{dt} = \frac{-f(z)}{f'(z)}. \tag{2}$$

Conversely, Euler's method applied to (2), gives rise to an iteration of the form (1). A dynamical system of type (2) is denoted by $\mathcal{N}(f)$. For this system we will interchangeably use the following terminologies: *vector field* [i.e. the expression on its r.h.s.], or *(Newton-)flow* [when we focus on its phase portrait(=family of all maximal trajectories as point sets)].

Obviously, zeros and poles for f are removable singularities for $\frac{f}{f'}$ and turn into *isolated equilibria* for $\mathcal{N}(f)$. Special attention should be paid to those points z where $f(z) \neq 0$ and $f'(z) = 0$. In these (isolated!) so-called *critical points* , the vector field $\mathcal{N}(f)$ is not well-defined. We overcome this complication by introducing an additional "damping factor" $(1 + |f(z)|^4)^{-1}|f'(z)|^2 (\geq 0)$ and considering a system $\overline{\mathcal{N}}(f)$ of the form

$$\frac{dz}{dt} = -(1 + |f(z)|^4)^{-1} \overline{f'(z)} f(z). \tag{3}$$

Clearly, $\overline{\mathcal{N}}(f)$ may be regarded as another infinitesimal version of Newton's iteration (1). Note that, where both $\mathcal{N}(f)$ and $\overline{\mathcal{N}}(f)$ are well-defined, their phase portraits coincide, including the orientations of the trajectories (cf. Fig. 1). Moreover, $\overline{\mathcal{N}}(f)$ is a smooth, even real (but not complex) analytic vector field on the *whole* plane. In the sequel, we refer to $\overline{\mathcal{N}}(f)$ as to a *desingularized Newton flow* for f on $\mathbb{C}$.

Integration of (2) yields:

$$f(z(t)) = e^{-t} f(z_0),\ z(0) = z_0, \tag{4}$$

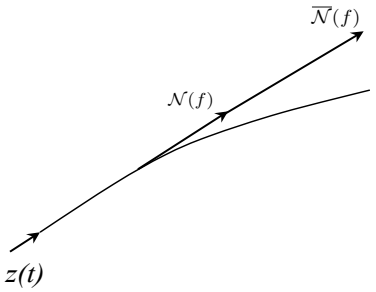

Figure 1: $\mathcal{N}(f)$ versus $\overline{\mathcal{N}}(f)$.

where $z(t)$ denotes the maximal trajectory for $\mathcal{N}(f)$ through a point z_0. So we have

$$\mathcal{N}(f)\text{-trajectories and also those of } \overline{\mathcal{N}}(f), \text{ are made up of lines arg } f(z) = \text{constant}. \quad (5)$$

It is easily verified that these Newton flows fulfil a *duality property* which will play an important role in the sequel:

$$\mathcal{N}(f) = -\mathcal{N}(\frac{1}{f}) \text{ and } \overline{\mathcal{N}}(f) = -\overline{\mathcal{N}}(\frac{1}{f}). \quad (6)$$

As a consequence of (5), (6), and using properties of (multi-)conformal mappings, we picture the local phase portraits of $\mathcal{N}(f)$ and $\overline{\mathcal{N}}(f)$ around their equilibria. See the comment on Fig.2, where $N(f)$, $P(f)$ and $C(f)$ stands for respectively the set of zeros, poles and critical points of f.

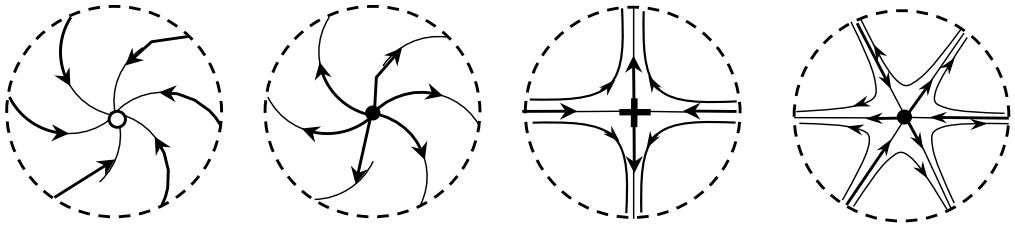

Figure 2: Local phase portraits around equilibria of $\overline{\mathcal{N}}(f)$

Comment on Fig. 2:
Fig. 2-$(a), (b)$: In case of a k-fold zero (pole) the Newton flow exhibits an attractor (repellor) and each (principal) value of arg$f$ appears precisely k times on equally distributed incoming (outgoing) trajectories. Moreover, the (positively measured) angle between two different incoming (outgoing) trajectories intersect under a non vanishing angle ($= \frac{\Delta}{k}$), where Δ stands for the difference of the arg$f$ values on these trajectories. In the sequel we will use: If two incoming (outgoing) trajectories at a *simple* zero (pole) admit the same arg$f$ value, those trajectories coincide.
Fig. 2-$(c), (d)$: In case of a k-fold critical point (i.e. a k-fold zero for f', no zero for f) the Newton flow exhibits a k-fold saddle, the stable (unstable) separatrices being equally

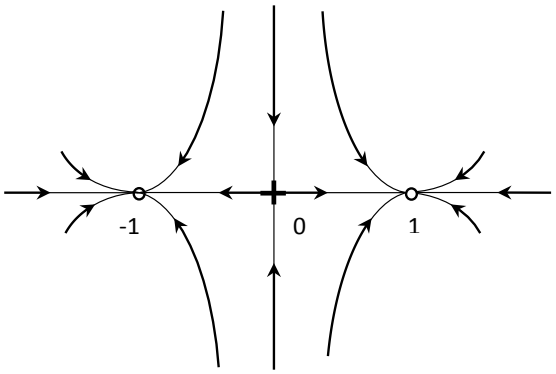

Figure 3: Phaseportrait $\overline{\mathcal{N}}(z^2-1)$

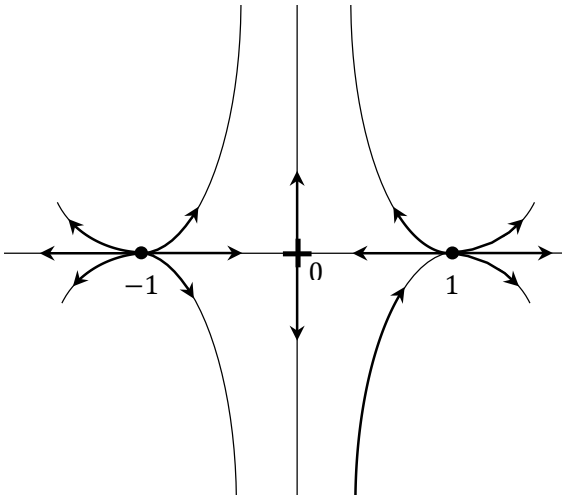

Figure 4: Phaseportrait $\overline{\mathcal{N}}(\frac{1}{z^2-1})$

distributed around this point. The two unstable (stable) separatrices at a 1-fold saddle, see Fig.2(c), constitute the local unstable (stable) manifold at this saddle point.

In the sequel we shall need:

Remark 1.1. Let z_0 be either a *simple* zero, pole or critical point for f. Then z_0 is a hyperbolic[1] equilibrium for $\overline{\mathcal{N}}(f)$. (In case of a zero or critical point for f, this follows by inspection of the linearization of the r.h.s. of $\overline{\mathcal{N}}(f)$: in case of a pole use (6).)

Remark 1.2. (Desingularized meromorphic Newton flows in $\mathbb{R}^2$-setting)
If we put $F : (\mathrm{Re}(z), \mathrm{Im}(z))^T (= (x_1, x_2)^T) \mapsto (\mathrm{Re}f(z), \mathrm{Im}f(z))^T$, the desingularized Newton flow $\overline{\mathcal{N}}(f)$ takes the form

$$\begin{aligned} \frac{d}{dt}(x_1, x_2)^T &= -[1 + |F(x_1, x_2)|^4]^{-1} \det(DF(x_1, x_2))(DF)^{-1}(x_1, x_2)F(x_1, x_2) \qquad (7) \\ &= -[1 + |F(x_1, x_2)|^4]^{-1} \tilde{DF}(x_1, x_2)F(x_1, x_2), \end{aligned}$$

[1] An equilibrium for a C^1- vector field on $\mathbb{R}^2$ is called hyperbolic if the Jacobi matrix at this equilibrium has only eigenvalues with non vanishing real parts(cf.[20]).

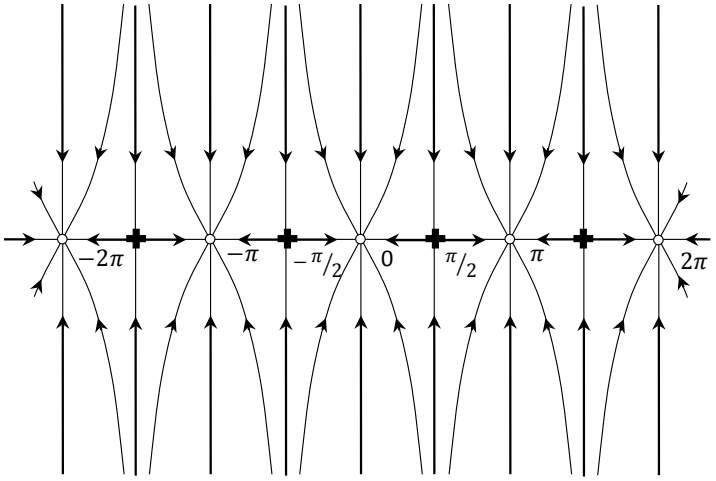

Figure 5: Phaseportrait $\overline{\mathcal{N}}(\sin z)$

where $(\cdot)^T$ stands for transpose, and $\tilde{DF}(\cdot)$ for the co-factor (adjoint) matrix[2] of the Jacobi matrix $DF(\cdot)$ of F. (The r.h.s. of (7) vanishes at points corresponding to poles of f)

We end up with some pictures illustrating the above explanation.

[2]i.e. $\tilde{DF}(x_1, x_2) \cdot DF(x_1, x_2) = \det(DF(x_1, x_2))I_2$, where I_2 stands for the 2×2-unit matrix.

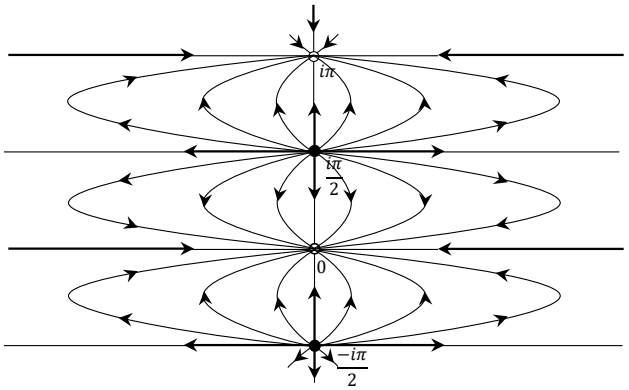

Figure 6: Phaseportrait of $\overline{\mathcal{N}}(\tanh z)$

2 Rational Newton flows

Here we present some earlier results on meromorphic Newton flows in the special case of rational functions. Throughout this section, let f be a (*non-constant*) rational function. By means of the transformation $w = \frac{1}{z}$ we may regard f as a function on the extended complex plane $\mathbb{C} \cup \{z = \infty\}$. As usual, we identify the latter set with the sphere S^2 (as a Riemann surface) and the set $\mathcal{R}$ of extended functions f with the set of all (non-constant) meromorphic functions on S^2. The transformation $w=\frac{1}{z}$ turns the *planar rational Newton flow* $\overline{\mathcal{N}}(f)$, $f \in \mathcal{R}$, into a *smooth* vector field on S^2, denoted $\overline{\overline{\mathcal{N}}}(f)$, cf. [23], [36]. In the theory on such vector fields the concept of structural stability plays an important role, see e.g. [32] or [20]. Roughly speaking, structural stability of $\overline{\overline{\mathcal{N}}}(f)$ means "topological invariance of its phase portrait under sufficiently small perturbations of the problem data". Here we briefly summarize the results as obtained by Jongen, Jonker, Twilt (cf. [22], [23], [24]):

Theorem 2.1. (*Structural stability for rational Newton flows*)
Let $f \in \mathcal{R}$, then:

(i) Characterization:
The flow $\overline{\overline{\mathcal{N}}}(f)$, $f \in \mathcal{R}$, is structurally stable iff f fulfils the following conditions:

- *All finite zeros and poles for f are simple.*
- *All critical points for f, possibly including $z = \infty$, are simple.*
- *No two critical points for f are connected by an $\overline{\overline{\mathcal{N}}}(f)$-trajectory.*

(ii) Genericity:
For "almost all" functions f in $\mathcal{R}$, the flows $\overline{\overline{\mathcal{N}}}(f)$ are structurally stable, i.e. the functions f as in (i) constitute an open and dense subset of $\mathcal{R}$ (w.r.t. an appropriate topology on $\mathcal{R}$).

(iii) Classification:
The conjugacy classes of the stucturally stable flows $\overline{\overline{\mathcal{N}}}(f)$ can be classified in terms of certain sphere graphs that are generated by the phase portraits of these flows.

(iv) Representation:
Up to conjugacy for flows and (topological) equivalency for graphs, there is a 1-1-correspondence between the set of all structurally stable flows $\overline{\overline{\mathcal{N}}}(f)$ and the set of all so-called Newton graphs, i.e., cellularly embedded sphere graphs that fulfil some combinatorial (Hall) condition.

The purpose of the present paper is to find out wether similar results hold for *elliptic* Newton flows (i.e., meromorphic Newton flows in the case of elliptic functions). See also the forthcoming Section 13.1.

Phase portraits of rational Newton flows (even structurally stable) on $\mathbb{C}$ are presented in Fig. 3 and 4. The simplest example of a spherical rational Newton flow is the so-called North-South flow, given by $\overline{\overline{\mathcal{N}}}(z^n)$, see Fig. 7; structurally stable if $n = 1$. Intuitively, it is clear that the phase portraits of $\overline{\overline{\mathcal{N}}}(z^n)$ and $\overline{\overline{\mathcal{N}}}((\frac{z-a}{z-b})^n), a \neq b$, are topologically equivalent (i.e. equal up to conjugacy), see see Fig. 7 and 8.

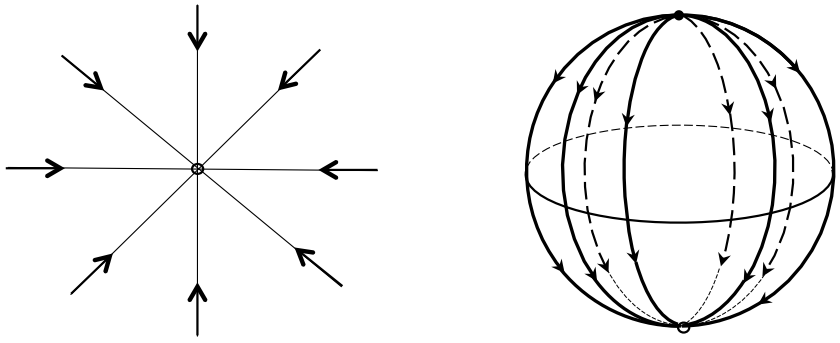

$\overline{\mathcal{N}}(z^n)$ $\qquad\qquad$ $\overline{\overline{\mathcal{N}}}(z^n)$

Figure 7: The planar and spherical North-South flow

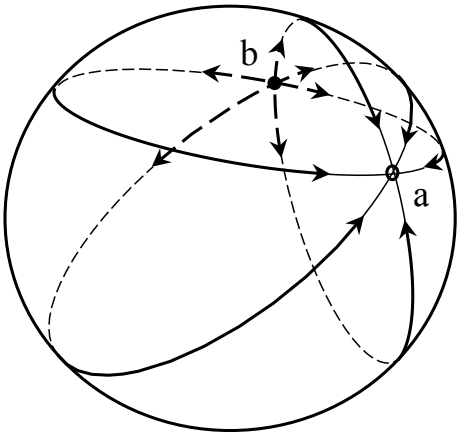

Figure 8: $\overline{\overline{\mathcal{N}}}((\frac{z-a}{z-b})^n)$

3 Elliptic Newton flows: definition

Throughout this section, let f be a (non-constant) elliptic, i.e. a meromorphic and doubly periodic function of order r ($2 \leq r < \infty$) with $(\omega_1,\ \omega_2)$ as a pair of *basic periods.*[3] We may assume that $\mathrm{Im}\frac{\omega_2}{\omega_1} > 0$. The associated period lattice is denoted by Λ, and $P_{\omega_1,\,\omega_2}$ stands for the "half open/half closed" period parallelogram $\{t_1\omega_1 + t_2\omega_2 \mid 0 \leq t_1 < 1,\ 0 \leq t_2 < 1\}$. On P_{ω_1,ω_2}, the function f has r zeros and r poles (counted by multiplicity).

By Liouville's Theorem, these sets of zeros and poles determine f up to a multiplicative constant $C(\neq 0)$, and thus also the class $[f]$ of all elliptic functions of the form $Cf, C(\neq 0)$.

Let T_{ω_1,ω_2} be the torus obtained from P_{ω_1,ω_2} by identifying opposite sides in the boundary of this parallelogram. The planar, desingularized Newton flow $\overline{\mathcal{N}}(f)$ is doubly periodic on $\mathbb{C}$ with periods (ω_1,ω_2). Hence, this flow may be interpreted as a smooth (not complex analytic) vector field -say $\overline{\overline{\mathcal{N}}}(f_{\omega_1,\omega_2})$- on T_{ω_1,ω_2}; its trajectories correspond to the lines $\arg f(z) =$ constant, cf. (5). We refer to $\overline{\overline{\mathcal{N}}}(f_{\omega_1,\omega_2})$ as the *(desingularized) elliptic Newton flow* for f on T_{ω_1,ω_2}.

If g is another function in $[f]$, the planar flows $\overline{\mathcal{N}}(g)$ and $\overline{\mathcal{N}}(f)$ have equal phase portraits, as follows by inspection of the expressions of these flows in Section 1; see also Fig.1. Hence, the flows $\overline{\overline{\mathcal{N}}}(f_{\omega_1,\omega_2})$ and $\overline{\overline{\mathcal{N}}}(g_{\omega_1,\omega_2})$, both defined on T_{ω_1,ω_2}, have equal phase portraits.

Next, we choose another pair of basic periods for f, say (ω_1',ω_2'), with $\mathrm{Im}\frac{\omega_2'}{\omega_1'} > 0$, i.e. (ω_1,ω_2) and (ω_1',ω_2') generate the same lattice Λ and are related by a unimodular[4] linear transfomation M. Note that under M the zeros/poles for f on P_{ω_1,ω_2} are mapped onto the zeros/poles for f on $P_{\omega_1',\omega_2'}$.
The above introduction of the concept "elliptic Newton flow for f" leads to different flows (being defined on different tori T_{ω_1,ω_2} and $T_{\omega_1',\omega_2'}$). However, from a topological point of view, all these flows may be considered as equal:

Lemma 3.1. *Let (ω_1,ω_2) and (ω_1',ω_2') be pairs of basic periods for f. Then, the unimodular mapping from (ω_1,ω_2) to (ω_1',ω_2') induces a homeomorphism from T_{ω_1,ω_2} to $T_{\omega_1',\omega_2'}$ such that the phase portraits of $\overline{\overline{\mathcal{N}}}(f_{\omega_1,\omega_2})$ and $\overline{\overline{\mathcal{N}}}(f_{\omega_1',\omega_2'})$ correspond under this homeomorphism, thereby respecting the orientations of the trajectories.*

Proof. We turn over from $\overline{\overline{\mathcal{N}}}(f_{\omega_1,\omega_2})$ and $\overline{\overline{\mathcal{N}}}(f_{\omega_1',\omega_2'})$ to their $\mathbb{R}^2$-settings, say $\overline{\mathcal{N}}(F)$ resp. $\overline{\mathcal{N}}(F')$, cf. Remark 1.2. (Note that $\overline{\mathcal{N}}(F)$=$\overline{\mathcal{N}}(F')$). The linear isomorphism, given by the basis transfomation (Ω) from (ω_1,ω_2) to $(1,i)$ -considered as two ordered bases for $\mathbb{C}$ as the real vector space $\mathbb{R}^2$- is given by a 2×2-matrix, also denoted Ω. Analogously, we define Ω' with respect to (ω_1',ω_2') and $(1,i)$. The (linear) unimodular transformation from (ω_1,ω_2) to (ω_1',ω_2') is given by a 2×2-matrix M. We put

$$H = \Omega' M \Omega^{-1} \text{ and } H(x^T) = y^T, x = (x_1,x_2), y = (y_1,y_2) \in \mathbb{R}^2.$$

Then F=$F'\circ H$. The flow $\overline{\mathcal{N}}(F)$ takes the form

$$\frac{dx^T}{dt} = -[1+|F(x)|^4]^{-1}\tilde{DF}(x)F(x). \tag{8}$$

By the Chain Rule, this equation turns -under the transformation $x^T = H^{-1}(y^T)$- into:

$$\frac{dy^T}{dt} = -[1+|F'(y)|^4]^{-1}\det(H)\tilde{DF'}(y)F'(y).$$

[3] i.e. each period is of the form $n\omega_1 + m\omega_2, n, m \in \mathbb{Z}$. In particular, $\mathrm{Im}\frac{\omega_2}{\omega_1} \neq 0$ (cf. [27], [6]).

[4] M is given by a 2×2-matrix with coefficients in $\mathbb{Z}$ and determinant $+1$(cf. [6]).

Apart from the mutiplicative factor $\det(H)$ -always strictly positive- this is the expression for the desingularized Newton flow $\overline{\mathcal{N}}(F^{'})$. Hence, under H the phase portrait of $\overline{\mathcal{N}}(F)$ remains invariant. It follows that the phase portraits of $\overline{\overline{\mathcal{N}}}(f_{\omega_1,\omega_2})$ and $\overline{\overline{\mathcal{N}}}(f_{\omega_1^{'},\omega_2^{'}})$ correspond under the homeomorphism from T_{ω_1,ω_2} to $T_{\omega_1^{'},\omega_2^{'}}$, induced by M. □

The above lemma, together with the preceding observation, leads to:

Definition 3.2. If f is an elliptic function of order r, then:

(1) The elliptic Newton flow for f , denoted $\overline{\overline{\mathcal{N}}}([f])$, is the collection of all flows $\overline{\overline{\mathcal{N}}}(g_{\omega_1,\omega_2})$, for any $g \in [f]$ and any pair (ω_1, ω_2) generating the period lattice Λ of f.

(2) The set of all elliptic Newton flows of order r with respect to a given period lattice Λ is denoted $N_r(\Lambda)$.

This definition might look rather complicated. However, a natural interpretation is possible. To see this, let us consider the quotient space $T(\Lambda) := \mathbb{C}/\Lambda$, endowed with the complex analytic structure[5] determined by the pair (ω_1, ω_2). A pair $(\omega_1^{'}, \omega_2^{'})$, related to (ω_1, ω_2) by a unimodular map, generates the same lattice Λ and determines on $T(\Lambda)$ another -but isomorphic- complex analytic structure (cf. [14]). Each parallelogram P_{ω_1,ω_2} resp. $P_{\omega_1^{'},\omega_2^{'}}$ contains precisely one representative for each of the classes mod Λ. Hence, the tori T_{ω_1,ω_2} and $T_{\omega_1^{'},\omega_2^{'}}$ may be identified with $T(\Lambda)$, endowed with isomorphic complex analytic structures. Now, the flows $\overline{\overline{\mathcal{N}}}(f_{\omega_1,\omega_2})$ and $\overline{\overline{\mathcal{N}}}(f_{\omega_1^{'},\omega_2^{'}})$ can be interpreted as smooth flows on $T(\Lambda)$ with *the same phase portraits*. Regarding flows on $T(\Lambda)$ with the same phase portraits as equal, compare the "desingularization" step leading from (2) to (3) and see also Fig. 1, we may interprete the elliptic Newton flow $\overline{\overline{\mathcal{N}}}([f])$ as a smooth vector field on the compact torus $T(\Lambda)$. Consequently, it is allowed to apply the theory for smooth vector fields on compact two-dimensional differential manifolds. For example: Since there are no closed orbits by (4), and applying the Poincaré-Bendixson-Schwartz Theorem, cf. [21], [22], [32], we find:

Lemma 3.3. *The limiting set of any (maximal) trajectory of $\overline{\overline{\mathcal{N}}}([f])$ tends -for increasing t- to either a zero or a critical point for f on $T(\Lambda)$, and -for decreasing t- to either a pole or a critical point for f on $T(\Lambda)$.*

We also have:

Remark 3.4. Hyperbolic equilibria for $\overline{\mathcal{N}}(f)$ correspond to such equilibria for $\overline{\overline{\mathcal{N}}}([f])$.

4 Elliptic Newton flows: representation

Let f be as introduced in Section 3, i.e. an elliptic function of order r ($2 \leq r < \infty$) with (ω_1, ω_2), $\mathrm{Im}\frac{\omega_2}{\omega_1} > 0$, as an (arbitrary) pair of basic periods generating a period lattice Λ. The set of all such functions is denoted by $E_r(\Lambda)$.

Let the zeros and poles for f on P_{ω_1,ω_2} be $a_1, \cdots, a_r$, resp. $b_1, \cdots, b_r$ (counted by multiplicity). Then we have: (cf. [28])

$$a_i \neq b_j, i, j = 1, \cdots, r \text{ and } a_1 + \cdots + a_r = b_1 + \cdots + b_r \text{ mod } \Lambda. \tag{9}$$

We may consider f as a meromorphic function on the quotient space $T(\Lambda) := \mathbb{C}/\Lambda$. The zeros and poles for f on $T(\Lambda)$ are given by respectively: $[a_1], \cdots, [a_r]$ and $[b_1], \cdots, [b_r]$, where $[\cdot]$ stands for the congruency class mod Λ of a number in $\mathbb{C}$. Apparently, from (9) it follows:

$$[a_i] \neq [b_j], i, j = 1, \cdots, r \text{ and } [a_1] + \cdots + [a_r] = [b_1] + \cdots + [b_r]. \tag{10}$$

[5] As coordinate neighborhoods in $T(\Lambda)$ take open subsets of $\mathbb{C}$ that contain no points congruent to one another mod Λ.

Moreover, a parallelogram of the type P_{ω_1,ω_2} contains one representative of each of these classes: the r zeros/poles for f on this parallelogram.

An elliptic Newton flow $\overline{\overline{\mathcal{N}}}([f])(\in N_r(\Lambda))$ corresponds uniquely to the class $[f]$. So we may identify the set $N_r(\Lambda)$ with the set $\{[f]|f \in E_r(\Lambda)\}$.

On its turn, the class $[f]$ is uniquely determined (cf. Section 3) by sets of zeros/poles, say $\{a_1,\cdots,a_r\}/\ \{b_1,\cdots,b_r\}$, both situated in some P_{ω_1,ω_2}. Thus, the sets

$$\{[a_1],\cdots,[a_r]\},\{[b_1],\cdots,[b_r]\}$$

fulfill the conditions (10). Conversely, we have:
Let two sets $\{[a_1],\cdots,[a_r]\},\ \{[b_1],\cdots,[b_r]\}$ of classes mod Λ (repetitions permitted!), fulfilling conditions (10), be given. Choose (the unique)representatives, say $a_1,\cdots,a_r$ and $b_1,\cdots,b_r$ of these classes situated in a half open/half closed parallelogram spanned by an (arbitrary) pair of basic periods of Λ. We put

$$b_r^{'} = a_1 +\cdots+ a_r - b_1 -\cdots- b_{r-1},$$

thus $b_r^{'} = b_r \bmod \Lambda$ and $[b_r^{'}] \neq [b_j], j = 1,\cdots,r-1$, and consider functions of the form

$$C\frac{\sigma(z-a_1)\cdots\sigma(z-a_r)}{\sigma(z-b_1)\cdots\sigma(z-b_{r-1})\sigma(z-b_r^{'})}, \tag{11}$$

where $C(\neq 0)$ is an arbitrary constant, and σ stands for the Weierstrass sigma function (cf. [28]) corresponding to Λ. Since σ is a holomorphic, quasi-periodic function with only simple zeros, cf. [28], at the lattice points of Λ, a function given by (11) is elliptic (with respect to Λ) of order r. The zeros and poles are $a_1,\cdots,a_r$ resp. $b_1,\cdots,b_r$. Such a function determines precisely one element of $N_r(\Lambda)$. (Note that if we choose representatives in an other period parallelogram we obtain a representative of the same Newton flow, cf. Section 3).

Altogether, we have proved:

Lemma 4.1. *Given a lattice Λ, then the flows in $N_r(\Lambda)$ are represented by the set of all ordered pairs $(\{[a_1],\cdots,[a_r]\},\ \{[b_1],\cdots,[b_r]\})$ of sets of classes* mod Λ *that fulfil (10).*

Remark 4.2. Interchanging the roles of $(\{[a_1],\cdots,[a_r]\}$ and $\{[b_1],\cdots,[b_r]\})$ reflects the duality property, cf. (6). In fact, we have $\overline{\overline{\mathcal{N}}}([\frac{1}{f}]) = -\overline{\overline{\mathcal{N}}}([f])$.

On the subset $V_r(\Lambda)$ in $T^r(\Lambda)\times T^r(\Lambda)$ of pairs $(c,d),\ c := ([c_1],\cdots,[c_r]), d := ([d_1],\cdots,[d_r])$, that fulfil condition (10), we define an equivalence relation ($\approx$):

$$(c,d) \approx (c^{'},d^{'}) \text{ iff } \{[c_1],\cdots,[c_r]\} = \{[c_1^{'}],\cdots,[c_r^{'}]\} \text{ and } \{[d_1],\cdots,[d_r]\} = \{[d_1^{'}],\cdots,[d_r^{'}]\}$$

The topology τ_0 on $E_r(\Lambda)$

Clearly, the set $V_r(\Lambda)/\approx$ may be identified with the representation space for $N_r(\Lambda)$ in Lemma 4.1 , and thus with $\{[f] \mid f \in E_r(\Lambda)\}$. Hence, this space can be endowed with a topology which is successively induced by the quotient topology on $T(\Lambda) = (\mathbb{C}/\Lambda))$, the product topology on $T^r(\Lambda)\times T^r(\Lambda)$, the relative topology on $V_r(\Lambda)$ as a subset of $T^r(\Lambda)\times T^r(\Lambda)$, and the quotient topology w.r.t. the relation $\approx$.
Finally, we endow $E_r(\Lambda)$ with the weakest topology, say τ_0, making the mapping

$$E_r(\Lambda) \to N_r(\Lambda) : f \mapsto [f]$$

continuous.

The topology τ_0 on $E_r(\Lambda)$ is induced by the Euclidean topology on $\mathbb{C}$, and is natural in the following sense: Given f in $E_r(\Lambda)$ and $\epsilon > 0$ sufficiently small, a τ_0-neighbourhood $\mathcal{O}$ of

f exists such that for any $g \in \mathcal{O}$, the zeros (poles) for g are contained in ε-neighbourhoods of the zeros (poles) for f.

Uptill now, we dealt with elliptic Newton flows $\overline{\overline{\mathcal{N}}}(f)$ with respect to an arbitrary, but fixed, lattice, namely the lattice Λ for f. Now, we turn over to a different lattice, say Λ^*, i.e., pairs of basic periods for Λ and Λ^* are not necessarily related by a unimodular transformation. Firstly, we treat a simple case: For $\alpha \in \mathbb{C}\backslash\{0\}$, we define $f^\alpha(z) := f(\alpha^{-1}z)$. Thus f^α is an elliptic function, of order r, with basic periods $(\alpha\omega_1, \alpha\omega_2)$ generating the lattice $\Lambda^* = \alpha\Lambda$.

The following lemma is in the same spirit as Lemma 3.1. The proof (also based on the Chain Rule) will be omitted.

Lemma 4.3. *The transformation $z \mapsto w := \alpha z$ induces a homeomorphism from the torus T_{ω_1,ω_2} onto $T_{\alpha\omega_1,\alpha\omega_2}$, such that the phase portraits of the flows $\overline{\overline{\mathcal{N}}}([f])$ and $\overline{\overline{\mathcal{N}}}([f^\alpha])$ correspond under this homeomorphism, thereby respecting the orientations of the trajectories.*

In other words: from a topological point of view, the Newton flows $\overline{\overline{\mathcal{N}}}([f]) \in N_r(\Lambda)$ and $\overline{\overline{\mathcal{N}}}([f^\alpha]) \in N_r(\alpha\Lambda)$ may be considered as equal.

More general, we call the Newton flows $\overline{\overline{\mathcal{N}}}([f]) \in N_r(\Lambda)$ and $\overline{\overline{\mathcal{N}}}([g]) \in N_r(\Lambda^*)$ equivalent ($\sim$) if they attain representatives, say $\overline{\overline{\mathcal{N}}}(f_{\omega_1,\omega_2})$, respectively $\overline{\overline{\mathcal{N}}}(g_{\omega_1^*,\omega_2^*})$, and there is a homeomorphism $T_{\omega_1,\omega_2} \to T_{\omega_1^*,\omega_2^*}$, induced by the linear (over $\mathbb{R}$) basis transformation $(\omega_1, \omega_2) \mapsto (\omega_1^*, \omega_2^*)$, such that their phase portraits correspond under this homeomorphism, thereby respecting the orientations of the trajectories.

From now on, we choose for (ω_1, ω_2) a pair of so-called reduced[6] periods for f, such that the quotient $\tau = \frac{\omega_2}{\omega_1}$ satisfies the conditions:

$$\begin{cases} \text{Im } \tau > 0, |\tau| \geq 1, -\frac{1}{2} \leq \text{Re } \tau < \frac{1}{2}, \\ \text{Re } \tau \leq 0, \text{ if } |\tau| = 1 \end{cases} \tag{12}$$

(Such a choice is always possible (cf. [6]). Moreover, τ is unique in the following sense: if $(\omega_1^{'}, \omega_2^{'})$ is another pair of reduced periods for f, such that $\tau^{'} = \frac{\omega_2^{'}}{\omega_1^{'}}$ also satisfies the conditions (12), then $\tau = \tau^{'}$).

We emphasize that τ depends on the given lattice Λ, not on the incidental choice of the elliptic functions f with Λ as period lattice. We put $D := \{\tau \in \mathbb{C} \mid \tau \text{ fulfills (12)}\}$).

Lemma 4.4. *Let f be -as before- an elliptic function of order r with Λ as period lattice, and let Λ^* be an arbitrary lattice. Then, there exists a function, say f^*, with $f^* \in E_r(\Lambda^*)$, such that $\overline{\overline{\mathcal{N}}}([f]) \sim \overline{\overline{\mathcal{N}}}([f^*])$.*

Proof. Choose (ω_1, ω_2), respectively (ω_1^*, ω_2^*), as pairs of reduced periods for Λ and Λ^* such that $\frac{\omega_2}{\omega_1} = \tau$ and $\frac{\omega_2^*}{\omega_1^*} = \tau^*$ satisfy (12). Then, $(1, \tau)$ and $(1, \tau^*)$ are pairs of primitive periods for the lattices $\Lambda_{1,\tau}(=(\frac{1}{\omega_1}\Lambda))$, respectively $\Lambda^*_{1,\tau^*}(=(\frac{1}{\omega_1^*}\Lambda^*))$. Let $\mathcal{F}$ be the linear basis transformation from $(1, \tau)$ to $(1, \tau^*)$ and choose the linear basis transformations Ω and Ω^* from $(1, \tau)$ to $(1, i)$, resp. from $(1, \tau^*)$ to $(1, i)$, as Ω and Ω^*, in the proof of Lemma 3.1.

We consider $\overline{\overline{\mathcal{N}}}([f^{\frac{1}{\omega_1}}])$: a flow in $N_r(\Lambda_{1,\tau})$, determined by two tuples of classes mod $\Lambda_{1,\tau}$, say $\{[a_1], \cdot, [a_r]\}/\{[b_1], \cdot, [b_r]\}$, and satisfying (10). Under $\mathcal{F}$ these tuples turn into tuples of classes mod Λ^*_{1,τ^*}, say $\{[a_1^*], \cdots, [a_r^*]\}/\{[b_1^*], \cdots, [b_r^*]\}$ satisfying (10) as well.

[6]The pair of basic periods (ω_1, ω_2) for f is called *reduced* or *primitive* if $|\omega_1|$ is minimal among all periods for f , whereas $|\omega_2|$ is minimal among all periods ω for f with the property $\text{Im}\frac{\omega_2}{\omega_1} > 0$ (cf. [6]).

By Lemma 4.1, the latter tuples determine a Newton flow, say $\overline{\overline{\mathcal{N}}}([g])$, in $N_r(\Lambda^*_{1,\tau^*})$. The transfomation $\Omega^*\mathcal{F}\Omega^{-1}$ induces an equivalency: $\overline{\overline{\mathcal{N}}}([f^{\frac{1}{\omega_1}}]) \sim \overline{\overline{\mathcal{N}}}([g])$. The proof -based on the Chain Rule- is similar to the proof of Lemma 3.1, and will be deleted. We define f^* as $f^* := g^{\omega_1}$. Thus, by Lemma 4.3: $\overline{\overline{\mathcal{N}}}([f^*]) = \overline{\overline{\mathcal{N}}}([g^{\omega_1}]) \sim \overline{\overline{\mathcal{N}}}([g])$, $\overline{\overline{\mathcal{N}}}([f]) \sim \overline{\overline{\mathcal{N}}}([f^{\frac{1}{\omega_1}}])$. Altogether, we find: $\overline{\overline{\mathcal{N}}}([f]) \sim \overline{\overline{\mathcal{N}}}([f^*])$. □

Remark 4.5. Note that if -in Lemma 4.4- we have $\Lambda = \Lambda^*$, i.e. the basic periods for Λ, and Λ^* are related by unimodular transformations, then: $f = f^*$. Moreover, the function f^* is uniquely determined by f, and $g \in [f]$ implies $g^* \in [f^*]$.

We summarize the results, obtained in this (and the preceding) section:

Theorem 4.6. *When studying (topological) features of elliptic Newton flows of order r, it is enough to choose a fixed (but arbitrary) lattice Λ, determining a unique parameter τ in the fundamental domain D, as specified in (12). Then, any Newton flow in $N_r(\Lambda)$ can be represented by a flow $\overline{\overline{\mathcal{N}}}(f_{1,\tau})$ on a torus $T_{1,\tau}$, where $f_{1,\tau}$ is of the form (11) with $C = 1$, and $(1, \tau)$ stands for a pair of reduced periods. If Λ^* is any other lattice, then there is an f^* in $E_r(\Lambda^*)$ such that $\overline{\overline{\mathcal{N}}}([f]) \sim \overline{\overline{\mathcal{N}}}([f^*])$. In particular, we may choose $\Lambda^* = \Lambda_{1,i}$, i.e. $\tau = i$.*

We end up by presenting two pictures of Newton flows for $\mathrm{sn}_{\omega_1,\omega_2}$, where $\mathrm{sn}_{\omega_1,\omega_2}$ stands for a Jacobian function. This is a 2nd order elliptic function, attaining only simple zeros, poles and critical points. This function is characterized by the basic periods $4K, 2iK'$, and so does the phase portrait of its Newton flow. Here K, K' are two parameters defined in terms of the Weierstrass function $\wp_{\omega_1,\omega_2}$

It turns out that for the phase portrait there are -up to conjugacy- only two possibilities (rectangular or not), corresponding to the form of the parallelogram $P_{1,\tau}$ with $(1, \tau)$ in D and $\tau = (\frac{2iK'}{4K})$ mod 1. In fact, these conjugacy classes are determined by the stable and unstable manifolds at the saddles of the flow (cf. [9]). Hence, it is sufficient to select for each possibility one suitably chosen example. See Fig. 9 [non-rectangular, equiharmonic subcase, given by $\tau = \frac{1}{3}\sqrt{3}\exp(\frac{\pi i}{6})$] and Fig. 10 [rectangular subcase given by $\mathrm{Re}\tau = 0$]. For a detailed argumentation, see our previous work [9]; compare also the forthcoming Remarks 6.14, 6.15.

Note that in Fig. 9, 10 the points, labelled by $0, 4K, 2iK'$ and $4K + 2iK'$ correspond to the same toroidal zero for $\mathrm{sn}_{\omega_1,\omega_2}$ (denoted by $\circ_1$) , whereas both $2K$ and $2K + 2iK'$ correspond to the other zero (denoted by $\circ_2$) Similarly, $2K + iK'$ stands for a pole (denoted by $\bullet_3$) on the torus, the pair $(iK', 4K + iK')$ for the other pole (denoted by $\bullet_4$). The four torodial critical points (denoted by $+_5, \cdots, +_8$) are represented by respectively the pairs $(K, K + 2iK'), (3K, 3K + 2iK')$ and the points $K + iK'$ and $3K + iK'$; see e.g. [1] or [27].

It is well-known that the periods $4K, 2iK'$ are not independent of each other, but related via a parameter $m, 0 < m < 1$, see e.g. [1]. In the situation of Fig. 10: if $m \downarrow 0$, then $4K \to 2\pi, \pm 2iK' \to \infty$ and the phase portraits of $\overline{\mathcal{N}}(\mathrm{sn}_{\omega_1,\omega_2})$ turn into that of $\overline{\mathcal{N}}(\sin)$; if $m \uparrow 1$, then $\pm 4K \to \infty, 2iK' \to 2\pi i$ and the phase portraits of $\overline{\mathcal{N}}(\mathrm{sn}_{\omega_1,\omega_2})$ turn into that of $\overline{\mathcal{N}}(\tanh)$; compare also Fig. 5, 6.

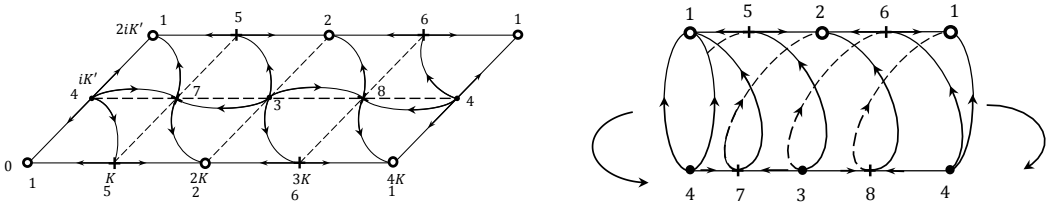

Figure 9: Newton flows for sn; non-rectangular case; $\tau = \frac{1}{3}\sqrt{3}\exp(\frac{\pi i}{6})$

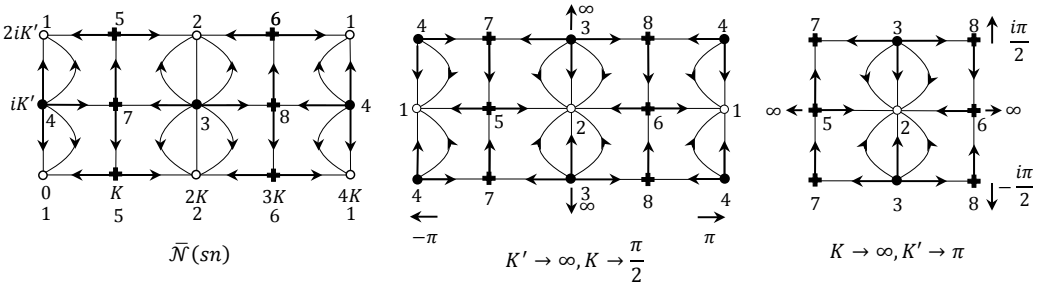

Figure 10: Newton flows for sn; rectangular case; Re τ=0

5 Structural stability: Genericity and Characterization

Adopting the notations introduced in the preceding section, let f be a function in $E_r(\Lambda)$ and $\overline{\overline{\mathcal{N}}}([f])$ ($\in N_r(\Lambda)$) its associated Newton flow (as a smooth vector field on the torus $T(\Lambda)$).

By $X(T(\Lambda))$ we mean the set of all C^1-vector fields on $T(\Lambda)$, endowed with the C^1-topology (cf. [18]). We consider the map:

$$\mathcal{F}_\Lambda : E_r(\Lambda) \to X(T(\Lambda)) : f \mapsto \overline{\overline{\mathcal{N}}}([f])$$

The topology τ_0 on $E_r(\Lambda)$ and the C^1-topology on $X(T(\Lambda))$ are matched by:

Lemma 5.1. *The map $\mathcal{F}_\Lambda$ is $\tau_0 - C^1$ continuous.*

Proof. In accordance with Theorem 4.6 and (11) we assume

$$f(z) = \frac{\sigma(z-a_1)\cdots\sigma(z-a_r)}{\sigma(z-b_1)\cdots\sigma(z-b_{r-1})\sigma(z-b_r')}.$$

Put $p(z) = \sigma(z-a_1)\cdots\sigma(z-a_r)$ and $q(z) = \sigma(z-b_1)\cdots\sigma(z-b_{r-1})\sigma(z-b_r')$. Then, the planar version $\overline{\mathcal{N}}(f)$ of the flow $\overline{\overline{\mathcal{N}}}([f])$ takes the form: (cf. (3))

$$\frac{dz}{dt} = -(|p(z)|^4 + |q(z)|^4)^{-1}(p(z)\overline{p'(z)}|q(z)|^2 - q(z)\overline{q'(z)}|p(z)|^2) \tag{13}$$

The expression in the r.h.s. is well-defined (since $|p(z)|^4 + |q(z)|^4 \neq 0$ for all z) and depends - as function (F) on $\mathbb{R}^2$- continuously differentiable on x(=Re z) and y(=Im z). So does the Jacobi matrix (DF) of F. Analogously, a function $g \in E_r(\Lambda)$ chosen τ_0-close to f , gives

rise to a system $\overline{\mathcal{N}}(g)$ and a function G with Jacobi matrix DG. Taking into account the very definition of C^1-topology on $X(T(\Lambda))$, the mapping $\mathcal{F}_\Lambda$ is continuous as a consequence of the following observation: If -w.r.t. the topology τ_0- the function g approaches f , i.e. the zeros and poles for g approach those for f, then G and DG approach F, respectively DF on every compact subset of $\mathbb{R}^2$. □

Next, we make the concept of structural stability for elliptic Newton flows more precise (compare also Section 2):

Definition 5.2. Let f, g be two functions in $E_r(\Lambda)$. Then, the associated Newton flows are called *conjugate*, denoted $\overline{\overline{\mathcal{N}}}([f]) \sim \overline{\overline{\mathcal{N}}}([g])$, if there is a homeomorphism from $T(\Lambda)$ onto itself, mapping maximal trajectories of $\overline{\overline{\mathcal{N}}}([f])$ onto those of $\overline{\overline{\mathcal{N}}}([g])$, thereby respecting the orientation of these trajectories.

Note that the above definition is compatible with the concept of " equivalent representations of elliptic Newton flows" as introduced in Section 4; compare also (the comment on) Definition 3.2.

Definition 5.3. The flow $\overline{\overline{\mathcal{N}}}([f])$ in $N_r(\Lambda)$ is called *(τ_0-)structurally stable* if there is a τ_0-neighborhood $\mathcal{O}$ of f, such that for all $g \in \mathcal{O}$ we have: $\overline{\overline{\mathcal{N}}}([f]) \sim \overline{\overline{\mathcal{N}}}([g])$.
The set of all structurally stable Newton flows $\overline{\overline{\mathcal{N}}}([f])$ is denoted $\tilde{N}_r(\Lambda)$.

From Lemma 5.1 it follows:

Corollary 5.4. *If $\overline{\overline{\mathcal{N}}}([f])$, as an element of $\mathcal{X}(T(\Lambda))$, is C^1-structurally stable ([32]) , then this flow is also τ_0-structurally stable.*

So, when discussing structural stability in the case of elliptic Newton flows, we may skip the adjectives C^1 and τ_0.

Definition 5.5. The function f in $E_r(\Lambda)$ is called *non-degenerate* if:

- All zeros, poles and critical points for f are simple;
- No two critical points for f are connected by a $\overline{\overline{\mathcal{N}}}([f])$-trajectory.

The set of all non degenerate functions in $E_r(\Lambda)$ is denoted by $\tilde{E}_r(\Lambda)$.

Note: if f is non-degenerate, then $\frac{1}{f}$ is non-degenerate.
The main result of this section is:

Theorem 5.6. *Genericity and characterization of structural stability.*

(1) The set $\tilde{E}_r(\Lambda)$ is open and dense in $E_r(\Lambda)$)

(2) $\overline{\overline{\mathcal{N}}}([f])$ is structurally stable if and only if f in $\tilde{E}_r(\Lambda)$

Proof. Will be postponed until the end of this section. □

We choose another lattice, say Λ^*. The functions f and g in $E_r(\Lambda)$ determine respectively, the unique functions f^* and g^* in $E_r(\Lambda^*)$, compare Lemma 4.4. Then the following assertions are easily verified:

- $\overline{\overline{\mathcal{N}}}([f]) \sim \overline{\overline{\mathcal{N}}}([g])$ if and only if $\overline{\overline{\mathcal{N}}}([f^*]) \sim \overline{\overline{\mathcal{N}}}([g^*])$
- $\overline{\overline{\mathcal{N}}}([f])$ is structurally stable if and only if $\overline{\overline{\mathcal{N}}}([f^*])$ is structurally stable.

- f in $\tilde{E}_r(\Lambda)$ if and only if f^* in $\tilde{E}_r(\Lambda^*)$

Hence, the map

$$E_r(\Lambda) \to E_r(\Lambda^*) : f \mapsto f^*$$

induces bijections between $\tilde{E}_r(\Lambda)$ and $\tilde{E}_r(\Lambda^*)$ and between $\tilde{N}_r(\Lambda)$ and $\tilde{N}_r(\Lambda^*)$. As a consequence (compare also Theorem 4.6) we may assume without loss of generality that:

$$\Lambda = \Lambda_{1,\tau}, \tau \in D, \text{ and } f \text{ is of the form (11) with } C = 1.$$

Hence, we suppress -unless strictly necessary- references to the pair $(1, \tau)$, the lattice Λ, and the class $[\cdot]$. So we shall write $\Lambda, T, E_r, N_r, \overline{\overline{\mathcal{N}}}(f)$ instead of resp. $\Lambda_{1,\tau}, T(\Lambda), E_r(\Lambda), N_r(\Lambda)$ and $\overline{\overline{\mathcal{N}}}([f])$.

Steady streams

As an intermezzo, we look at (elliptic) Newton flows from a slightly different point of view. To this aim, we consider a *steady stream* on $\mathbb{C}$ (cf. [27]) with complex potential

$$w(z) = -\log f(z) \tag{14}$$

The *stream lines* are given by the lines $\arg f(z) =$ constant, and the *velocity field* of this stream by $\overline{w'(z)}$. Zeros and poles for f of order n and m respectively, are just the *sinks* and *sources* of strength n, respectively m. Moreover, it is easily verified that the so called *stagnation points* of the steady stream (i.e., the zeros for $\overline{w'(z)}$) are the critical points of the planar Newton flow $\mathcal{N}(f)$. Altogether, we may conclude that the velocity field of the steady stream given by $w(z)$ and the (desingularized) planar Newton flow $\mathcal{N}(f)$ exhibit equal phase portraits.

From now on, we assume that f has -on the period parallelogram $P(= P_{\omega_1,\omega_2} = P_{1,\tau})$- the points $(\mathbf{a_1}, \cdots, \mathbf{a_A})$ and $(\mathbf{b_1}, \cdots, \mathbf{b_B})$ as zeros, resp. poles, with multiplicities $n_1, \cdots, n_A$, resp. $m_1, \cdots, m_B$ We even may assume[7] that all these zeros and poles are situated inside P (not on its boundary), cf. Fig. 11.

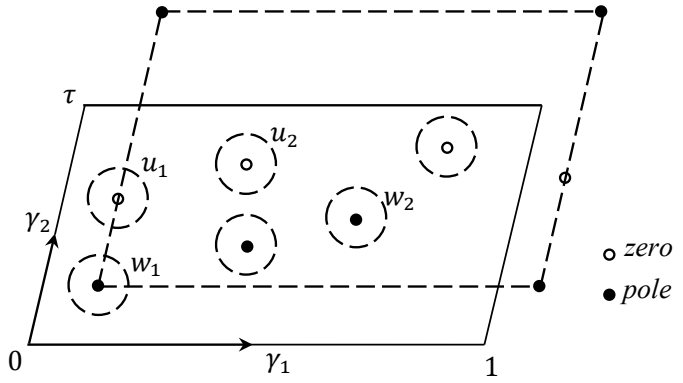

Figure 11: All zeros and poles for f inside $P = P_{1,\tau}$; after shift

[7] If this is not the case, an (arbitrary small) shift of P is always possible such that the resulting parallelogram satisfies our assumption (cf. Fig. 11 and [28]).

Since f is elliptic of order r, we have:

$$\begin{cases} n_1 + \cdots + n_A = m_1 + \cdots + m_B = r \\ n_1\mathbf{a_1} + \cdots + n_A\mathbf{a_A} = m_1\mathbf{b_1} + \cdots + m_B\mathbf{b_B} \bmod \Lambda, \text{ i.e.} \\ \mathbf{b_B} = \frac{1}{m_B}[n_1\mathbf{a_1} + \cdots + n_A\mathbf{a_A} - m_1\mathbf{b_1} - \cdots - m_{B-1}\mathbf{b_{B-1}} + \lambda^0], \text{ some } \lambda^0 \in \Lambda. \end{cases} \tag{15}$$

Note that there is an explicit formula for λ^0. In fact, we have:

$$\lambda^0 = -\eta(f(\gamma_2))\omega_1 + \eta(f(\gamma_1))\omega_2,$$

where $\omega_1(=1)$ and $\omega_2(=\tau)$ are basic (reduced) periods for Λ, and $\eta(\cdot)$ stands for winding numbers of the curves $f(\gamma_1)$ and $f(\gamma_2)$ (compare Fig. 11 and [28]).

The derivative f' is an elliptic function of order $(m_1+1)+\cdots+(m_B+1) = r+B$, and

$$\sharp(\text{crit. points for } f) = r + B - (n_1 - 1) - \cdots - (n_A - 1) = A + B(=: K)$$

In view of our assumptions on f we have: (cf. (11))

$$\begin{aligned} f(z) &= \frac{\sigma^{n_1}(z-\mathbf{a_1})\cdots\sigma^{n_A}(z-\mathbf{a_A})}{\sigma^{m_1}(z-\mathbf{b_1})\cdots\sigma^{m_B-1}(z-\mathbf{b_B})\sigma(z-\mathbf{b_B'})}, \text{ with} \\ \mathbf{b_B'} &= n_1\mathbf{a_1} + \cdots + n_A\mathbf{a_A} - m_1\mathbf{b_1} - \cdots - (m_B-1)\mathbf{b_B}, \\ &\text{and thus } \mathbf{b_B'} = \mathbf{b_B} \bmod \Lambda. \end{aligned} \tag{16}$$

So, by (14)

$$\begin{aligned} w'(z) = &- n_1\frac{\sigma'(z-\mathbf{a_1})}{\sigma(z-\mathbf{a_1})} - \cdots - n_A\frac{\sigma'(z-\mathbf{a_A})}{\sigma(z-\mathbf{a_A})} + m_1\frac{\sigma'(z-\mathbf{b_1})}{\sigma(z-\mathbf{b_1})} + \cdots \\ &+ (m_B-1)\frac{\sigma'(z-\mathbf{b_B})}{\sigma(z-\mathbf{b_B})} + \frac{\sigma'(z-\mathbf{b_B'})}{\sigma(z-\mathbf{b_B'})} \\ = &- n_1\zeta(z-\mathbf{a_1}) - \cdots - n_A\zeta(z-\mathbf{a_A}) + m_1\zeta(z-\mathbf{b_1}) + \cdots + (m_B-1)\zeta(z-\mathbf{b_B}) + \zeta(z-\mathbf{b_B'}) \end{aligned}$$

where ζ stands for the Weierstrass zeta function (cf. [28]) associated with the lattice $\Lambda(=\Lambda_{1,\tau})$. Since ζ is a quasi-periodic, meromorphic function with only poles (all simple!) in the points of the lattice Λ, the function $w'(z)$ is elliptic of order $K(=A+B)$ with K (simple) poles given by: $\mathbf{a_1},\cdots,\mathbf{a_A},\mathbf{b_1},\cdots,\mathbf{b_B}$, situated in its period parallelogram P. It follows that $w'(z)$ has also K zeros (counted by multiplicity) on P. These zeros correspond with the critical points for $\overline{\overline{\mathcal{N}}}(f)$ on the torus T.

Since $\zeta' = -\wp$, where $\wp$ stands for the (elliptic!) Weierstrass $\wp$-function (cf. [28]) associated with $\Lambda(=\Lambda_{1,\tau})$, we find (use also $\mathbf{b_B'} = \mathbf{b_B} \bmod \Lambda$):

$$w''(z) = n_1\wp(z-\mathbf{a_1}) + \cdots + n_A\wp(z-\mathbf{a_A}) - m_1\wp(z-\mathbf{b_1}) - \cdots - m_B\wp(z-\mathbf{b_B}) \tag{17}$$

From (15) and (16) it follows: $\mathbf{b_B}$ is determined by $\mathbf{a_1},\cdots,\mathbf{a_A},\mathbf{b_1},\cdots,\mathbf{b_{B-1}}$. In mutually disjoint and suitably small[8] neighborhoods, say $U_1,\cdots,U_A$, and $W_1,\cdots,W_{B-1}$, of respectively $\mathbf{a_1},\cdots,\mathbf{a_A},\mathbf{b_1},\cdots,\mathbf{b_{B-1}}$ we choose arbitrary points $a_1,\cdots,a_A,b_1,\cdots,b_{B-1}$ and put, with fixed values n_i, m_j :

$$b_B := \frac{1}{m_B}[n_1a_1 + \cdots + n_Aa_A - m_1b_1 - \cdots - m_{B-1}b_{B-1} + \lambda^0]. \tag{18}$$

[8]Choose these neighborhoods so that they are contained in the period parallelogram P, cf Fig. 11.

In this way $a_1,\cdots,a_A,b_1,\cdots,b_{B-1}$ are close to respectively $\mathbf{a_1},\cdots,\mathbf{a_A},\mathbf{b_1},\cdots,\mathbf{b_{B-1}}$ and b_B is close to $\mathbf{b_B}$. Finally, we put

$$b_B^{'} = n_1a_1 +\cdots+ n_Aa_A - m_1b_1\cdots- m_{B-1}b_{B-1} - (m_B-1)b_B \quad \text{(close to } \mathbf{b_B^{'}}\text{)}. \tag{19}$$

Perturbating $\mathbf{a_1},\cdots,\mathbf{a_A},\mathbf{b_1},\cdots,\mathbf{b_{B-1}}$ into respectively $a_1,\cdots,a_A,b_1,\cdots,b_{B-1}$, and putting $\check{a} = (a_1,\cdots,a_A),\check{b} = (b_1,\cdots,b_{B-1})$, we consider functions[9] $\mathbf{f}(z;\check{a},\check{b})$ on the product space $\mathbb{C}\times U_1\times\cdots U_A\times W_1\times\cdots W_{B-1}$ given by: (compare (16))

$$\mathbf{f}(z;\check{a},\check{b}) = \frac{\sigma^{n_1}(z-a_1)\cdots\sigma^{n_A}(z-a_A)}{\sigma^{m_1}(z-b_1)\cdots\sigma^{m_B-1}(z-b_B(\check{a},\check{b}))\sigma(z-b_B^{'}(\check{a},\check{b}))}. \tag{20}$$

Then, for each $(\check{a},\check{b})$ in $U_1\times\cdots U_A\times W_1\times\cdots W_{B-1}$, the function $f|_{\check{a},\check{b}}(\cdot) := \mathbf{f}(\cdot;\check{a},\check{b})$ is elliptic in z, of order r. The points $a_1,\cdots,a_A$, resp. $b_1,\cdots,b_B$ are the zeros and poles for $f|_{\check{a},\check{b}}$ on P (of multiplicity $n_1,\cdots,n_A$, resp. $m_1,\cdots,m_B$). Moreover, $f|_{\check{a},\check{b}}$ has $K(=A+B)$ critical points on P (counted by multiplicity). Note that the Newton flow $\overline{\overline{\mathcal{N}}}(f|_{\check{a},\check{b}})$ on T is represented by the pair $(\check{a},\check{b})$ in $U_1\times\cdots U_A\times W_1\times\cdots W_{B-1}$, i.e. by

$$\begin{array}{cccccc} a_1, & \cdots, & a_A; & b_1, & \cdots, & b_{B-1}, \\ \uparrow & & \uparrow & \uparrow & & \uparrow \\ 1\times & & 1\times & 1\times & & 1\times \end{array} \qquad \begin{array}{l}\text{arbitrarily chosen in suitably small} \\ \text{neighbourhoods } U_1\times\cdots U_A\times W_1\times\cdots W_{B-1}\end{array}$$

but also by the pair (a,b) in the quotient space $V_r(\Lambda)/\approx$ as introduced in Section 4, i.e. by

$$\begin{array}{cccccccc} (([a_1], & \cdots, & [a_A]), & ([b_1], & \cdots, & [b_B])), \\ \uparrow & & \uparrow & \uparrow & & \uparrow \\ n_1\times & & n_A\times & m_1\times & & m_B\times \end{array} \qquad \text{that fulfil condition (10)}$$

Apparently, we have:

- If $(\check{a},\check{b}) = (\check{\mathbf{a}},\check{\mathbf{b}})$, then $f|_{\check{\mathbf{a}},\check{\mathbf{b}}}(z) = f(z)$ and thus $\overline{\overline{\mathcal{N}}}(f|_{\check{\mathbf{a}},\check{\mathbf{b}}}) = \overline{\overline{\mathcal{N}}}(f)$;
- If $A = B = r$ (thus $K = 2r$), then

$$\begin{array}{l}(\check{a},\check{b}) = (a_1,\cdots,a_r;b_1,\cdots,b_{r-1}) \in U_1\times\cdots U_r\times W_1\times\cdots W_{r-1}, \text{ and} \\ (a,b) = (([a_1],\cdots,[a_r]),([b_1],\cdots,[b_r])) + \text{ condition (10)}\end{array}$$

Now we have the following useful lemma:

Lemma 5.7. *Let $K(=A+B)>2$. Then:*
Under suitably chosen -but arbitrarily small- perturbations of the zeros and poles for f, thereby preserving the multiplicities of these zeros and poles, the Newton flow $\overline{\overline{\mathcal{N}}}(f))$ turns into a flow $\overline{\overline{\mathcal{N}}}(f|_{\check{a},\check{b}})$ with only (K different)1-fold saddles.

Proof. We consider $\hat{w}(z;\check{a},\check{b}) := -\log\mathbf{f}(z;\check{a},\check{b})$ and write:

$$\frac{\partial\hat{w}}{\partial z} = \hat{w}^{'}(z;\check{a},\check{b});\ \frac{\partial^2\hat{w}}{\partial^2 z} = \hat{w}^{''}(z;\check{a},\check{b}).$$

[9]Note that, when perturbing $(\mathbf{a},\mathbf{b})$ in the indicated way, the winding numbers $\eta(\mathbf{f}_{(\cdot,a,b)}(\gamma_1))$, $\eta(\mathbf{f}_{(\cdot,a,b)}(\gamma_2))$, and thus also λ^0, remain unchanged.

These are meromorphic functions in each of the variables $z, a_1, \cdots, a_A, b_1, \cdots, b_{B-1}$.
Define:

$$\Sigma = \{(z;\check{a},\check{b}) \mid \hat{w}'(z;\check{a},\check{b}) = 0\} \qquad \text{"critical set"}$$
$$\Sigma_{nd} = \{(z;\check{a},\check{b}) \mid \hat{w}'(z;\check{a},\check{b}) = 0, \hat{w}''(z;\check{a},\check{b}) \neq 0\} \qquad \text{"non-degenerate critical set"}$$
$$\Sigma_d = \{(z;\check{a},\check{b}) \mid \hat{w}'(z;\check{a},\check{b}) = 0, \hat{w}''(z;\check{a},\check{b}) = 0\} \qquad \text{"degenerate critical set"}$$

Since the $a_i, i = 1, \cdots, A$, and $b_j, j = 1, \cdots, B$, are poles for $\hat{w}'(\cdot;\check{a},\check{b})$ as an elliptic function in z, we have: If $(z;\check{a},\check{b}) \in \Sigma$, then:

$$\begin{cases} z \neq a_i \bmod \Lambda, z \neq b_j \bmod \Lambda, z \neq b_B' \bmod \Lambda, \text{ and (by construction)} \\ a_{i_1} \neq a_{i_2} \bmod \Lambda, i_1 \neq i_2, i_1, i_2 = 1, \cdots, A; b_{j_1} \neq b_{j_2} \bmod \Lambda, j_1 \neq j_2, j_1, j_2 = 1, \cdots, B-1. \end{cases}$$

The subset $\mathcal{V}$ of elements $(z;\check{a},\check{b}) \in \mathbb{C} \times U_1 \times \cdots U_A \times W_1 \times \cdots W_{B-1}$ that fulfills these inequalities is open in $\mathbb{C} \times \mathbb{C}^A \times \mathbb{C}^{B-1}$. On this set $\mathcal{V}$ (that contains the critical set Σ), the function $\hat{w}'$ is analytic in each of its variables. (Thus Σ is a closed subset of $\mathcal{V}$). For the partial derivatives of $\hat{w}'$ on $\mathcal{V}$ we find: (use (14), (20), compare also (17) and Footnote 9)

$$\frac{\partial \hat{w}'}{\partial z} : n_1 \wp(z - a_1) + \cdots + n_A \wp(z - a_A) - m_1 \wp(z - b_1) - \cdots - m_B \wp(z - b_B)$$
$$\frac{\partial \hat{w}'}{\partial a_i} : \frac{\partial}{\partial a_i}[-n_1 \zeta(z - a_1) \cdots - n_A \zeta(z - a_A) + m_1 \zeta(z - b_1) \cdots + (m_B - 1)\zeta(z - b_B) + \zeta(z - b_B')]$$
$$= [\text{ using the formulas (18) and (19)}]$$
$$= [-n_i \wp(z - a_i) + (m_B - 1)[\frac{n_i}{m_B}]\wp(z - b_B) + (n_i - (m_B - 1)[\frac{n_i}{m_B}])\wp(z - b_B')]$$
$$= -n_i(\wp(z - a_i) - \wp(z - b_B)) \qquad (i = 1, \cdots, A)$$

In a similar way:

$$\frac{\partial \hat{w}'}{\partial b_j} : m_j(\wp(z - b_i) - \wp(z - b_B)) \quad (j = 1, \cdots, B - 1)$$
$$[\frac{\partial \hat{w}'}{\partial b_B} = 0 \quad (m_B = 1, 2, \cdots)]$$

By the Addition Theorem of the $\wp$-function [cf. [28]], we have:

$$\frac{\partial \hat{w}'}{\partial a_i} : -\frac{\sigma(a_i - b_B)\sigma(2z - a_i - b_B)}{\sigma^2(z - a_i)\sigma^2(z - b_B)}, i = 1, \cdots, A$$

So, let $(z;\check{a},\check{b})$ in $\mathcal{V}$, then

$$\frac{\partial \hat{w}'}{\partial a_i}|_{(z;\check{a},\check{b})} = 0, \text{ some } i \in \{1, \cdots, A\} \Leftrightarrow$$

$$\begin{cases} a_i = b_B \bmod \Lambda, & [\text{in contradiction with "}a_i, b_B \text{ different"}] \\ \text{ or} & \\ 2z = a_i + b_B \bmod \Lambda & [\text{ if } 2z = a_{i_1} + b_B \bmod \Lambda, 2z = a_{i_2} + b_B \bmod \Lambda, i_1 \neq i_2, \\ & \text{then } a_{i_1} = a_{i_2}; \text{ in contradiction with "}a_{i_1}, a_{i_2} \text{ different"}] \end{cases}$$

From this follows:

If $(z;\breve{a},\breve{b}) \in \mathcal{V}$, then at most one of $\frac{\partial \hat{w}^{'}}{\partial a_i}|_{(z;\breve{a},\breve{b})}, i = 1,\cdots,A$, vanishes. By a similar reasoning, we even may conclude:

$$\begin{cases} \text{At most one of the partial derivatives} \\ \frac{\partial \hat{w}^{'}}{\partial a_i}(z;\breve{a},\breve{b}), \frac{\partial \hat{w}^{'}}{\partial b_j}(z;\breve{a},\breve{b}), (z;\breve{a},\breve{b}) \in \mathcal{V}, i = 1,\cdots,A, j = 1,\cdots,B-1, \\ \text{vanishes, and thus, } \mathbf{in\ case\ K > 2:} \\ \frac{\partial \hat{w}^{'}}{\partial a_i}(z;\breve{a},\breve{b}) \neq 0, \frac{\partial \hat{w}^{'}}{\partial b_j}(z;\breve{a},\breve{b}) \neq 0, \\ \text{for at least one } i \in \{1,\cdots,A\} \text{ or } j \in \{1,\cdots,B-1.\} \end{cases} \tag{21}$$

The latter conclusion cannot be drawn in case $K = 2$; however, see the forthcoming Remark 5.8. Note that always $K \geq 2$.

Under the assumption that $K > 2$: let $\mathbf{z_1}, \mathbf{z_2},\cdots,\mathbf{z_L}$ be the different critical points for $f = (\mathbf{f}(\cdot,\breve{\mathbf{a}},\breve{\mathbf{b}}))$ with multiplicities $K_1,\cdots,K_L, K_1 \geq \cdots \geq K_L \geq 1, K_1 + \cdots + K_L = K$. If $(\breve{a},\breve{b})$ tends to $(\breve{\mathbf{a}},\breve{\mathbf{b}})$, then K_l of the K critical points for $\mathbf{f}(\cdot,\breve{a},\breve{b})$(counted by multiplicity) tend to the K_l-fold saddle $\mathbf{z_l}$ for $\overline{\overline{\mathcal{N}}}(f)$). It follows that, if $(\breve{a},\breve{b})$ is sufficiently close to $(\breve{\mathbf{a}},\breve{\mathbf{b}})$, then K_l critical points for $\mathbf{f}(\cdot,\breve{a},\breve{b})$(counted by multiplicity) are situated in, suitably small, disjunct neighborhoods, say V_l, around $\mathbf{z_l}, l = 1,\cdots,L$. We choose $(\breve{a},\breve{b})$ so close to $(\breve{\mathbf{a}},\breve{\mathbf{b}})$ that this condition holds. If all the critical points for f, i.e. the saddles of $\overline{\overline{\mathcal{N}}}(f)$), are simple, there is nothing to prove. So, let $K_1 > 1$, thus $\hat{w}^{''}(\mathbf{z_1};\breve{\mathbf{a}},\breve{\mathbf{b}}) = 0$, i.e. $(\mathbf{z_1};\breve{\mathbf{a}},\breve{\mathbf{b}}) \in \Sigma_d \subset \Sigma$. Without loss of generality, we assume (see (21)) that $\frac{\partial \hat{w}^{'}}{\partial a_i}(\mathbf{z_1};\breve{\mathbf{a}},\breve{\mathbf{b}}) \neq 0$. According to the Implicit Function Theorem a local parametrization of Σ around $(\mathbf{z_1};\breve{\mathbf{a}},\breve{\mathbf{b}})$ exists, given by:

$$(z; a_1(z, a_2,\cdots,a_A, b_1,\cdots,b_{B-1}), a_2,\cdots,a_A, b_1,\cdots,b_{B-1}),$$

where $a_1(\mathbf{z_1},\mathbf{a_2},\cdots,\mathbf{a_A},\mathbf{b_1},\cdots,\mathbf{b_{B-1}}) = \mathbf{a_1}$. Thus, at $(\mathbf{z_1};\breve{\mathbf{a}},\breve{\mathbf{b}})$ we have:

$$\hat{w}^{''} + [\frac{\partial \hat{w}^{'}}{\partial a_1}][\frac{\partial a_1}{\partial z}(z, a_2,\cdots)] = 0.$$

Since $\hat{w}^{''}(\mathbf{z_1};\breve{\mathbf{a}},\breve{\mathbf{b}}) = 0$ and $\frac{\partial \hat{w}^{'}}{\partial a_i}(\mathbf{z_1};\breve{\mathbf{a}},\breve{\mathbf{b}}) \neq 0$, it follows that

$$\frac{\partial a_1}{\partial z}(\mathbf{z_1},\breve{\mathbf{a}},\breve{\mathbf{b}}) = 0$$

Note that $a_1(z, a_2,\cdots,a_A, b_1,\cdots,b_{B-1})$, depends complex differentiable on z. So the zeros for $\frac{\partial a_1}{\partial z}(z; a_2,\cdots,a_A, b_1,\cdots,b_{B-1})$ are *isolated*. Thus, on a *reduced* neighborhood of $(\mathbf{z_1},\breve{\mathbf{a}},\breve{\mathbf{b}})$, say $\hat{U}$, neither $\frac{\partial a_1}{\partial z}(\cdot)$ nor $\frac{\partial \hat{w}^{'}}{\partial a_1}$ vanish. If z tends to $\mathbf{z_1}$, then:

$$(z; a_1(z, \mathbf{a_2},\cdots,\mathbf{a_A},\mathbf{b_1},\cdots,\mathbf{b_{B-1}}), \mathbf{a_2},\cdots,\mathbf{a_A},\mathbf{b_1},\cdots,\mathbf{b_{B-1}})$$

tends to $(\mathbf{z_1},\breve{\mathbf{a}},\breve{\mathbf{b}})$ along Σ, and we cross $\hat{U}$, meeting elements $(z,\breve{a},\breve{b}) \in \Sigma$, such that

$$\begin{cases} \hat{w}^{''}(z,\breve{a},\breve{b}) + \frac{\partial \hat{w}^{'}}{\partial a_1}(z,\breve{a},\breve{b})\frac{\partial a_1}{\partial z}(z,\breve{a},\breve{b}) = 0 \\ \frac{\partial \hat{w}^{'}}{\partial a_1}(z,\breve{a},\breve{b}) \neq 0, \frac{\partial a_1}{\partial z}(z,\breve{a},\breve{b}) \neq 0 \end{cases}$$

Thus,

$$\hat{w}^{''}(z,\breve{a},\breve{b}) \neq 0.$$

Hence, we have: $(z,\breve{a},\breve{b}) \in \Sigma_{nd}$. So, the K_1 critical points for $\mathbf{f}(\cdot;\breve{a},\breve{b})$ that approach $\mathbf{z_1}$ via the curve

$$(z; a_1(z, \mathbf{a_2},\cdots,\mathbf{a_A},\mathbf{b_1},\cdots,\mathbf{b_{B-1}}), \mathbf{a_2},\cdots,\mathbf{a_A},\mathbf{b_1},\cdots,\mathbf{b_{B-1}})$$

are all simple, whereas the critical points for $\mathbf{f}(\cdot, \check{a}, \check{b})$ approaching $\mathbf{z_2}, \cdots, \mathbf{z_L}$ are still situated in respectively $V_2, \cdots, V_L$. If $K_2 > 1$, we repeat the above procedure with respect to $\mathbf{z_2}$, etc. In finitely many steps we arrive at a flow $\overline{\overline{\mathcal{N}}}(\mathbf{f}|_{\check{a},\check{b}})$ with only simple saddles and $(\check{a}, \check{b})$ arbitrary close to $(\check{\mathbf{a}}, \check{\mathbf{b}})$. □

Remark 5.8. The case $A = B = 1$(i.e. $K = 2$).
If $K = 2$, then the function f has -on T- only one zero and one pole, both of order r; the corresponding flow $\overline{\overline{\mathcal{N}}}(f)$) is referred to as to a *nuclear* Newton flow. In this case, the assertion of Lemma 5.7 is also true. In fact, even a stronger result holds:

> " All nuclear Newton flows -of any order r- are conjugate , in particular each of them has precisely two saddles (simple) and there are no saddle connections".

Nuclear Newton flows will play an important role in the sequel, but we postpone the discussion on this subject untill Section 11.

We end up by presenting the (already announced) proof of Theorem 5.6

Proof of Theorem 5.6:

The "density part" of Assertion 1: Let $\mathcal{O}$ be an arbitrarily small τ_0-neighbourhood of a function f as in Lemma 5.7. We split up each of the A different zeros for f and the B different poles for f into n_i resp. m_j mutually different points, contained in disjoint neighbourhoods U_i resp. $W_j, i = 1, \cdots, A, j = 1, \cdots, B$(compare Fig.11). In this way, we obtain $2r$ different points, giving rize to an elliptic function of the the form (11), with these points as the r simple zeros resp. r simple poles in P. We may assume that this function is still situated in $\mathcal{O}$, see the introduction of the topology τ_0 in Section 4. Now, we apply Lemma 5.7 (case $A = B = r, K = 2r$) and find in $\mathcal{O}$ an elliptic function, of order r with only simple zeros, poles and critical points. This function is non-degenerate if the corresponding Newton flow does not exhibit trajectories that connect two of its critical points. If this is the case, none of the straight lines connecting two critical values for our function, passes through the point $0 \in \mathbb{C}$. If not, then adding an arbitrarily small constant $c \in \mathbb{C}$ to f does not affect the position of its critical points, and yields a function -still in[10] $\mathcal{O}$- with only simple zeros and poles. By choosing c suitably, we find a function, renamed f, such that none of the straight lines connecting critical values (for different critical points) contains $0 \in \mathbb{C}$. So, we have: $f \in \tilde{E}_r$, i.e., $\tilde{E}_r$ is dense in E_r.

The "if part" of Assertion 2: Let $f \in \tilde{E}_r$. Then all equilibria for $\overline{\overline{\mathcal{N}}}(f)$ are simple, and thus hyperbolic (cf. Remarks 1.1 and 3.4). Moreover, there are neither saddle-connections nor closed orbits (compare (4)). Now, the Baggis-Peixoto Theorem for structurally stable C^1-vector fields on compact 2-dimensional manifolds (cf. [32]) yields that $\overline{\overline{\mathcal{N}}}(f)$ is C^1-structurally stable, and by Corollary 5.4 also τ_0-structural stable.

The "only if part" of Assertion 2: Suppose that $f \notin \tilde{E}_r$, but $\overline{\overline{\mathcal{N}}}(f)$ in $\tilde{N}_r$. Then there is a τ_0-neighbourhood of f, say $\mathcal{O}$, such that for all $g \in \mathcal{O}$: $\overline{\overline{\mathcal{N}}}(f) \sim \overline{\overline{\mathcal{N}}}(g)$. Since $\tilde{E}_r$ is dense in E_r(already proved), we may assume that $g \in \tilde{E}_r$. So, $\overline{\overline{\mathcal{N}}}(g)$ has precisely r hyperbolic attractors/repellors and does not admit "saddle connections". This must also be true for $\overline{\overline{\mathcal{N}}}(f)$, in contradiction with $f \notin \tilde{E}_r$.

The "openess part" of Assertion 1: This a direct consequence of the Assertion 2 (which is already proved).

[10] Note that at simple zeros an analytic function is conformal. In case of a pole, use also (6).

6 Structural stable elliptic Newton flows: Classification

Throughout this section, let f be a non-degenerate elliptic function of order r. Thus the flow $\overline{\overline{\mathcal{N}}}(f)$ is structurally stable.
Now, the following definition makes sense (compare Definition 5.5 and Lemma 3.3)

Definition 6.1. The graph $\mathcal{G}(f)$, $f \in \tilde{E}_r$, on the torus T is given by:

- Vertices are the r zeros for f on T (as attractors for $\overline{\overline{\mathcal{N}}}(f)$).
- Edges are the $2r$ unstable manifolds at the critical points for f on T as $\overline{\overline{\mathcal{N}}}(f)$-saddles.

Note that the faces of $\mathcal{G}(f)$ are precisely the r *basins of repulsion* of the poles, say $[b_j], j = 1,\cdots,r$ for f on T (as repellors for $\overline{\overline{\mathcal{N}}}(f)$) and will be denoted by $F_{b_j}(f)$; their boundaries by $\partial F_{b_j}(f)$. These boundaries , consisting of *unstable manifolds* at saddles for $\overline{\overline{\mathcal{N}}}(f)$, are subgraphs of $\mathcal{G}(f)$.

Analogously, we define the graph[11], say $\mathcal{G}^*(f)$, on the poles and the stable $\overline{\overline{\mathcal{N}}}(f)$-manifolds at the critical points for f on T.

Lemma 6.2. *Both $\mathcal{G}(f)$ and $\mathcal{G}^*(f)$ are multigraphs[12] embedded in T.*

Proof. If $\mathcal{G}(f)$ would have a loop, the two unstable $\overline{\overline{\mathcal{N}}}(f)$-separatrices at some critical point for f would approach the same zero, say $[a]$, on T. In that case, the zeros (simple!) for f in the plane, corresponding to $[a]$, will then be approached by two *different* trajectories (of the planar version $\overline{\mathcal{N}}(f)$) with the same value of $\arg f$. This is impossible (cf. the Comment on Fig.2). The second part of the assertion follows by interchanging the roles of the poles and zeros for f. □

Corollary 6.3. *An edge in $\mathcal{G}(f)$ or $\mathcal{G}^*(f)$ is contained in the boundaries of two different faces.*

Next we introduce a graph on T, denoted $\mathcal{G}(f) \wedge \mathcal{G}^*(f)$, which may be considered as the "common refinement of $\mathcal{G}(f)$) and $\mathcal{G}^*(f)$":

Definition 6.4. The *vertices* of $\mathcal{G}(f) \wedge \mathcal{G}^*(f)$ are defined as the zeros, poles and critical points for f, whereas the *edges* are the stable and unstable separatrices of $\overline{\overline{\mathcal{N}}}(f)$ at the critical points for f.

The faces of $\mathcal{G}(f) \wedge \mathcal{G}^*(f)$ are the so-called *canonical regions* for $\overline{\overline{\mathcal{N}}}(f)$, i.e. the connected components of what is left after deleting from T all the $\overline{\overline{\mathcal{N}}}(f)$-equilibria and all stable and unstable manifolds at the saddles of $\overline{\overline{\mathcal{N}}}(f)$. A priori, the canonical regions of a C^1-structurally stable flow on T(without closed orbits) are of one of the Types 1,2,3 in Fig. 12 (cf. [33]). However, by Lemma 6.2 the flow $\overline{\overline{\mathcal{N}}}(f)$- although structurally stable - cannot admit canonical regions of Types 2 and 3.

So. we only have to deal with canonical regions of Type 1. Since all zeros, poles and critical points for f are simple, we find: (see (5) and the Comment on Fig. 2)

Lemma 6.5. *In a canonical region of $\overline{\overline{\mathcal{N}}}(f)$, the angles (anti-clockwise measured) at the pole and the zero are well-defined, strictly positive and equal.*

[11] $\mathcal{G}(f)$ and $\mathcal{G}^*(f)$ are *geometrical duals*; see also Section 7.

[12] i.e., multiple edges are allowed, but no loops (cf. [16]); note however that the concept of multigraph in ([31]) includes loops.

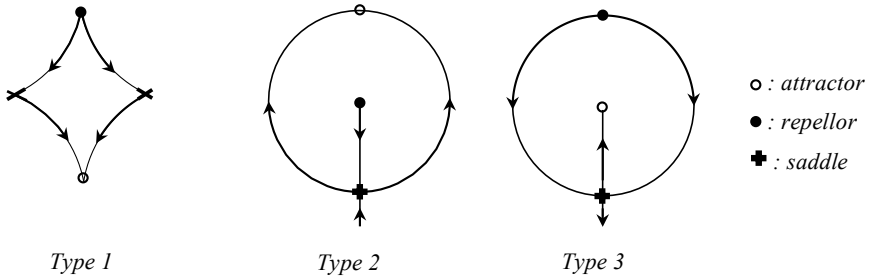

Figure 12: The canonical regions of a structural stable flow on T

Since a face $F_{b_j}(f)$ is built up from all canonical regions that have $[b_j]$ in common, we find:

Corollary 6.6. *All (anti-clockwise measured) angles spanning a sector of $F_{b_j}(f)$ at the vertices in its boundary, are non-vanishing and sum up to 2π.*

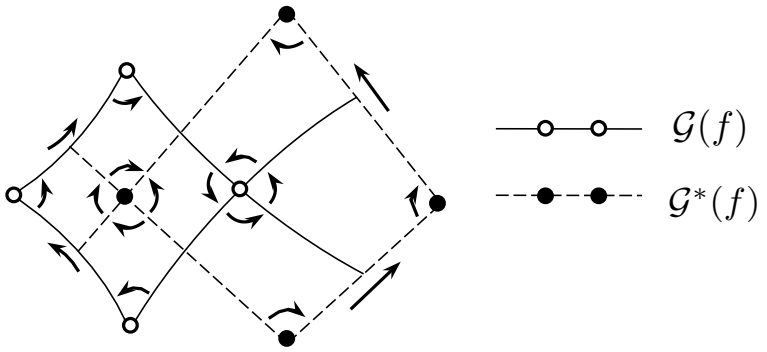

Figure 13: Oriented facial walks on $\mathcal{G}(f)$ and $\mathcal{G}^*(f)$.

Lemma 6.7. *Each subgraph $\partial F_{b_j}(f)$ is Eulerian*[13].

Proof. Traverse the set of all canonical regions centered at $[b_j]$ once. In this way we determine a closed walk, say w_{b_j}, through all the vertices and edges of $\partial F_{b_j}(f)$; see Fig. 13. By Corollary 6.3, this walk contains each edge of $\partial F_{b_j}(f)$ only once (since otherwise the two stable separatrices at the saddle on such an edge must originate from $[b_j]$). So, w_{b_j} is the desired Euler trail. □

The walk w_{b_j} in the above proof will be referred to as to the *facial walk* for $\partial F_{b_j}(f)$. Analogously, we define the (Eulerian!) facial walks on the boundaries of the $\mathcal{G}^*(f)$-faces(i.e., the *basins of attraction* of the zeros, say $[a_i], i = 1, \cdots, r$, for f on T (as attractors for $\overline{\overline{\mathcal{N}}}(f)$).

Remark 6.8. Note that in these facial walks the same vertex may occur more than once. However, by Lemma 6.2, a vertex in a facial walk cannot be adjacent to itself.

[13] i.e. the graph $\partial F_{b_j}(f)$ admits a so-called *Euler trail*: a closed walk that traverses each edge exactly once and goes through all vertices. We do not distinguish between an Euler trail and its cyclic shift

We endow (the faces of) $\mathcal{G}(f)$ with a coherent orientation as follows:
For each facial walk we demand that the (constant) values of $\arg f(z)$ on consecutive edges form an increasing sequence. This is imposed by the anti-clockwise ordering of the $\mathcal{G}(f)$-edges around a common vertex, which on its turn induces clockwise orientations of the $\mathcal{G}^*(f)$-edges incident to a given vertex. This leads to an orientation of (the facial walks on) $\mathcal{G}^*(f)$ which is opposite to the orientation of $\mathcal{G}(f)$ as chosen before; see Fig.13. From now, on we assume that all graphs $\mathcal{G}(f)$ and $\mathcal{G}^*(f), f \in \tilde{E}_r$, are oriented in this way: $\mathcal{G}(f)$ always clockwise; $\mathcal{G}^*(f)$ always anti-clockwise.

Lemma 6.9. *The (multi)graphs $\mathcal{G}(f)$ and $\mathcal{G}^*(f)$ are connected and cellularly embedded*[14].

Proof. We focus on $\mathcal{G}(f)$ and follow the treatise [31] closely. Consider the r facial walks w_{b_j} , and put $l_j =$ length w_{b_j}. Consider for each w_{b_j} a so-called *facial polygon*, i.e. a polygon in the plane with l_j sides labelled by the edges of $\partial F_{b_j}(f)$(taking the orientation of w_{b_j} into account) , so that each polygon is disjoint from the other polygons. Now we take all facial polygons. Each $\mathcal{G}(f)$-edge occurs precisely once in two different facial walks and this determines orientations of the sides of the polygons. By identifying each side with its mate, we construct (cf. [31]) an orientable, connected surface S , homeomorphic to T, and -in S- a 2-cell embedded graph, which is -up to an homeomorphism-equal to $\mathcal{G}(f)$. In particular, the graph $\mathcal{G}(f)$ is connected and orientable as well. Finally, we note that a 2-cell embedding is always cellular (cf. [31]). □

The *abstract directed graph*, underlying $\mathcal{G}(f) \wedge \mathcal{G}^*(f)$, will be denoted by $\mathbb{P}(f)$, where the directions are induced by the orientations of the (un)stable separatrices at $\overline{\overline{\mathcal{N}}}(f)$-saddles. Each canonical region is represented by a quadruple of directed edges in $\mathbb{P}(f)$, and is associated with precisely one pole, one zero (in opposite position) and two critical points for f on T. Following Peixoto ([32], [33]), such a quadruple is called a *distinguished set* (of Type 1). The graph $\mathbb{P}(f)$), together with the collection of all distinguished sets is denoted by $\mathbb{P}^d(f)$. We say "$\mathbb{P}^d(f)$ is realized by the distinguished graph of $\overline{\overline{\mathcal{N}}}(f)$ on T".

We need a classical result due to Peixoto (cf. [33]) on structurally, C^1-stable vector fields on 2-dimensional compact manifolds. In the context of our elliptic Newton flows this yields (together with Corollary 5.4): if $f, h \in \tilde{E}_r$, then:

$$\overline{\overline{\mathcal{N}}}(f) \sim \overline{\overline{\mathcal{N}}}(h) \quad \Leftrightarrow \quad \mathbb{P}^d(f) \sim \mathbb{P}^d(h). \tag{22}$$

Here, $\sim$ in the l.h.s stands for "conjugacy" and $\sim$ in the r.h.s. for *isomorphism between* $\mathbb{P}^d(f)$ and $\mathbb{P}^d(h)$ (as directed abstract graphs) , preserving the distinguished sets and respecting the cyclic ordering (induced by the embedding in T) of the distinguished sets around a common vertex.

Lemma 6.10. *Let $\overline{\overline{\mathcal{N}}}(f)$ and $\overline{\overline{\mathcal{N}}}(h)$ be structurally stable (thus $f, h \in \tilde{E}_r$), then:*

$$\overline{\overline{\mathcal{N}}}(f) \sim \overline{\overline{\mathcal{N}}}(h) \Leftrightarrow \mathcal{G}(f) \sim \mathcal{G}(h) (\textit{and thus also } \mathcal{G}^*(f) \sim \mathcal{G}^*(h)),$$

where $\sim$ in the r.h.s. stands for equivalency between the graphs (i.e., an isomorphism respecting their orientations).

Proof. Apply (22) to $\overline{\overline{\mathcal{N}}}(f)$ and $\overline{\overline{\mathcal{N}}}(h)$. □

[14] i.e. each face is homeomorphic to an *open* disk in $\mathbb{R}^2$.

Graph $\mathcal{G}(\frac{1}{f})$ is also well-defined (with as faces $F_{a_i}(\frac{1}{f})$) and associated with the structurally stable flow $\overline{\overline{\mathcal{N}}}(\frac{1}{f})$ $(=-\overline{\overline{\mathcal{N}}}(f))$.
$\overline{\overline{\mathcal{N}}}(\frac{1}{f})$ is the dual version of $\overline{\overline{\mathcal{N}}}(f)$, i.e., $\overline{\overline{\mathcal{N}}}(\frac{1}{f})$ is obtained from $\overline{\overline{\mathcal{N}}}(f)$ by reversing the orientations of the trajectories of the latter flow, thereby changing repellers into attractors and vice versa.
Clearly, $\mathcal{G}(\frac{1}{f})$ and $\mathcal{G}^*(f)$ coincide, be it with opposite orientations, i.e., $\mathcal{G}(\frac{1}{f}) = -\mathcal{G}^*(f)$, where, due to our convention on orientations, $\mathcal{G}(\frac{1}{f})$ is clockwise oriented.
Similarly: $\mathcal{G}(f) = -\mathcal{G}^*(\frac{1}{f})$. Note that, in general, $\overline{\overline{\mathcal{N}}}(f)$ and $\overline{\overline{\mathcal{N}}}(\frac{1}{f})$ are *not* conjugate. In the special case where $\overline{\overline{\mathcal{N}}}(f) \sim \overline{\overline{\mathcal{N}}}(\frac{1}{f})$ we call $\overline{\overline{\mathcal{N}}}(f)$ *self dual*, and we have:

$$\overline{\overline{\mathcal{N}}}(f) \sim \overline{\overline{\mathcal{N}}}(\frac{1}{f}) \Leftrightarrow \mathcal{G}(f) \sim \mathcal{G}(\frac{1}{f}) \text{ (thus also } \mathcal{G}^*(f) \sim \mathcal{G}^*(\frac{1}{f})).$$

Given an arbitrary pair of functions $f, h \in \tilde{E}_r$, we consider the two pairs of graphs $(\mathcal{G}(f), \mathcal{G}^*(f))$ and $(\mathcal{G}(h), \mathcal{G}^*(h))$. Concerning the equivalency $\sim$ between these graphs there are *precisely* two -a priori- different combinations possible:

1. $\mathcal{G}(f) \sim \mathcal{G}(h)$, and thus also $\mathcal{G}^*(f) \sim \mathcal{G}^*(h)$.
2. $\mathcal{G}(f) \sim -\mathcal{G}^*(h)$, and thus also $-\mathcal{G}^*(f) \sim \mathcal{G}(h)$

Applying Lemma 6.10 and using $\mathcal{G}(f) = -\mathcal{G}^*(\frac{1}{f})$, $\mathcal{G}(h) = -\mathcal{G}^*(\frac{1}{h})$, we find:

In Case 1: $\overline{\overline{\mathcal{N}}}(f) \sim \overline{\overline{\mathcal{N}}}(h)$ and also $\overline{\overline{\mathcal{N}}}(\frac{1}{f}) \sim \overline{\overline{\mathcal{N}}}(\frac{1}{h})$.
In Case 2: $\overline{\overline{\mathcal{N}}}(f) \sim \overline{\overline{\mathcal{N}}}(\frac{1}{h})$ and also $\overline{\overline{\mathcal{N}}}(\frac{1}{f}) \sim \overline{\overline{\mathcal{N}}}(h)$.

We summarize the above observations as follows:

Theorem 6.11. (*Classification of structurally stable elliptic Newton flows by graphs.*)
For $f \in \tilde{E}_r$, the phase portrait of the flow $\overline{\overline{\mathcal{N}}}(f)$ is -up to conjugacy and duality- completely determined by the graph $\mathcal{G}(f)$ (and also by $\mathcal{G}^*(f)(= -\mathcal{G}(\frac{1}{f}))$).

Remark 6.12. (On self-duality)

$$\mathcal{G}(f) \sim \mathcal{G}(\frac{1}{f}) \wedge \mathcal{G}(f) \sim \mathcal{G}(h) \Leftrightarrow \mathcal{G}(f) \sim \mathcal{G}(\frac{1}{f}) \wedge \mathcal{G}(h) \sim \mathcal{G}(\frac{1}{h}) \Leftrightarrow \overline{\overline{\mathcal{N}}}(f) \sim \overline{\overline{\mathcal{N}}}(\frac{1}{f}) \sim \overline{\overline{\mathcal{N}}}(h) \sim \overline{\overline{\mathcal{N}}}(\frac{1}{h})$$

Corollary 6.13. *Any two structurally stable 2^{nd} order elliptic Newton flows are conjugate.*

Proof. Let $\overline{\overline{\mathcal{N}}}(f), f \in \tilde{E}_2$, be chosen arbitrarily. By Corollary 6.3, the two faces of $\mathcal{G}(f)$ share their boundaries. So, the common facial walk w_f of these faces is built up from the four $\mathcal{G}(f)$-edges and the two $\mathcal{G}(f)$-vertices (each appearing twice but not consecutive!). Hence, compare the construction in the proof of Lemma 6.9 and see Fig. 14, $\mathcal{G}(f)$ is determined by the *positively* oriented walk w_f. The same holds for any other flow $\overline{\overline{\mathcal{N}}}(h)$ with facial walk $w_h, h \in \tilde{E}_2$. Apparently, we have $w_f \sim w_h$ and thus $\mathcal{G}(f) \sim \mathcal{G}(h)$. In particular, put $h = \frac{1}{f}$, see again Fig.14, we find $\mathcal{G}(f) \sim \mathcal{G}(\frac{1}{f})$. Now, the assertion follows from Remark 6.12. □

Remark 6.14. For basically the same proof of Corollary 6.13 , see [10] and also Remark 9.3.

Remark 6.15. The flow $\overline{\overline{\mathcal{N}}}(\mathrm{sn})$, in the non-rectangular case (cf. Fig.9) exhibits an example of a 2^{nd} order structurally stable elliptic Newton flow. By Corollary 6.13, this is the only possibility (up to conjugacy) for a flow in $\tilde{N}_2$. Note that the flow in Fig.10 (rectangular case!) is not structurally stable (because of the saddle connections).

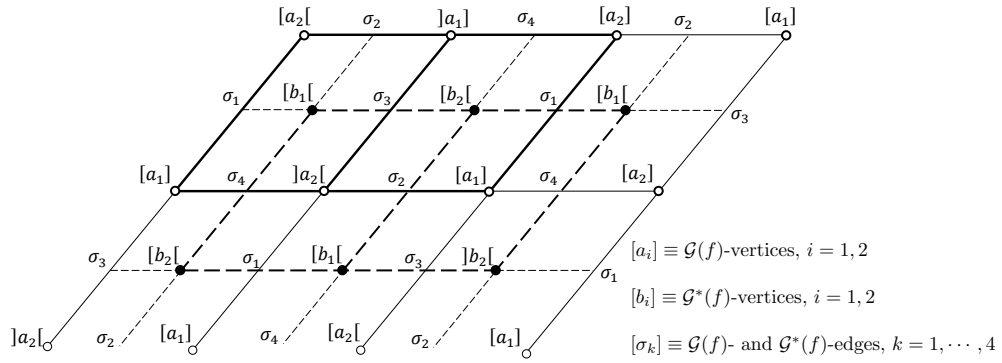

Figure 14: The graphs $\mathcal{G}(f)$ and $\mathcal{G}^*(f), f \in \tilde{E}_2$.

We proceed by introducing flows that are closely related to $\mathcal{N}(f)$, $\overline{\mathcal{N}}(f)$ and $\overline{\overline{\mathcal{N}}}(f)$: the so-called *rotated Newton flows*,

Definition 6.16. For $f \in E_r$, let $\mathcal{N}^\perp(f)$ be a dynamical system of the type

$$\frac{dz}{dt} = \frac{-if(z)}{f'(z)}.$$

Apparently, $\mathcal{N}^\perp(f)(= i\mathcal{N}(f))$ is a complex analytic vector field outside the set $C(f)$ of critical points for f. Proceeding as in Section 1 [in particular, the transition (2) $\rightarrow$ (3)], we turn $\mathcal{N}^\perp(f)$ into a smooth system on the whole plane, say $\overline{\mathcal{N}}^\perp(f)$, with -on $\mathbb{C}\backslash C(f)$- the same phase portrait as $\mathcal{N}^\perp(f)$. The function f, being elliptic, the system $\overline{\mathcal{N}}^\perp(f)$ can be interpreted as a smooth flow on T and as such it will be referred to as to $\overline{\overline{\mathcal{N}}}^\perp(f)$, in particular: (cf. Sections 3, 4)

$$\overline{\overline{\mathcal{N}}}^\perp(f) \text{ is smooth, and } \overline{\overline{\mathcal{N}}}^\perp(\frac{1}{f}) = -\overline{\overline{\mathcal{N}}}^\perp(f)$$

Lemma 6.17. *Let $z^\perp(t)$ be the (maximal) $\mathcal{N}^\perp(f)$-trajectory through a non-equilibrium $\check{z} = z^\perp(0)$, then:*

1. *$f(z^\perp(t)) = e^{-it} f(\check{z})$[thus $|f(z^\perp(t))| =$ constant $(\neq 0)$].*
2. *A zero or pole for f is a center for $\mathcal{N}^\perp(f)$[thus also for $\overline{\mathcal{N}}^\perp(f)$, $\overline{\overline{\mathcal{N}}}^\perp(f)$].*
3. *A k-fold critical point for f is a k-fold saddle for $\overline{\mathcal{N}}^\perp(f)$ [thus also for $\overline{\overline{\mathcal{N}}}^\perp(f)$].*

Proof. Assertions 1., 3. are proved as in Section 1. Note that outside $N(f) \cup P(f)$ the flow $\mathcal{N}^\perp(f)$ can be considered as the Newton flow for $h(z) = \exp(i \log(f(z)))$.
For Assertion 2. : let z_0 be a zero or pole for f with multiplicity k, thus an isolated zero for $\mathcal{N}^\perp(f)$. In a neighborhood of z_0, system $\mathcal{N}^\perp(f)$ is linearly approximated by:

$$\frac{dz}{dt} = \frac{-i(z - z_0)}{k}.$$

Thus z_0 is a non-degenerate equilibrium for $\mathcal{N}^\perp(f)$ with characteristic roots $\pm\frac{i}{k}$. By the first assertion in the lemma, a regular integral curve through a point $\check{z}$ close to z_0, but $\neq z_0$,

cannot end up at, or leave from z_0. Hence, this point is neither a focus, nor a centro-focus for $\mathcal{N}^{\perp}(f)$ (cf. [2]) and must be a center for $\mathcal{N}^{\perp}(f)$. □

In view of the above Assertion 1., a closed orbit for $\overline{\overline{\mathcal{N}}}^{\perp}(f)$ cannot be a limit cycle, and -by 2.- a separatrix $z^{\perp}(t)$ leaving a saddle σ_1, must approach a saddle σ_2. Moreover, this separatrix cannot connect σ_1 to itself (i.e. $\sigma_1 \neq \sigma_2$). In fact, let $\sigma_1 = \sigma_2$. This would lead to (cf. (5)):

$$\lim_{t\downarrow 0} \arg\, h(z^{\perp}(t)) = \arg\, h(\sigma_1) \text{ and also } \lim_{t\uparrow 0} \arg\, h(z^{\perp}(t)) = \arg\, h(\sigma_1),$$

which is impossible, see Fig. 15 and the Comment on Fig. 2.

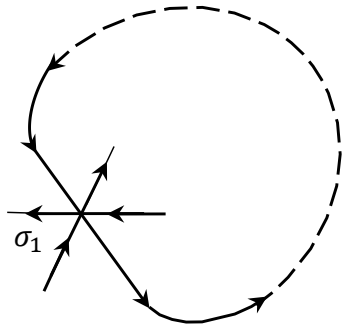

Figure 15: No "self-connected" $\overline{\overline{\mathcal{N}}}^{\perp}(h)$-saddles ; σ_1 is 2-fold.

Note that -when introducing rotated Newton flows- no restrictions were laid upon the function f. But now, we return to the case of non-degenerate functions f. Then $\overline{\overline{\mathcal{N}}}^{\perp}(f)$ has $2r$ simple saddles (corresponding to the critical points for f) with altogether $4r$ separatrices, connecting *different* saddles. So, we may introduce:

Definition 6.18. The graph $\mathcal{G}^{\perp}(f), f \in \check{E}_r$, on the torus T is given by:

- Vertices are the $2r$ critical points for f (as saddles for $\overline{\overline{\mathcal{N}}}^{\perp}(f)$) on T.
- Edges are the $4r$ separatrices at the critical points for f (as $\overline{\overline{\mathcal{N}}}^{\perp}(f)$-saddles) on T.

Since all zeros and poles for f are centers for $\overline{\overline{\mathcal{N}}}^{\perp}(f)$, each $\mathcal{G}^{\perp}(f)$-face contains only one zero or one pole for f. Moreover, the graph $\mathcal{G}^{\perp}(f)$ is cellularly embedded. Hence, the graph $\mathcal{G}^{\perp}(f)$ has $2r$ faces.

Let c be an arbitrary, strictly positive real number and put $L_c = \{z \mid |f(z)| = c\}$.

Lemma 6.19. *Then there holds:*

(1) The level set L_c is a regular curve in $\mathbb{R}^2$ (i.e., grad $|f(z)| \neq 0$ for all $z \in L_c$) if and only if L_c contains no critical points for f.

(2) The graph $\mathcal{G}^{\perp}(f), f \in \check{E}_r$, is connected. In particular, $f(z)$ admits the same absolute value at all critical points z.

Proof. (1): Use the Cauchy-Riemann equations.
(2): Apply Euler's theorem. □

We orient the edges of $\mathcal{G}^{\perp}(f)$ according to their orientation as $\overline{\overline{\mathcal{N}}}^{\perp}(f)$-trajectories. Let A_i and B_j be open subsets of $\mathbb{C}$, corresponding to the (open) faces of $\mathcal{G}^{\perp}(f)$ that are determined by the zero a_i, respectively the pole b_j, for f. Hence, the boundaries of A_i are anti-clockwise oriented, but those of B_j clockwise. Since $\overline{\overline{\mathcal{N}}}^{\perp}(\frac{1}{f}) = -\overline{\overline{\mathcal{N}}}^{\perp}(f)$ we have: reversing the orientations in $\mathcal{G}^{\perp}(f)$ turns this graph into $\mathcal{G}^{\perp}(\frac{1}{f})$ and thus, by Lemma 6.19 (2): $|f(z)| = 1$ on $\mathcal{G}^{\perp}(f)$. See Fig. 16 for (parts of) the graphs $\mathcal{G}^{\perp}(f)$, $\mathcal{G}(f)$, $\mathcal{G}^{*}(f)$ and $\mathcal{G}^{\perp}(\frac{1}{f})$, $\mathcal{G}(\frac{1}{f})$, $\mathcal{G}^{*}(\frac{1}{f})$. A canonical $\overline{\overline{\mathcal{N}}}(f)$region, with $[a_i]$,$[b_j]$ in opposite position, and the saddles σ, σ' consecutive w.r.t. the orientation of A_i(or B_j), will be denoted by $R_{ij}(\sigma, \sigma')$ and is contained in $F_{a_i}(\frac{1}{f}) \cap F_{b_j}(f)$. Note that, in general, this intersection contains more canonical regions of type $R_{ij}(\cdot, \cdot)$. But even so, these regions are separated by canonical regions, not of this type; compare Remark 6.8. In view of (5) and Lemmas 6.17 (1): Under f the net of $\overline{\overline{\mathcal{N}}}(f)$- and $\overline{\overline{\mathcal{N}}}(f)^{\perp}$-trajectories on $R_{ij}(\sigma, \sigma')$ is homeomorphically mapped onto a polar net in a sector of the $u + iv$-plane (u=Re(f), v=Im(f)), namely

$$s_{i,j}(\sigma, \sigma') = \{(u, v) \mid 0 < u^2 + v^2 < \infty, \arg f(\sigma) < \arctan(\frac{v}{u}) < \arg f(\sigma')\}.$$

Analogously, $\frac{1}{f}$ maps the net of $\overline{\overline{\mathcal{N}}}(f)$- and $\overline{\overline{\mathcal{N}}}(f)^{\perp}$-trajectories on $R_{ji}(\sigma, \sigma')$ onto a polar net in a sector of the $U + iV$-plane (U=Re($\frac{1}{f}$), V=Im($\frac{1}{f}$)), namely

$$S_{i,j}(\sigma, \sigma') = \{(U, V) \mid 0 < U^2 + V^2 < \infty, -\arg f(\sigma) < \arctan(\frac{V}{U}) < -\arg f(\sigma')\}.$$

So, the polar nets on $s_{i,j}(\sigma, \sigma')$ and $S_{i,j}(\sigma, \sigma')$ correspond under the inversion[15]:

$$U = \frac{u}{u^2 + v^2}, V = \frac{v}{u^2 + v^2}.$$

Next we turn to the relationship between Newton flows and steady streams.

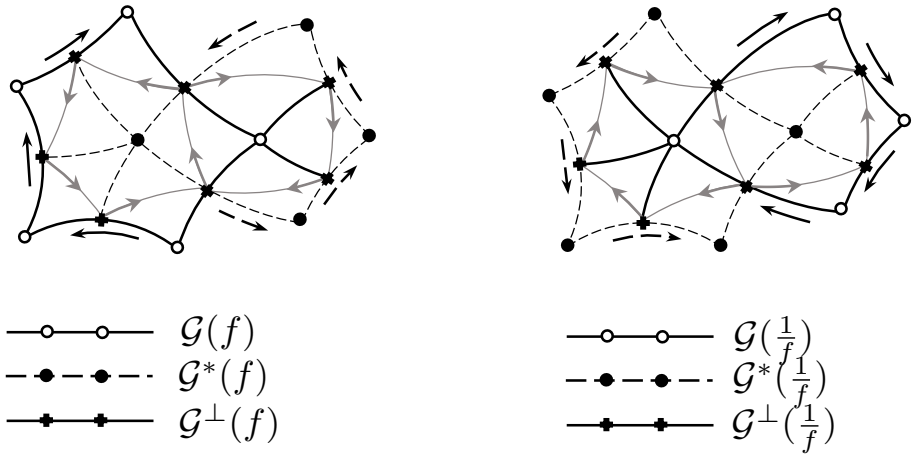

Figure 16: The graphs $\mathcal{G}(\cdot)$, $\mathcal{G}^{*}(\cdot)$ and $\mathcal{G}^{\perp}(\cdot)$ for f and $\frac{1}{f}$ in $\tilde{E}_r$.

[15] Here we use that in a canonical region the angles at the zero and the pole are equal.

Remark 6.20. *Newton flows as steady streams.*

For $f \in \check{E}_r$, we consider the planar *steady stream* ([27]) with complex potential $w(z) = -\log f(z)$, potential function $\Phi(x,y) = -\log|f(z)|$ and stream function $\psi(x,y) = -\arg f(z)$, where $x = \mathrm{Re}(z), y = \mathrm{Im}(z)$. Then the *equipotential lines* are given by $-\log|f(z)| =$ constant, the *stream lines* by $-\arg f(z) =$ constant and the *velocity field* $V(z)(= \mathrm{grad}\Phi)$ by the complex conjugate of $w'(z)$, i.e.

$$V(z) = \frac{|w'(z)|^2}{w'(z)} = \frac{-|w'(z)|^2 f(z)}{f'(z)} (= |w'(z)|^2 \mathcal{N}(f)).$$

Moreover, the zeros (poles) for f are just the sinks (sources) of strength 1, whereas the critical points for f are the 1-fold stagnation points of the stream, compare also Section 5. So, the "orthogonal net of the stream- and equipotential-lines" of the planar steady stream is a combination of the phase portraits of $\overline{\mathcal{N}}(f)$ and $\overline{\mathcal{N}}^{\perp}(f)$, see Fig. 17.

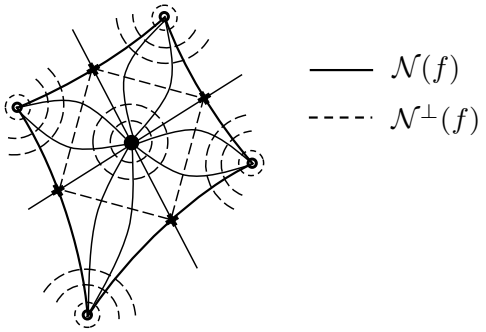

Figure 17: The steady stream $w(z) = -\log f(z), f \in \check{E}_r$.

Hence we may interprete the pair $(\overline{\overline{\mathcal{N}}}(f), \overline{\overline{\mathcal{N}}}^{\perp}(f))$ as a toroidal desingularized version of our planar steady stream. Finally, we clarify the "steady stream character" of the structurally stable elliptic Newton flows from the point of view of the Riemann surface T.
Firstly, we note that the polar net on open (!) sectors as $s_{i,j}(\sigma,\sigma')$ and $S_{i,j}(\sigma,\sigma')$ are just the stream and equipotential lines of the steady stream with complex potential $-\log(u+iv)$, resp. $-\log(U+iV)$. In particular , these stream and equipotential lines exhibit the phase portraits of resp. the flows $\mathcal{N}(u+iv)(= -(u+iv)), \mathcal{N}(u+iv)^{\perp}(= -i(u+iv))$, resp. $\mathcal{N}(U+iV)(= -(U+iV)), \mathcal{N}(U+iV)^{\perp}(= -i(U+iV))$ on $s_{i,j}(\sigma,\sigma')$ and $S_{i,j}(\sigma,\sigma')$ respectively. Now the collection

$$\{F_{a_i}(\frac{1}{f})\backslash[a_i], F_{b_j}(f)\backslash[b_j]; i,j = 1,\cdots r\}$$

exhibits a covering of $\check{T}$ with open neighborhoods. Apparently, only in the case of pairs $(F_{a_i}(\frac{1}{f})\backslash[a_i], F_{b_j}(f)\backslash[b_j])$ a non-empty intersection is possible. Even so, the intersection

$$F_{a_i}(\frac{1}{f})\backslash[a_i] \cap F_{b_j}(f)\backslash[b_j]$$

consists of the disjoint union of sets of the type $R_{ij}(\cdot,\cdot)$, say $R_{ij}^1, \cdots, R_{ij}^s$. (Note that $[a_i]$ occurs in w_{b_j} as many times as $[b_j]$ occurs in w_{a_i}). This turns our covering into an atlas for $\check{T}$ with smooth (even complex analytic) coordinate transformations, induced by the

inversion $(u+iv)) \leftrightarrow (1/(u+iv)) = U+iV$. With aid of this atlas, we may interprete $\overline{\overline{\mathcal{N}}}(f)$ and $\overline{\overline{\mathcal{N}}}^{\perp}(f)$ on each canonical region as the pull back of the most simple[16] planar flows $\mathcal{N}(u+iv), \mathcal{N}^{\perp}(u+iv)$, and $\mathcal{N}(U+iV), \mathcal{N}^{\perp}(U+iV)$ on the various sectors $s_{i,j}(\cdot,\cdot)$ and $S_{i,j}(\cdot,\cdot)$ respectively. Glueing the canonical regions $R_{ij}(\cdot,\cdot)$ along the $\overline{\overline{\mathcal{N}}}(f)$-trajectories in their common boundaries, we obtain the restrictions to $\check{T}$ of our original (rotated) Newton flows. In particular, the flows $\mathcal{N}(u+iv)(=-(u+iv))$ and $\mathcal{N}(U+iV)(=-(U+iV))$ lead to an analytic function on $\check{T}$, namely the restriction $f|\check{T}$, with as isolated singularities the zeros, poles and critical points for f. By continuous extension to this singularities, we find the original flows $\overline{\overline{\mathcal{N}}}(f)$ and $\overline{\overline{\mathcal{N}}}^{\perp}(f)$. For an illustration, see Fig. 18, 19.

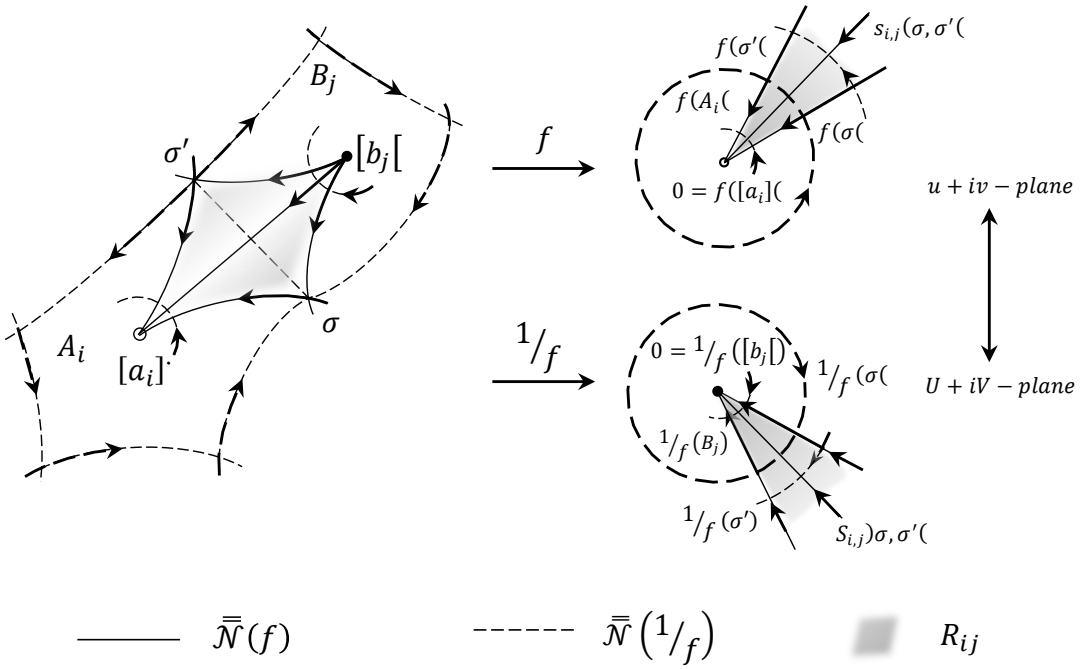

Figure 18: The canonical regions R_{ij}, and the sectors $s_{i,j}(\sigma,\sigma')$ and $S_{i,j}(\sigma,\sigma')$.

[16] On the sectors $s_{i,j}(\sigma,\sigma')$ resp. $S_{i,j}(\sigma,\sigma')$ the flows $\mathcal{N}(u+iv)$, resp. $\mathcal{N}(U+iV)$ are North-South flows, cf. Section 2.

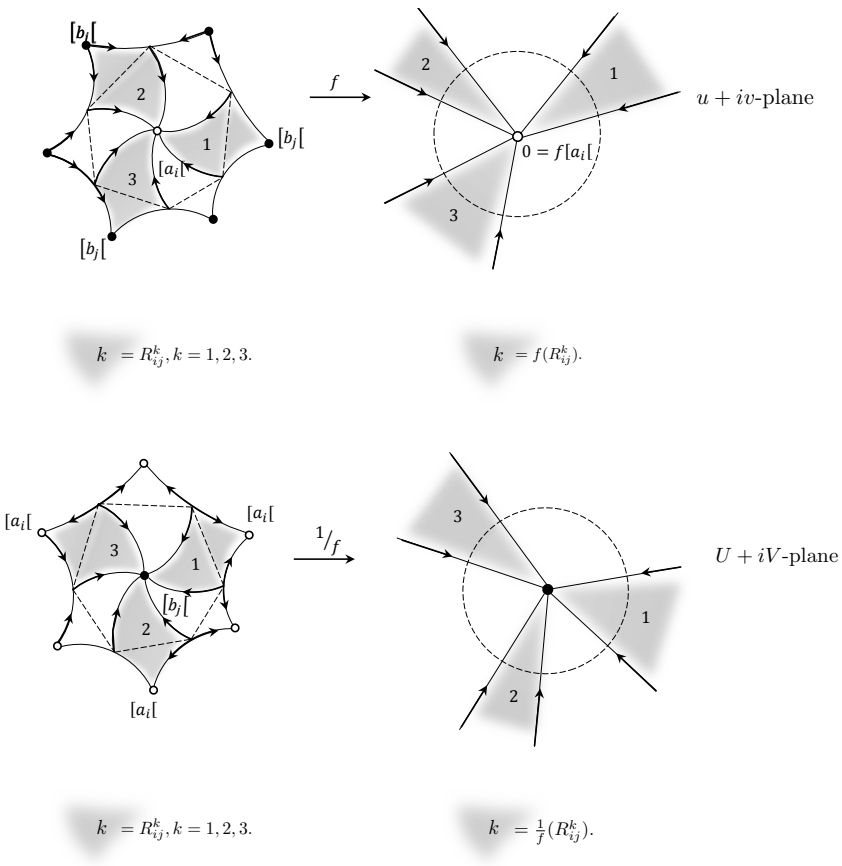

Figure 19: $F_{a_i}(\frac{1}{f})\backslash[a_i] \cap F_{b_j}(f)\backslash[b_j]$ and its images under f and $\frac{1}{f}$ $(s = 3)$.

7 Newton graphs

Throughout this section, the graph $\mathcal{G}$ is a cellular embedding in T, seen as a compact, orientable, Hausdorff topological space, of an abstract multigraph $\mathbf{G}$ with r vertices, $2r$ edges ($r \geq 2$); $r =$*order* $\mathcal{G}$.

The forthcoming analysis strongly relies on some concepts from classical graph theory on surfaces, which- in order to fix terminology-will be briefly reviewed[17]:

7.1. Cellularity; geometric duals

Since $\mathcal{G}$ is cellularly embedded, we may consider (cf. [31]) the *rotation system* Π for $\mathcal{G}$:

$$\Pi = \{\pi_v \,|\, \text{all vertices } v \text{ in } \mathbf{G}\},$$

where the local *rotation* π_v at v is the cyclic permutation of the edges incident with v such that $\pi_v(e)$ is the successor of e in the anti-clockwise ordering around v.

If $e(= v'v'')$ stands for an edge, with end vertices v' and v'', we define a Π-*walk* (facial walk[18]), say w, on $\mathbf{G}$ as follows:

The face traversal procedure.
Consider an edge $e_1 = (v_1v_2)$ and the closed walk[19] $w = v_1e_1v_2e_2v_3 \cdots v_ke_kv_1$, which is determined by the requirement that, for $i = 1, \cdots, \ell$, we have $\pi_{v_{i+1}}(e_i) = e_{i+1}$, where $e_{\ell+1} = e_1$ and ℓ is minimal.

Apparently, such "minimal" ℓ exists since $\mathbf{G}$ is finite. Note that each edge occurs *either once* in two different Π-walks, or *twice* (with opposites orientations) in *only one* Π-*walk*; in particular, the first edge in the same direction which is repeated when traversing w, is e_1. As in the proof of Lemma 6.9, these Π-walks can be used to construct (patching the facial polygons along identically labelled sides) an orientable(!) surface S and in S, a so-called *2-cell* embedded graph with faces determined by the facial polygons. Since there are precisely r facial walks, S is homeomorphic to T and the 2-cell embedded graph is isomorphic to $\mathcal{G}$. By the *Heffter-Edmonds-Ringel rotation principle*, the graph $\mathcal{G}$ is uniquely determined up to homeomorphism by its rotation system. We say: $\mathcal{G}$ is generated by Π.
From now on, we suppress the role of the underlying abstract graph $\mathbf{G}$ and will not distinguish between the vertices of $\mathcal{G}$ and those of $\mathbf{G}$. Occasionally, $\mathcal{G}$ will be referred to as to the pair ($\mathcal{G}$, Π). The $\mathcal{G}$-faces (as well as the corresponding facial polygons) are denoted by F_j; their boundaries (as well as the corresponding Π-walks) by $\partial F_j, j = 1, \cdots, r$. We denote the sets of all vertices, edges and faces of $\mathcal{G}$ by $V(\mathcal{G}), E(\mathcal{G})$ and $F(\mathcal{G})$ respectively.

The embedding of $\mathcal{G}$ into the orientable surface T induces an anti-clockwise orientation on the edges around each vertex v. In the sequel we assume that the local rotations π_v are endowed with this orientation (so that the inverse permutation π_v^{-1} are clockwise).

Given a cellularly embedded toroidal ($\mathcal{G}$, Π), the abstract graph $\mathbf{G}^*$ is defined as follows:

- The r vertices $\{v^*\}$ are represented by the Π-walks in $\mathcal{G}$,

[17] Again we follow the treatise [31] closely. Note however, that in [31] a multigraph may exhibit loops, whereas in our case this possibility for $\mathcal{G}$ is ruled out.
[18] Compare the facial walk w_{b_j} in Section 6.
[19] We shall not distinguish between w and its cyclic shifts.

- Two vertices are connected by an edge e^* iff the representing Π-walks share an edge e.

Hence, between the $\mathcal{G}$-edges and $\mathbf{G}^*$-edges, there is a bijective correspondence: $e \leftrightarrow e^*$.
In particular, $\mathbf{G}^*$ has $2r$ edges, and an edge e^* is a loop[20] iff e shows up twice in a Π-walk of $\mathcal{G}$.

The graph $\mathbf{G}^*$ admits a 2-cell embedding in T: the *(geometric) dual* $(\mathcal{G}^*, \Pi^*)$. In fact, if the vertex v^* in $(\mathcal{G}^*, \Pi^*)$ is represented[21] by the Π-walk $(e_1 - \cdots - e_l)$, then the cyclic permutation on the $\mathbf{G}^*$-edges incident with v^*, say $\pi^*_{v^*}$, is defined by $\pi^*_{v^*} = (e_1^* - \cdots - e_l^*)$. Each Π^*-walk of length ℓ corresponds to precisely one $\mathcal{G}$-vertex of degree ℓ: compare Fig. 13, where $\mathcal{G} = \mathcal{G}(f)$ and $\mathcal{G}^*$=$\mathcal{G}^*(f)$. Note that the anti-clockwise orientation of the local rotation systems π_v induces a clockwise orientation on the Π-walk $(e_1 - \cdots - e_l)$ and thus a clockwise orientation on $\pi^*_{v^*}$. All together it follows that $(\mathcal{G}^*, \Pi^*)^*$=$(\mathcal{G}, \Pi)$.

Finally, we note that two cellularly embedded graphs in T are isomorphic, then also their duals.

7.2. The E(Euler)-property

In contradistinction to the case of facial walks in $\mathcal{G}(f)$, $f \in \tilde{E}_r$, see Lemma 6.7, a Π-walk in $\mathcal{G}$ is-in general- *not* an Euler-trail. So, we need an additional condition:

Definition 7.1. $(\mathcal{G}, \Pi)$ has the *E(Euler)-property* if every Π-walk is Eulerian.

For an example of a second order graph $(\mathcal{G}, \Pi)$ that has the *E-property*, see Fig. 20-(i). This it not so for the third order graphs $(\mathcal{G}, \Pi)$ in Fig. 20-(ii), (iii), whereas the graph in Fig. 20 (iv) does not even fulfil the initial conditions laid upon $\mathcal{G}$ (because there are 3 vertices and only 5 edges). Note, however, that also in the latter case the Euler Characteristic vanishes, so that this multigraph is toroidal as well.

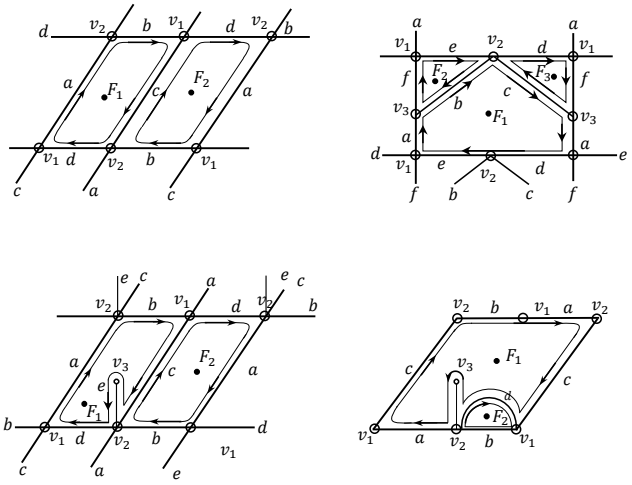

Figure 20: Four multigraphs, cellularly embedded in T

[20] In contradistinction to our assumption on $\mathcal{G}$, the graph $\mathbf{G}^*$ may admit loops.
[21] We say: v^* is "'located' in the $\mathcal{G}$-face, determined by the Π-walk $(e_1 - \cdots - e_l)$.

Lemma 7.2. *If* $(\mathcal{G},\ \Pi)$ *has the E-property, then this is also true for* $(\mathcal{G}^*,\ \Pi^*)$.

Proof. Recall that the conditions "E-property holds for $\mathcal{G}$" and "non-occurrence of loops in $\mathcal{G}^*$" are equivalent and apply $(\mathcal{G}^*)^*{=}\mathcal{G}$. □

From now, on we assume that both $\mathcal{G}$ and $\mathcal{G}^*$ are multigraphs and fulfil the *E-property*. In particular, each edge in these graphs is adjacent to *two different* faces.

Let v be an arbitrary vertex in $\mathcal{G}$, contained in the boundary ∂F of a face F and e_1ve_2 a subwalk of the Π-walk w_F. The *different* edges e_1, e_2 are consecutive w.r.t. the (*clockwise*) orientation of w_F. The *facial local sector* of F at v, spanned by the ordered pair $(e_1,\ e_2)$, is referred to as to a *F-sector at v*. Note that if v occurs more than once in w_F , two F-sectors at v cannot share an edge (because in that case the common edge would show up twice in w_F). Hence, F-sectors at v must be separated by facial sectors at v that do not belong to F. So, if e_1ve_2 and $e_1^{'}ve_2^{'}$ are subwalks of w_F, spanning two facial F-sectors at v, then e_1, e_2, $e_1^{'}$ and $e_2^{'}$ must be different. Thus each vertex in ∂F has even degree.

Apparently, the number of all facial sectors at v equals the degree of v, and in $\mathcal{G}$ there are altogether $\delta_1+\cdots+\delta_r(=4r)$ facial sectors, where the δ_i's stand for the degrees of the vertices in $\mathcal{G}$.

Similarly, there are $\delta_1^*+\cdots+\delta_r^*(=4r)$ facial sectors in $\mathcal{G}^*$ with the δ_j^*'s the degrees of the $\mathcal{G}^*$-vertices.

We write $F=F_{v^*}$, where v^* is the $\mathcal{G}^*$-vertex defined by F. So, $w_F=w_{F_{v^*}}$. Analogously, F_v^* stands for the $\mathcal{G}^*$-face determined by v. Then $e_2^*v^*e_1^*$ is a subwalk of $w_{F_v^*}$ and the *different* edges e_1^*, e_2^* are consecutive w.r.t. the *anti-clockwise* orientation of this facial walk. We say that the F_{v^*}-sector at v, spanned by the pair (e_1, e_2) and the F_v^* at v^* spanned by (e_1^*, e_2^*) are in *opposite position*; see Fig. 21. Altogether there are $4r$ of such (ordered) pairs of $\mathcal{G}$-, $\mathcal{G}^*$-vertices. Note that if v occurs p times in $w_{F_{v^*}}$, then v^* shows up also p times in $w_{F_v^*}$.

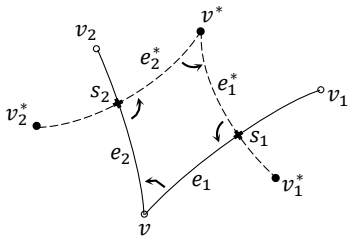

Figure 21: Pairs of facial sectors in opposite position.

The next step is to introduce the analogon of the *common refinement* $\mathcal{G}(f)\wedge\mathcal{G}^*(f)$.

To this aim:

Definition 7.3. The abstract graph $\mathbb{P}(\mathcal{G})$ is given as follows:

- There are $4r$ vertices (on three levels) represented by:

  - the $\mathcal{G}$-vertices [Level-1],
  - the pairs $s = (e, e^*), e \in E(\mathcal{G}), e^* \in E(\mathcal{G}^*)$ [Level-2],
  - the $\mathcal{G}^*$-vertices [Level-3].

- There are $8r$ edges:

  - a vertex on Level-2, represented by (e, e^*) is connected to two different vertices on Level-1, namely the $\mathcal{G}$-vertices incident with e, and to two different vertices on Level-3, namely the $\mathcal{G}^*$-vertices incident with e^*.
  - vertices on Level-1 are not connected with vertices on Level-3.

$\mathbb{P}(\mathcal{G})$-vertices on the Levels-1, -3 are denoted as the corresponding $\mathcal{G}-, \mathcal{G}^*-$vertices. The graph $\mathbb{P}(\mathcal{G})$ is directed by the convention: vertices on Level-1 (resp. Level-3) are the end- (resp. begin-)points of its edges.

We claim the existence of a cellular embedding of $\mathbb{P}(\mathcal{G})$ in T, denoted $\mathcal{G} \wedge \mathcal{G}^*$, with faces determined by the $4r$ pairs of facial sectors in *opposite position*. In order to verify this claim, consider an arbitrary pair of such sectors, given by the subwalks $e_1 v e_2$ and $e_1^* v^* e_2^*$ with $s_\ell = (e_\ell, e_\ell^*), \ell = 1, 2$; compare Fig.21. We specify local rotation systems on $\mathbb{P}(\mathcal{G})$ at v and v^* by π_v and $\pi_{v^*}^*$ respectively. The rotation systems at s_1 and s_2 are given by the cyclic permutations $(s_1 v, s_1 v_1^*, s_1 v_1, s_1 v^*)$, respectively $(s_2 v, s_2 v^*, s_2 v_2, s_2 v_2^*)$, where v_ℓ and v_ℓ^* stand for the vertices incident with e_ℓ and e_ℓ^* that are different from respectively v and $v^*, \ell = 1, 2$. The resulting rotation system for $\mathbb{P}(\mathcal{G})$ is called (Π, Π^*). Now starting from $v s_2$ we find the (Π, Π^*)-walk $(v s_2, s_2 v^*, v^* s_1, s_1 v)$.

This yields a cellular embedding of $(\mathbb{P}(\mathcal{G}), (\Pi, \Pi^*))$ into a surface homeomorphic to T (because the alternating sum of the numbers of vertices, edges and (Π, Π^*)-walks in $\mathbb{P}(\mathcal{G})$ vanishes). This embedding is denoted by $\mathcal{G} \wedge \mathcal{G}^*$, and can be viewed as the common refinement of $\mathcal{G}$ and $\mathcal{G}^*$. Each face in $\mathcal{G} \wedge \mathcal{G}^*$ is represented by a quadruple of directed edges in $\mathbb{P}(\mathcal{G})$ and is associated with exactly one vertex on Level 1, one vertex on Level 3 (in opposite position) and two vertices on Level 2. Moreover, each $\mathcal{G}$-face ($\mathcal{G}^*$-face) is built up from the sets of all $\mathcal{G} \wedge \mathcal{G}^*$-faces centered at a $\mathcal{G}^*$-vertex ($\mathcal{G}$-vertex), ordered in accordance with the orientation of $\mathcal{G}$ ($\mathcal{G}^*$). This observation turns the *abstract* graph $\mathbb{P}(\mathcal{G})$ into a distinguished graph $\mathbb{P}^d(\mathcal{G})$ with only distinguished sets of *Type 1* (in the sense of [33]).
Following Peixoto, the distinguished graph $\mathbb{P}^d(\mathcal{G})$ is realizable as *the* distinguished graph of a C^1-*structurally stable* vector field, say[22] $\mathcal{X}(\mathcal{G})$ on T, with:

- as hyperbolic attractors (repellors): the $\mathcal{G}$-vertices ($\mathcal{G}^*$-vertices),
- as 1-fold saddles: the other $\mathcal{G} \wedge \mathcal{G}^*$-vertices,
- as stable (unstable) manifolds at the saddles: the $\mathcal{G} \wedge \mathcal{G}^*$-edges with as begin point a $\mathcal{G}^*$-vertex (as end point a $\mathcal{G}$-vertex).
- as canonical regions (of Type 1): the faces of $\mathcal{G} \wedge \mathcal{G}^*$.

Note that $\mathcal{X}(\mathcal{G})$ exhibits *no* "saddle connections", *no* closed orbits and thus *no* limit cycles.

[22] Since $\mathcal{G}^*$ is determined by $\mathcal{G}$, we occasionally refer to $\mathcal{G}$ as to the distinguished graph of $\mathcal{X}(\mathcal{G})$.

In order to specify the roles of $\mathcal{G}$ and $\mathcal{G}^*$, we occasionally write $\mathcal{X}(\mathcal{G}) = \mathcal{X}_{\mathcal{G}\wedge\mathcal{G}^*}$.

Again, due to Peixoto's classification result ([33]) on structural stability, we have[23]:
If $\mathcal{H}$ is another connected multigraph of order r, cellularly embedded in T that fulfils the E-property, then:

$$\mathcal{X}_{\mathcal{G}\wedge\mathcal{G}^*} \sim \mathcal{X}_{\mathcal{H}\wedge\mathcal{H}^*} \Leftrightarrow \mathcal{G} \sim \mathcal{H},$$

where, as in Section 6, in the left hand side $\sim$ stands for conjugacy and in the right hand side for an equivalency (i.e., isomorphism between graphs respecting their orientations[24]).
The flow $\mathcal{X}(\mathcal{G}^*)$ is the *dual version* of $\mathcal{X}(\mathcal{G})$, i.e., $\mathcal{X}(\mathcal{G}^*)$ is obtained from $\mathcal{X}(\mathcal{G})$ by reversing the orientations of the trajectories of the latter flow, thereby changing repellors into attractors and vice versa. Apparently, the dual version of $\mathcal{X}(\mathcal{G}^*)$ is $\mathcal{X}(\mathcal{G})$.

Now, put $\mathcal{H} = \mathcal{G}^*$ and thus $\mathcal{G} = \mathcal{H}^*$, then we find:

$$\mathcal{X}(\mathcal{G}) \sim \mathcal{X}(\mathcal{G}^*) \Leftrightarrow \mathcal{G} \sim \mathcal{G}^*.$$

The above observation can be paraphrased as:

Lemma 7.4. *$\mathcal{X}(\mathcal{G})$ is self dual (i.e., $\mathcal{X}_{\mathcal{G}} \sim \mathcal{X}_{\mathcal{G}^*}$) iff $\mathcal{G}$ is self dual (i.e., $\mathcal{G} \sim \mathcal{G}^*$).*

Lemma 7.5. *Put*

$$\delta(\mathcal{G}) = \{\delta_i = \deg(v_i), v_i \in V(\mathcal{G}), i = 1, \cdots, r\} \text{ and}$$
$$\delta^*(\mathcal{G}) := \{\delta_j^* = \deg(v_j^*), v_j^* \in V(\mathcal{G}^*), j = 1, \cdots, r\}.$$

Then:

$$\mathcal{G} \sim \mathcal{G}^* \Leftrightarrow \delta(\mathcal{G}) = \delta^*(\mathcal{G}) (= \delta(\mathcal{G}^*)).$$

Proof. Note that the δ_i's, together with the claim "clockwise" ("anti-clockwise") fix the local rotations of $\mathcal{G}$ and $\mathcal{G}^*$. Now the Heffter-Edmonds-Ringel rotation principle together with $(\mathcal{G}^*)^* = \mathcal{G}$ proves the assertion. □

From Lemmata 7.4 and 7.5 it follows:

Corollary 7.6. *There holds: $\mathcal{X}(\mathcal{G}) \sim \mathcal{X}(\mathcal{G}^*) \Leftrightarrow \delta(\mathcal{G}) = \delta^*(\mathcal{G})$.*

7.3 The A(Angle)-property

Recall that $V(\mathcal{G}) = \{v_1, \cdots, v_r\}$ and $\delta_i = \deg(v_i)$. The δ_i anti-clockwise ordered edges, incident with the vertex v_i are denoted $e_{i(k)}$, $e_{i(\delta_i+1)} = e_{i(1)}, k = 1, \cdots, \delta_i$. Note that all these edges are different (because $\mathcal{G}$ is a multigraph). Since T is locally homeomorphic to an open disk, it is always possible to re-draw $\mathcal{G}$, thereby respecting Π such that the anti-clockwise measured angles at v_i between $e_{i(k)}$ and $e_{i(k+1)}$, say $2\pi\omega_{i(k)}$, are strictly positive and sum up to 2π. The resulting graph is again denoted by $\mathcal{G}$. Since $\mathcal{G}$ is a multigraph, we have altogether $4r(= \delta_1 + \cdots + \delta_r)$ "angles" $\omega_{i(k)}$. The set of all these angles is $A(\mathcal{G})$. The subset of all angles between edges that are consecutive edges in the Π-walk w_{F_j} that span a F_j-sector, is called the set of angles of F_j and will be denoted by $a(F_j)$. Finally, for fixed i, the set of all "angles" $\omega_{i(k)}, k = 1, \ldots, \delta_i$, is the "set $a(v_i)$ of angles at v_i".
Now, we introduce:

[23] In fact: $\mathcal{X}_{\mathcal{G}\wedge\mathcal{G}^*} \sim \mathcal{X}_{\mathcal{H}\wedge\mathcal{H}^*} \Leftrightarrow \mathbb{P}^d(\mathcal{G}) \sim \mathbb{P}^d(\mathcal{H})$, where $\sim$ is defined as in (22).

[24] More precisely: if Π and Π' are rotation systems for $\mathcal{G}$ resp. $\mathcal{H}$, then either $\pi'_{\varphi(v)} = \pi_v$ for all $v \in V(\mathcal{G})$, or $\pi'_{\varphi(v)} = \pi_v^{-1}$ for all $v \in V(\mathcal{G})$, where φ is a homeomorphism on T with $\varphi(\mathcal{G}) = \mathcal{H}$. In the first case we call φ orientation-preserving and in the second case orientation-reversing.

Definition 7.7. $\mathcal{G}$ has the *A(Angle)-property* if -possibly under a suitable local re-drawing- the angles in $A(\mathcal{G})$ can be chosen such that:

A_1 : $\omega_{i(k)} > 0$ for all $\omega_{i(k)} \in A(\mathcal{G})$.

A_2 : $\sum_{a(v_i)} \omega_{i(k)} = 1$, for all $i = 1,\cdots,r$.

A_3 : $\sum_{a(F_j)} \omega_{i(k)} = 1$, for all $j = 1,\cdots,r$.

Note that Conditions A_1 and A_2 can always be fulfilled; the crucial claim is Condition A_3. Moreover, the sets of angles at the vertices v of $\mathcal{G}$ that fulfil the conditions A_1 and A_2, fix the anti-clockwise oriented local rotations π_v. Hence, $\mathcal{G}$ is determined by these angles.

Let J be an arbitrary *non empty* subset of $\{1,\ldots,r\}$. The subgraph of $\mathcal{G}$ generated by all vertices and edges in the faces $F_j, j \in J$, is denoted by $\mathcal{G}(J)$. An *interior vertex* of $\mathcal{G}(J)$ is a vertex of $\mathcal{G}$ that is only incident with $\mathcal{G}$-faces labelled by J, whereas a vertex of $\mathcal{G}(J)$ is called *exterior* if it is incident with both a face labelled by J and a face *not* labelled by J. The sets of all interior, respectively all exterior vertices in $\mathcal{G}(J)$ are denoted by $\mathrm{Int}\mathcal{G}(J)$ and $\mathrm{Ext}\mathcal{G}(J)$ respectively. If $J = \{1,\ldots,r\}$, then $|\mathrm{Int}\mathcal{G}(J)| = |J| = |V(\mathcal{G}(J))| = |V(\mathcal{G})|(= r)$, where as usual $|.|$ stands for cardinality.

We have:

Lemma 7.8. *Assume that $\mathcal{G}$ fulfils the A-property. Then:*

$$|\mathrm{Int}\mathcal{G}(J)| < |J| < |V(\mathcal{G}(J))|, \text{ for all } J, \emptyset \neq J \subsetneq \{1,\cdots,r\} \tag{23}$$

Proof. By Definition 7.7

$$\sum_{j\in J} \sum_{a(F_j)} \omega_{i(k)} = |J|.$$

The contribution of any *interior* vertex of $\mathcal{G}(J)$ to the sum in the left-hand side of this equation is equal to 1, whereas each *exterior* vertex contributes with a number that is strictly between 0 and 1. Hence, we are done if- for the subsets J under consideration- we can prove that $\mathrm{Ext}\mathcal{G}(J) \neq \emptyset$. So, assume $\mathrm{Ext}\mathcal{G}(J)$ is empty, thus $\mathrm{Int}\mathcal{G}(J) \neq \emptyset$. Let J^C be the complement of J in $\{1,\ldots,r\}$. Thus $\emptyset \neq J^C \subsetneq \{1,\ldots,r\}$ and $\mathrm{Ext}\mathcal{G}(J^C)(=\mathrm{Ext}\mathcal{G}(J)) = \emptyset$. Hence, we also have $\mathrm{Int}\mathcal{G}(J^C) \neq \emptyset$. Now, the connectedness of $\mathcal{G}$ yields a contradiction. □

Remark 7.9. If $\mathcal{G}$ has the *A-property*, then: l.h.s. of (23) ⇔ r.h.s. of (23), so that one of these equalities is redundant.

Lemma 7.10. *If $\mathcal{G}$ fulfils $|J| < |V(\mathcal{G}(J))|$ for all J, $\emptyset \neq J \subsetneq \{1,\cdots,r\}$ (cf. (23)), then:*

Any assignment of an arbitrary vertex v_{i_0} to any face F_{j_0} adjacent to v_{i_0}, can be extended to a bijection $\mathcal{T} : V(\mathcal{G}) \to F(\mathcal{G})$, with $v \in V(\partial\mathcal{T}(v))$ and $\mathcal{T}(v_{i_0}) = F_{j_0}$, i.e., the assignment $v_{i_0} \mapsto F_{j_0}$ can be extended to a transversal of the vertex sets $V(\partial F_j), j = 1,\cdots,r$. (24)

Proof. Consider the vertex set $V(\partial F_j)$ of ∂F_j. Put for $j \in \{1,\cdots,r\}, p_j = 1$, if $j \neq j_0$, and $p_{j_0} = 0$. For *all non empty* subsets J of $\{1,\ldots,r\}$(i.e. including $J = \{1,\ldots,r\}$), we have

$$|V(\mathcal{G}(J))\backslash\{v_{i_0}\}| \geq \sum_{j\in J} p_j,$$

According to a slight generalization of Hall's theorem on distinct representatives(cf. [30]), these inequalities are necessary and sufficient for the existence of pairwise disjoint sets $X_1,\cdots,X_r$, such that

$$X_j \subset V(\partial F_j)\backslash\{v_{i_0}\}\ \text{, with } |X_j| = p_j, j = 1,\cdots,r.$$

Hence, the singletons(!) $X_j, j \in \{1,\cdots,r\}, j \neq j_0$, together with v_{i_0} yield the existence of the desired transversal $\mathcal{T}$. □

Now, let us re-label the angles of $\mathcal{G}$ by x_λ, with $\lambda = 1,\cdots,4r(=\sum_{i=1}^{r}\deg(v_i))$. We associate with $\mathcal{G}$ a $2r\times 4r$-matrix $M(\mathcal{G})$ with coefficients $m_{\ell\lambda}$:

$$m_{\ell\lambda} = \begin{cases} 1, & \text{if } \ell = 1,\cdots,r, \text{ and } x_\lambda \text{ is an angle at } v_\ell, \text{ i.e. } x_\lambda \text{ in } a(v_\ell); \\ 1, & \text{if } \ell = r+1,\cdots,2r, \text{ and } x_\lambda \text{ is an angle in } a(F_{\ell-r}); \\ 0, & \text{otherwise.} \end{cases}$$

Apparently, $\mathcal{G}$ has the *A-property* if and only if the following system of $2r$ equations and $4r$ inequalities has a solution:

$$\begin{cases} [M(\mathcal{G}) \ \mid -1].(x \mid 1)^T = (0,...,0)^T \\ x_\lambda > 0, \lambda = 1,\cdots,4r \end{cases} \tag{25}$$

Here, $[M(\mathcal{G}) \ \mid -1]$ stands for the matrix $M(\mathcal{G})$ augmented with a $(4r+1)$-st column, each of its elements being equal to -1, and $(x \mid 1) = (x_1,...,x_{4r},1)$.

Basically due to Stiemkes theorem (cf. [26]), System (25) has a solution *iff* System (26) below has no solution for which at least one of the inequalities is strict:

$$\begin{pmatrix} M(\mathcal{G})^T \\ ---- \\ -1\cdots -1 \end{pmatrix}.Z^T \geq (0,\cdots,0)^T, \text{ with } Z = (z_1,\cdots,z_i,\cdots,z_r,\cdots,z_{r+j},\cdots,z_{2r}) \tag{26}$$

Here,

$$\begin{pmatrix} M(\mathcal{G})^T \\ ---- \\ -1\cdots -1 \end{pmatrix}$$

stands for the matrix $M(\mathcal{G})^T$ augmented with a $(4r+1)$-st row, all its coefficients being equal to -1. For $i,j \in \{1,\cdots,r\}$, the pair (i,j) is called *associated*, notation $(i,j) \in \mathbf{O}$, if v_i and F_j share an angle.

Obviously, System (26) is equivalent with

$$\begin{cases} z_i + z_{r+j} \geq 0, \text{ for all } (i,j) \in \mathbf{O} \\ \sum_{\ell=1}^{2r} z_\ell \leq 0 \end{cases} \tag{27}$$

But now we are in the position to apply Lemma 7.10:

Lemma 7.11. *Consider a graph $\mathcal{G}$, not necessarily an E-graph. Then we have*

$$\mathcal{G} \text{ has the A-property} \Leftrightarrow |J| < |V(\mathcal{G}(J))| \text{ for all } J, \emptyset \neq J \subsetneq \{1,\cdots,r\}.$$

Proof. "⇒" See Lemma 7.8.
"⇐". Suppose that $Z = (z_1, \cdots, z_{2r})$ is a solution of System (27) for which at least one of the inequalities is not strict. We lead this assumption to a contradiction.

Consider an associated pair (i_0, j_0). So, the vertex v_{i_0} and the face F_{j_0} have an angle in common. Extend by Lemma 7.10, the assignment $v_{i_0} \mapsto F_{j_0}$ to a transversal $\mathcal{T}$ as in (24) and define $\tau(i)$ by $F_{\tau(i)} = \mathcal{T}(v_i)$. This means that v_i and $F_{\tau(i)}$ share an angle, thus $(i, \tau(i)) \in \mathbf{O}$; in particular $(i_0, \tau(i_0)) = (i_0, j_0) \in \mathbf{O}$. Since Z fulfills (27), we have: $z_i + z_{r+\tau(i)} \geq 0, i = 1, \cdots, r$, and moreover (use that $\mathcal{T}$ is bijective) also

$$\sum_{i=1}^{r}(z_i + z_{r+\tau(i)}) = \sum_{\ell=1,\ldots,2r} z_\ell \leq 0.$$

Hence, $z_i + z_{r+\tau(i)} = 0, i = 1, \cdots, r$. In particular, $z_{i_0} + z_{r+j_0} = 0$. Since the associated pair (i_0, j_0) was chosen arbitrarily, we have $z_i + z_{r+j} = 0$, for every combination $(i, j) \in \mathbf{O}$. This contradicts our assumption on Z. It follows that System (27) *does not have* a solution for which at least one of the inequalities is strict. Thus System (25) *does admit* a solution, i.e. $(\mathcal{G}, \Pi)$ has the *A-property.* □

Corollary 7.12. *Let $\mathcal{G}$ be a graph as in Lemma 7.11. Then there holds:*

$$\mathcal{G} \textit{ has the A-property} \Leftrightarrow \textit{ Condition } (24) \textit{ holds for } \mathcal{G}.$$

Proof. ⇒ See Lemmas 7.8, 7.10.
⇐ Follows from the (⇐ part) of the proof of Lemma 7.11. □

The (equivalent) conditions "$|J| < |V(\mathcal{G}(J))|$ for all J, $\emptyset \neq J \subsetneq \{1, \cdots, r\}$" and (24) will be referred to as to the *H(Hall)-condition*; see also Section 13.2.

As it is easily verified, the graphs $\mathcal{G}$ in Fig. 20(i), (ii) fulfil the *H-condition*, but $\mathcal{G}$ in Fig. 20(iii) not. Hence, by Lemma 7.11, or Corollary 7.12, the graphs $\mathcal{G}$ in Fig. 20(i), (ii) have the *A-property*, but this it not so for the graph in Fig. 20(iii).

7.4 Newton graphs

Definition 7.13. Cellularly embedded toroidal graphs that fulfil both the *A-and the E-properties* are called *Newton graphs.*

Lemma 7.14. *If $(\mathcal{G}, \Pi)$ is a Newton graph, then this is also true for $(\mathcal{G}^*, \Pi^*)$.*

Proof. In view of Lemma 7.2, we only have to show that $(\mathcal{G}^*, \Pi^*)$ has the *A-property.* Let v_0^* be a $\mathcal{G}^*$-vertex and consider an assignment $v_0^* \mapsto F_{v_0}^*$, where $F_{v_0}^*$ is a $\mathcal{G}^*$-face adjacent to v_0^* corresponding with the $\mathcal{G}$-vertex v_0. So the pair (v_0, v_0^*) is in opposite position, and v_0 is adjacent to the $\mathcal{G}^*$-face $F_{v_0^*}$. By assumption, $\mathcal{G}$ fulfills the A-property. So, we can extend (by Corollary 7.12) the assignment $v_0 \mapsto F_{v_0^*}$ to a transversal of the vertex sets of $\mathcal{G}$ (i.e., to pairs (v_i, v_i^*) in opposite position such that all v_i and v_i^* are different), and thus to a transversal $v_i^* \to F_{v_i}^*$ of the vertex sets of $\mathcal{G}^*$-faces (extending $v_0^* \mapsto F_{v_0^*}$). Now, application of Corollary 7.12 yields the assertion. □

The above result is easily verified by a geometric argument. Consider -under the assumption that the *A-and E-properties* hold for $\mathcal{G}$- the graph $\mathcal{G} \wedge \mathcal{G}^*$ on T and proceed in two steps: (see Fig. 22)
Step 1: Re-draw $\mathcal{G} \wedge \mathcal{G}^*$ locally around the vertices of $\mathcal{G}$ (solid lines) such that the angles in $A(\mathcal{G})$ fulfil the Conditions A1-A3 (in Definition 7.7).

Step 2: Due to Condition A3 for $\mathcal{G}$, we may re-draw $\mathcal{G} \wedge \mathcal{G}^*$ locally around the vertices of $\mathcal{G}^*$ (dotted lines) such that the $A(\mathcal{G})$- and $A(\mathcal{G}^*)$-angles of facial sectors in opposite position are equal.

We conclude that also $\mathcal{G}^*$ has the *A-property*, and find as a by-product:

Lemma 7.15. *If $\mathcal{G}$ is a Newton graph, we may assume -possibly after a suitable local re-drawing- that in each face of $\mathcal{G} \wedge \mathcal{G}^*$ the angles at the $\mathcal{G}$-and $\mathcal{G}^*$-vertices are equal (and non-vanishing).*

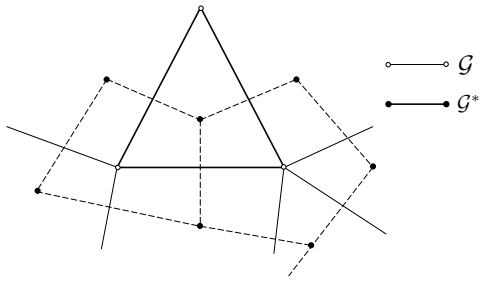

Figure 22: ($\mathcal{G}$, Π) and its dual ($\mathcal{G}^*$, Π^*); partial

From Corollary 6.6 and Lemma 6.7 it follows:

Corollary 7.16. *$\mathcal{G}(f)$ and $\mathcal{G}^*(f), f \in \tilde{E}_r$, are Newton graphs.*

In the forthcoming section we prove that in a certain sense the reverse is also true.

We end up this section with a lemma that we will use in the sequel:

Lemma 7.17. *Let $\mathcal{G}$ be of order $r = 2$ or 3. Then: If $r = 2$, the A-property always holds, whereas in Case $r = 3$ the E-property implies the A-property.*

Proof. Let J be an arbitrary *non empty, proper* subset of $\{1, \cdots, r\}$.
Case $r = 2$: Note that $|J| = 1$, thus $|V(\mathcal{G}(J)| > 1$ (because $\mathcal{G}$ has no loops). So we have: $|V(\mathcal{G}(J)| > |J|$, i.e., the *H-condition* holds, and Lemma 7.11 yields the assertion.
Case $r = 3$:
If $|J| = 1$, then $|V(\mathcal{G}(J)| > 1$(because $\mathcal{G}$ has no loops), thus $|V(\mathcal{G}(J)| > |J|$.
If $|J| = 2$, then $|J^c| = 1$ and $|V(\mathcal{G}(J^c)| \geq 2$ (since $\mathcal{G}$ has no loops). Moreover, by the *E-property*, each edge must be adjacent to at least two faces. This implies: $\mathrm{Int}\mathcal{G}(J^c) = \emptyset$. Thus $|\mathrm{Ext}\mathcal{G}(J)| = |\mathrm{Ext}\mathcal{G}(J^c)| = |V(\mathcal{G}(J^c)| \geq 2$ and $|V(\mathcal{G}(J)| = |\mathrm{Ext}\mathcal{G}(J)| + |\mathrm{Int}\mathcal{G}(J)|$. Distinguish now between two cases:

- $\mathrm{Int}\mathcal{G}(J) \neq \emptyset$, then $|V(\mathcal{G}(J)| > |J|$.
- $\mathrm{Int}\mathcal{G}(J) = \emptyset$, then the *three* vertices of $\mathcal{G}$ must be exterior vertices for $\mathcal{G}(J)$, thus also $|V(\mathcal{G}(J)| > |J|$. Hence, $|V(\mathcal{G}(J)| > |J|$ holds for all J under consideration, and Lemma 7.11 yields the assertion.

□

Remark 7.18. In contradistinction to the *A-property*, the *E-property* does not hold for all second order multigraphs $\mathcal{G}$; compare Fig. 23 (i), where the dual $\mathcal{G}^*$ admits a loop. From Fig. 23 (ii), it follows that Lemma 7.17 is not true in the case that $r = 4$. From Fig. 20 (ii) we learn that the A-property does not imply the *E-property*, even if $r = 3$.

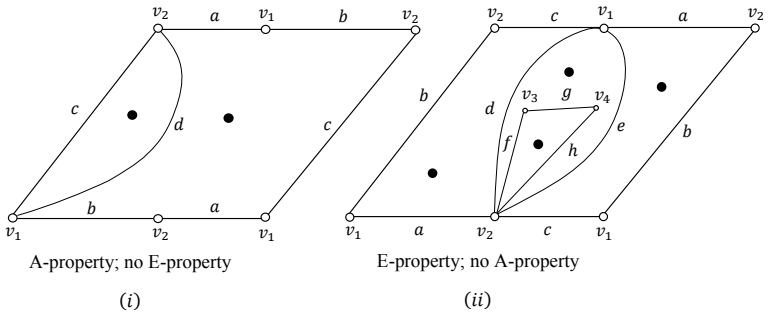

Figure 23: Two graphs $\mathcal{G}$.

8 The representation of a Newton graph by a structurally stable Newton flow.

In this section we prove that the reverse of Corollary 7.16 is also true.

Theorem 8.1. *Any Newton graph $\mathcal{G}$ of order r can be realized - up to equivalency - as the graph $\mathcal{G}(f), f \in \tilde{E}_r$.*

Proof. Based on several steps, see the end of this section. □

Starting point is an arbitrary Newton graph $\mathcal{G}$. We apply the results of Section 7. Let $\mathcal{X}(\mathcal{G})$ be a C^1-structurally stable vector field on T without limit cycles, determined - up to conjugacy - by $\mathcal{G} \wedge \mathcal{G}^*$, thus by the distinguished graph $\mathcal{G}$. (cf. Footnote 22)

The flow $\mathcal{X}(\mathcal{G})$ is gradient like, i.e. up to conjugacy equal to a gradient flow (with respect to a C^1-Riemannian metric R on T). This can be seen as follows:
An arbitrary equilibrium, say $\mathbf{x}$, of the (structurally stable!) flow $\mathcal{X}(\mathcal{G})$ is of hyperbolic type, i.e. the derivative $D_{\mathbf{x}}\mathcal{X}(\mathcal{G})$ has eigenvalues $\lambda_1(\mathbf{x}), \lambda_2(\mathbf{x})$ with non-vanishing real parts, cf. [32]. By the Theorem of Grobman-Hartman (cf. [17]) we have: (use also Theorem 8.1.8, Remark 8.1.10 in [21]): On a suitable $\mathbf{y}$-coordinate neighborhood [with $\mathbf{y}=(y_1, y_2)^T$] of $\mathbf{x}$, the phase portrait of $\mathcal{X}(\mathcal{G})$ is conjugate with the phase portrait around $\mathbf{y}= \mathbf{0}$ of one of the flows given by:

$$\mathbf{y}' = -\begin{pmatrix} \lambda_1 & 0 \\ 0 & \lambda_2 \end{pmatrix}\mathbf{y},\ \mathbf{y}(\mathbf{0}) = \mathbf{0},\ \text{with either } \lambda_1 = \lambda_2 = 1,\ \text{or } \lambda_1 = \lambda_2 = -1 \text{ or } \lambda_1 = -\lambda_2 = 1,$$

corresponding to the cases where $\mathbf{y}= \mathbf{0}$ stands for respectively a *stable star node*, an *unstable star node* and an *orthogonal saddle*; see Fig. 24.

Applying a flow box argument ("cutting" and "pasting" of local phase portraits), we find that $\mathcal{X}(\mathcal{G})$ is conjugate with a structurally stable smooth flow on T again denoted by $\mathcal{X}(\mathcal{G})$ with as equilibria: $2r$ star nodes (r of them being stable, the other r unstable) and $2r$ orthogonal saddles. The underlying "distinguished" graph is denoted - again - by $\mathcal{G}$. It follows that the angle between two $\mathcal{G}$-edges (i.e. unstable separatrices at saddles for $\mathcal{X}(\mathcal{G})$ incident with the same $\mathcal{G}$-vertex (i.e. a stable star node for $\mathcal{X}(\mathcal{G})$), may assumed to be well-defined and nonvanishing.

We adopt the notations/conventions as introduced in the preambule to Definition 7.7 (*Angle Property*). In particular, let the $\mathcal{G}$-vertex v_i stand for a stable node of $\mathcal{X}(\mathcal{G})$. In Fig. 25-(a) we present a picture of $\mathcal{X}(\mathcal{G})$ w.r.t. the $\mathbf{y}$-coordinates around $\mathbf{0}$ ($= v_i$). Here

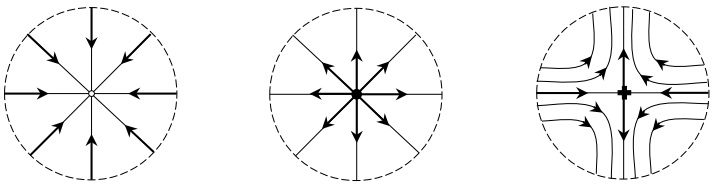

Figure 24: The possible local phase portraits of $\mathcal{X}(\mathcal{G})$ around $\mathbf{y}= \mathbf{0}$.

the bold lines stand for $\mathcal{G}$-edges, and the thin lines for other $\mathcal{X}(\mathcal{G})$-trajectories on a small disk D around $\mathbf{y}= \mathbf{0}$. Note that the angles $\omega_{i(k)}$ in this figure fulfil the conditions A_1, A_2 in Definition 7.7. In Fig. 25-(b), we consider a similar configuration of $\mathcal{X}(\mathcal{G})$-trajectories on D, approaching v_i, with as only additional condition that the tuples $(e_{i(1)}, \cdots, e_{i(\delta_i)})$ and $(e'_{i(1)}, \cdots, e'_{i(\delta_i)})$ are equally ordered. Consider the oriented arcs $\mathrm{arc}(i(k), i(k+1))$ and $\mathrm{arc}'(i(k), i(k+1))$ in the boundary ∂D of D, determined by respectively the consecutive pairs $(e_{i(k)}, e_{i(k+1)})$ and $(e'_{i(k)}, e'_{i(k+1)})$. Under suitable shrinking/stretching, these arcs can be identified. This yields an orientation preserving homeomorphism ψ from ∂D onto itself. It is easily proved that ψ can be extended to a homeomorphism $\Psi : D \to D$ mapping the $\mathcal{X}(\mathcal{G})$-trajectories in Fig. 25-(a) onto those in Fig. 25-(b). This procedure will be referred to as a local re-drawing (around v_i).

With the aid of local re-drawings, together with a "cut" and "paste" construction, the pair $(\mathcal{X}(\mathcal{G}), \mathcal{G})$ can be changed into an equivalent structurally stable flow (again denoted $\mathcal{X}(\mathcal{G})$) and an equivalent distinguished graph (again denoted $\mathcal{G}$), with pictures as Fig. 25-(b) instead of Fig. 25-(a). We conclude that the angles $\omega_i(k)$ in Fig. 25-(a) may be altered arbitrarily (provided that the Conditions A_1, A_2 in Definition 7.7 persist) without changing the topological types of $\mathcal{X}(\mathcal{G})$ and $\mathcal{G}$.

Note that any toroidal graph, equivalent with a Newton graph (such as the original graph $\mathcal{G}$), is also a Newton graph (cf. Defintion 7.1 and Lemma 7.11). Moreover, not only $\mathcal{G}$, but also $\mathcal{G}^*$ is Newtonian (cf. Lemma 7.14). Hence, compare (the proof of) Lemma 7.15, with the aid of local re-drawings around the vertices of $\mathcal{G}$ and $\mathcal{G}^*$, together with a "cut and past construction", it is easily shown that:

In each face of $\mathcal{G} \wedge \mathcal{G}^*$ (= canonical $\mathcal{X}(\mathcal{G})$-region), the angles at the $\mathcal{G}$- and $\mathcal{G}^*$-vertex (= a stable, respectively unstable, star node of $\mathcal{X}(\mathcal{G})$) are equal and non-vanishing.

With respect to the various local $\mathbf{y}$-coordinate systems around the $\mathcal{X}(\mathcal{G})$-equilibria , we define the $4r$ functions $h_i, h_i^*, h_j^{**}, i = 1, \cdots, r, j = 1, \cdots, 2r$, as follows:

$h_i(\mathbf{y}) = \frac{1}{2}(y_1^2 + y_2^2)$, in case of stable nodes at $\mathbf{y} = \mathbf{0}$ representing the r vertices v_i of $\mathcal{G}$,

$h_i^*(\mathbf{y}) = -\frac{1}{2}(y_1^2 + y_2^2)$, in case of unstable nodes at $\mathbf{y} = \mathbf{0}$ representing the r vertices v_i^* of $\mathcal{G}^*$,

$h_j^{**}(\mathbf{y}) = \frac{1}{2}(y_1^2 - y_2^2)$ in case of saddles at $\mathbf{y} = \mathbf{0}$ represented the $2r$ edges e_j of $\mathcal{G}$.

Note that each function exhibits a non-degenerate critical point at $\mathbf{y} = \mathbf{0}$. Moreover,

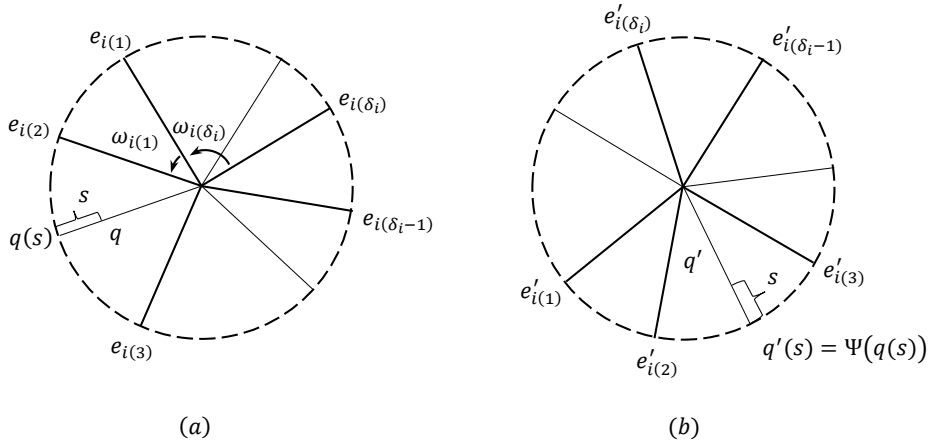

Figure 25: Local phase portraits of $\mathcal{X}(\mathcal{G})$ around a stable star node before and after local redrawing.

on a $\mathbf{y}$-coordinate neighborhood N around an equilibrium of $\mathcal{X}(\mathcal{G})$, the vector field $\mathcal{X}(\mathcal{G})$ is the negative gradient vector field [w.r.t. the standard Riemannian structure on N] of the associated function. Apparently, the flow $\mathcal{X}(\mathcal{G})$, being structurally stable on T (without limit cycles), together with the functions h_i, h_i^* and h_j^{**}, fulfils the Requirements (1)-(4) laid upon Theorem B in [35]. So, applying this theorem we may conclude that there is a function h on T such that:

1. The critical points of h coincide with the equilibria of $\mathcal{X}(\mathcal{G})$ and h coincides with the functions h_i, h_i^*, h_j^{**} plus a constant in some neighborhood of each critical point.
2. $Dh(x) \cdot \mathcal{X}(\mathcal{G})|_x < 0$ outside the critical point set $\mathrm{Crit}(h)$ of h.
3. The function h is *self indexing*, i.e. the value of h in a critical point β equals the Morse index of β (= #(negative eigenvalues of $D^2h(\beta)$). Thus: $h(\beta) = 0 (= 2)$, in case of a stable (unstable) node and $h(\beta) = 1$ in case of a saddle.

As a corollary, we have (cf. Theorem 8.2.8 in [21], and [35]), there is a variable (Riemannian) metric $R(\cdot)$ on T, such that:

$$\mathrm{grad}_R h = \mathcal{X}(\mathcal{G}),$$

where $\mathrm{grad}_R h$ is a vector field on T of the form: (w.r.t. local coordinates $\mathbf{x}$ for T)

$$\mathrm{grad}_R h(\mathbf{x}) = -R^{-1}(\mathbf{x}) D^T h(\mathbf{x}).$$

Here $R(\mathbf{x})$ is a symmetric, positive definite 2×2-matrix, with coefficients depending in a C^1-fashion on $\mathbf{x}$. Note that the direction of $\mathrm{grad}_R h$ is uniquely determined by the above transversality Condition 2., whereas on the neighborhoods N around the $\mathcal{X}(\mathcal{G})$-equilibria, the matrices $R(\cdot)$ are just the 2×2-unit matrix I_2. Moreover, $\mathrm{grad}_R h(\mathbf{x}) \neq 0$, if and only if $\mathbf{x}$ is outside the set $\mathrm{Crit}(h)$ (= set of $\mathcal{X}(\mathcal{G})$-equilibria).

For $\mathbf{x} \notin \mathrm{Crit}(h)$, let $\mathrm{grad}^{\perp}_{R(\mathbf{x})} h(\mathbf{x}) \neq 0$, be a vector R-orthogonal to $\mathrm{grad}_{R(\mathbf{x})} h(\mathbf{x})$, i.e.

$$(\mathrm{grad}^{\perp}_{R(\mathbf{x})} h(\mathbf{x}))^T . R(\mathbf{x}) . (-R^{-1}(\mathbf{x}) . D^T h(\mathbf{x}))[= -Dh(\mathbf{x}) . \mathrm{grad}^{\perp}_{R(\mathbf{x})} h(\mathbf{x})] = 0. \qquad (28)$$

Let x_0 be a point in the level set $L_c = \{x \in T \mid h(x) = c; c = \text{ constant}\}$. Then we have

- Assume $x_0 \notin \mathrm{Crit}(h)$, thus L_c is, locally around x_0, a regular curve. By (28) this local curve is R-orthogonal to the trajectory of $\mathcal{X}(\mathcal{G})$ $(= \mathrm{grad}_R h)$ through x_0.
- If $x_0 \in \mathrm{Crit}(h)$, then x_0 is either an isolated point, surrounded by closed regular curves $L_c, c \neq 0, 2$ (in the case where x_0 is a $\mathcal{X}(\mathcal{G})$-node), or a ramification point at the intersection of two (orthogonal) components of L_1 (in case of a $\mathcal{X}(\mathcal{G})$-saddle). This follows from the fact that on the neighborhoods N around the equilibria of $\mathcal{X}(\mathcal{G})$, the Riemannian metric R is just the standard one.

So, we may subdivide the level sets L_c into the disjunct union of maximal regular curves (to be referred to as to the level lines L_c) and single points (in $\mathrm{Crit}(h)$). Let $\mathbf{x}(t), \mathbf{x}(0) \notin \mathrm{Crit}(h)$ be a trajectory for $\mathcal{X}(\mathcal{G})$ $(= \mathrm{grad}_R h)$. Since $R^{-1}(\mathbf{x})$ is a symmetric, positive definite matrix:

$$\frac{d}{dt} h(\mathbf{x}(t))|_{t=0} = Dh(\mathbf{x}(0)).\mathbf{x}'(0) = Dh(\mathbf{x}(0)).(-R^{-1}(\mathbf{x}(0))).D^T h(\mathbf{x}(0))) < 0 \qquad (29)$$

So, $h(\mathbf{x}(t))$ decreases when t increases, and by the self indexing Condition 3: $0 \leq h(x) \leq 2$, all $x \in T$. By (29), when travelling along the boundary of an open canonical $\mathcal{X}(\mathcal{G})$-region[$=\mathcal{G} \wedge \mathcal{G}^*$-face], say $\overline{\overline{\mathcal{R}}}_{ij}$ in Fig. 26, the functional values of h vary strictly from 2 (at the unstable node v_j^*) via 1 (at a saddle σ_1 or σ_2) to 0 (at the stable node v_i). From this it follows -use also the transversality Condition 2 - that a level line L_c , entering $\overline{\overline{\mathcal{R}}}_{ij}$ through the boundary $\partial\overline{\overline{\mathcal{R}}}_{ij}$ between v_i and σ_1 [thus $0 < c < 1$], must leave this region through $\partial\overline{\overline{\mathcal{R}}}_{ij}$ between v_i and σ_2 . Also: if L_c enters $\overline{\overline{\mathcal{R}}}_{ij}$ through $\partial\overline{\overline{\mathcal{R}}}_{ij}$ between v_j^* and σ_1 [thus $1 < c < 2$], then it leaves $\overline{\overline{\mathcal{R}}}_{ij}$ through $\partial\overline{\overline{\mathcal{R}}}_{ij}$ between v_j^* and σ_2. By the same argumentation: the saddles σ_1 and σ_2 are connected by a level line L_1. Considering unions of all $\mathcal{G} \wedge \mathcal{G}^*$-faces incident with the same vertex representing a stable (unstable) attractor of $\mathcal{X}(\mathcal{G})$, we find: the level sets $L_c, c \neq 0, 1$ or 2, are closed smooth regular curves, either contractable to a stable attractor [in case $0 < c < 1$], or to an unstable attractor [in case $1 < c < 2$] . Altogether, a level line L_c is either a closed curve, or it connects two different $\mathcal{X}(\mathcal{G})$-saddles. Hence, the following definition makes sense: (compare also Definition 6.18)

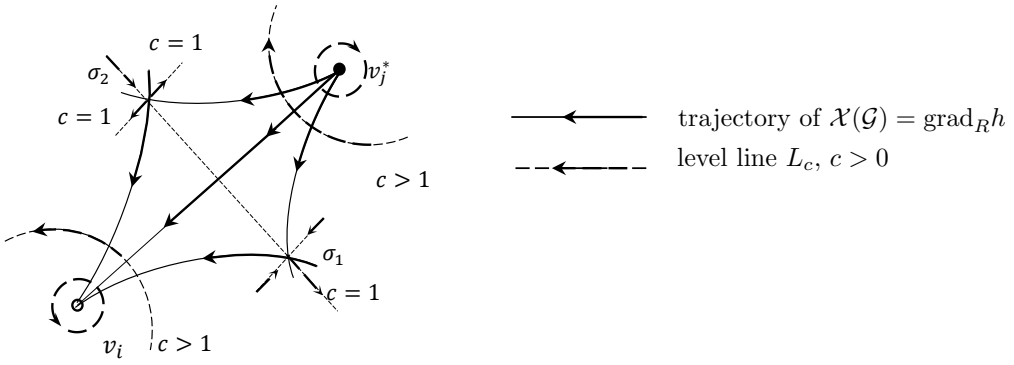

Figure 26: The canonical $\mathcal{X}(\mathcal{G})$-region $\overline{\overline{\mathcal{R}}}_{ij}$.

Definition 8.2. The graph $\mathcal{G}^\perp$ on the torus T is given by:

- Vertices are the $2r$ saddles for $\mathcal{X}(\mathcal{G})$ on T.
- Edges are the $4r$ level lines L_1 connecting different saddles of $\mathcal{X}(\mathcal{G})$.

Apparently, $\mathcal{G}^{\perp}$ is cellularly embedded, and by Euler's theorem this graph is connected (since there are $2r$ faces, determined by the stable and unstable nodes of $\mathcal{X}(\mathcal{G})$). So, the function h admits the same value on (the edges and vertices of) $\mathcal{G}^{\perp}$, whereas by the self indexing Condition 3 - we know that this value equals 1. Thus, the embedded graph $\mathcal{G}^{\perp}$ as a point set in T is just the level set L_1. This leads to Fig. 27, where we present the graphs $\mathcal{G}$, $\mathcal{G}^*$ and $\mathcal{G}^{\perp}$, together with some more level lines L_c. We endow the level lines $L_c, 0 < c < 1$ (the level lines $L_c, 1 < c < 2$) with the anti-clockwise (clock-wise) orientation. Doing so, we can turn $\mathcal{G}^{\perp}$ into a oriented graph; see Fig. 27.

We fix the vector field $\mathrm{grad}^{\perp}_{R(\mathbf{x})}h(\mathbf{x})$ by demanding that it has the same length as $\mathrm{grad}_R h(\mathbf{x})$ (w.r.t. the norm, induced by $R(\mathbf{x})$) and is oriented according to the orientation of the level line L_c through $\mathbf{x}$, see Fig. 26. So, by (28), we may interpret the net of $\mathcal{X}(\mathcal{G})$-trajectories and level lines L_c, as the R-orthogonal net of trajectories for the vector fields $\mathrm{grad}_R h$ and $\mathrm{grad}^{\perp}_R h$. The switch from $\mathcal{X}(\mathcal{G})$ to $\mathcal{X}(\mathcal{G}^*)$ $(=-\mathcal{X}(\mathcal{G}))$ causes the reverse of the orientations in this net. So, for the open canonical regions of $\mathcal{X}(\mathcal{G})$ and $\mathcal{X}(\mathcal{G}^*)$, we have $\overline{\overline{\mathcal{R}}}_{ij} = \overline{\overline{\mathcal{R}}}^*_{ji}$ (as point sets). However, the role of v_i and v_j^*, and of σ_1 and σ_2 (w.r.t. the orientations of the trajectories) is exchanged. see Fig. 28, where the equal angles at v_i and v_j^* in $\overline{\overline{\mathcal{R}}}_{ij}$ and $\overline{\overline{\mathcal{R}}}^*_{ji}$ are denoted by α.
Reasoning as in the case of the function h for $\mathcal{X}(\mathcal{G})$, we find a self indexing smooth function, say g, for $\mathcal{X}(\mathcal{G}^*)$ with the following property:
"When traveling along the boundary of $\overline{\overline{\mathcal{R}}}^*_{ji}$, the functional values of g vary strictly from 2 (at the unstable node v_i) via 1 (at a saddle σ_1 or σ_2) to 0 (at the stable node v_j^*)."

Consider an arbitrary $\mathcal{X}(\mathcal{G})$-trajectory, say γ_{Δ}, in $\overline{\overline{\mathcal{R}}}_{ij}$, approachng v_i under a positive angle Δ with the $\mathcal{G}$-edge $(=\mathcal{X}(\mathcal{G})$-trajectory) $v_i\sigma_1$; see Fig. 28. The set of all such trajectories is parametrized by the values of Δ in the interval $(0, \alpha)$ and the functional values of h (or g) on $\overline{\overline{\mathcal{R}}}_{ij}$. We map γ_{Δ} onto the half ray $r(x)\exp(i\Delta), x \in \gamma_{\Delta}$, where

$$r(x) = h(x), \text{ if } x \text{ is on } \gamma_{\Delta} \text{ between } v_i \text{ and } p \ (=\text{intersection } \gamma_{\Delta} \cap L_1),$$
$$r(x) = \frac{1}{g(x)}, \text{ if } x \text{ is on } \gamma_{\Delta} \text{ between } p \text{ and } v_j^*.$$

In this way, the R-orthogonal net of trajectories for $\mathcal{X}(\mathcal{G})$ $(=\mathrm{grad}_R h)$ and $\mathrm{grad}^{\perp}_R h$ on $\overline{\overline{\mathcal{R}}}_{ij}$ can be homeomorphically mapped onto the polar net on the open sector , say $s(\overline{\overline{\mathcal{R}}}_{ij})$, in the complex plane as in Fig. 29-(a). Here 0 corresponds to v_i, and $\sigma_1^{'}$, $\sigma_2^{'}$ (both situated on the unit circle) are related to respectively σ_1 and σ_2.

Similarly, the trajectory $\gamma^*_{\Delta^*}$ in $\overline{\overline{\mathcal{R}}}^*_{ji}$ can be mapped onto the half ray $\frac{1}{r(x)}\exp(i\Delta^*), x \in \gamma^*_{\Delta^*}$, where Δ^* is the angle at v_j^* between this trajectory and the $\mathcal{G}^*$-edge $v_j^*\sigma_1$, see Fig. 28, where $\Delta^* = \Delta$ (apart from orientation). Hence, the R-orthogonal net of trajectories for $\mathcal{X}(\mathcal{G}^*)$ $(=-\mathrm{grad}_R h)$ and $-\mathrm{grad}^{\perp}_R h$ on $\overline{\overline{\mathcal{R}}}^*_{ji}$ can be homeomorphically mapped onto the polar net on the sector, obtained from $s(\overline{\overline{\mathcal{R}}}_{ij})$ by reflection in the real axis. We call this sector $S(\overline{\overline{\mathcal{R}}}^*_{ji})$. Here 0 corresponds to v_j^*, and $(\sigma_1^*)'$, $(\sigma_2^*)'$ (both situated on the unit circle) are related to respectively σ_1 and σ_2. Reversing the orientations of the polar net in the latter section, we obtain a polar net, oriented as the $\mathcal{X}(\mathcal{G})$ $(=\mathrm{grad}_R h)$ and $\mathrm{grad}^{\perp}_R h$-trajectories on $\overline{\overline{\mathcal{R}}}_{ij}$. Endowed with this polar net we rename $S(\overline{\overline{\mathcal{R}}}^*_{ji})$ as $S(\overline{\overline{\mathcal{R}}}_{ij})$. Apparently, the polar nets on $s(\overline{\overline{\mathcal{R}}}_{ij})$ and $S(\overline{\overline{\mathcal{R}}}_{ij})$ correspond under the inversion $z \to \frac{1}{z}$. Compare Fig. 29-(a),(b). In the same way, we map a neighbouring region $\overline{\overline{\mathcal{R}}}_{ij'}$ as in Fig. 28, homeomorphically onto the sector $s(\overline{\overline{\mathcal{R}}}_{ij'})$ in Fig. 29-(a) and also onto $S(\overline{\overline{\mathcal{R}}}_{ij'})$ in Fig. 29-(c). Repeating this procedure we are able to map all canonical regions of $\mathcal{X}(\mathcal{G})$ onto (the closures of) sectors of the types

$s(\cdot)$ and $S(\cdot)$ in such a way that together they cover -for each value of i and j a copy of the complex plane. (Compare also Fig. 18 and 19).

In analogy with Remark 6.20 , we consider the reduced torus $\check{T} = T\backslash\{\mathcal{G} \wedge \mathcal{G}^*\text{-vertices}$, and on $\check{T}$ the covering by open neighborhoods

$$\{F^*_{v_i}\backslash v_i, F_{v_j^*}\backslash v_j^*\}, i, j = 1.\cdots, r,$$

, where $F^*_{v_i}$ and $F_{v_j^*}$ stand for the basins of $\mathcal{X}(\mathcal{G})$ for respectively v_i and v_j^*. Again, only intersections of the type $(F^*_{v_i}\backslash v_i) \cap (F_{v_j^*}\backslash v_j^*)$ are possibly non-empty. Even so, such an intersection consists of the disjoint union of regions of the type $\overline{\overline{\mathcal{R}}}_{ij}$, say $\overline{\overline{\mathcal{R}}}^1_{ij}, \cdots, \overline{\overline{\mathcal{R}}}^s_{ij}$, s is the amount of vertices v_i(vertices v_j^*) in the Π-walks of $F_{v_j^*}$ (of $F^*_{v_i}$). Note that at v_i, (resp. v_j^*) these regions $\overline{\overline{\mathcal{R}}}^k_{ij}$, are endowed with the anti-clockwise (clockwise) cyclic orientation, and are separated by regions not of this type; compare Remark 6.8 and Section 7.2.

Now, we proceed as in Remark 6.20: The open covering of $\check{T}$ provides this manifold with a complex analytic structure, exhibiting coordinate transfomations

$$s(\overline{\overline{\mathcal{R}}}^k_{ij}) \leftrightarrow S(\overline{\overline{\mathcal{R}}}^k_{ij}), i, j = 1.\cdots, r,$$

induced by the inversion $z \to \frac{1}{z}$. We pull back the restrictions of the function z (resp. $\frac{1}{z}$) on the various sectors $s(\overline{\overline{\mathcal{R}}}^k_{ij})$, resp. $S(\overline{\overline{\mathcal{R}}}^k_{ij})$ to $\check{T}$. By glueing all canonical regions for $\mathcal{X}(\mathcal{G})$ along the trajectories in their common boundaries, we construct a complex analytic function on $\check{T}$. Continuous extension to T, yields a meromorphic function, say f on T, with r simple zeros (poles) at v_i (v_j^*) and $2r$ simple saddles at $\sigma_1, \cdots, \sigma_{2r}$. Since $\overline{\mathcal{N}}(z) = -z; \overline{\mathcal{N}}(\frac{1}{z}) = -\frac{1}{z}$, we find $\mathcal{X}(\mathcal{G}) = \overline{\overline{\mathcal{N}}}(f)$, thus $\mathcal{G} = \mathcal{G}(f)$. This proves Lemma 8.1.

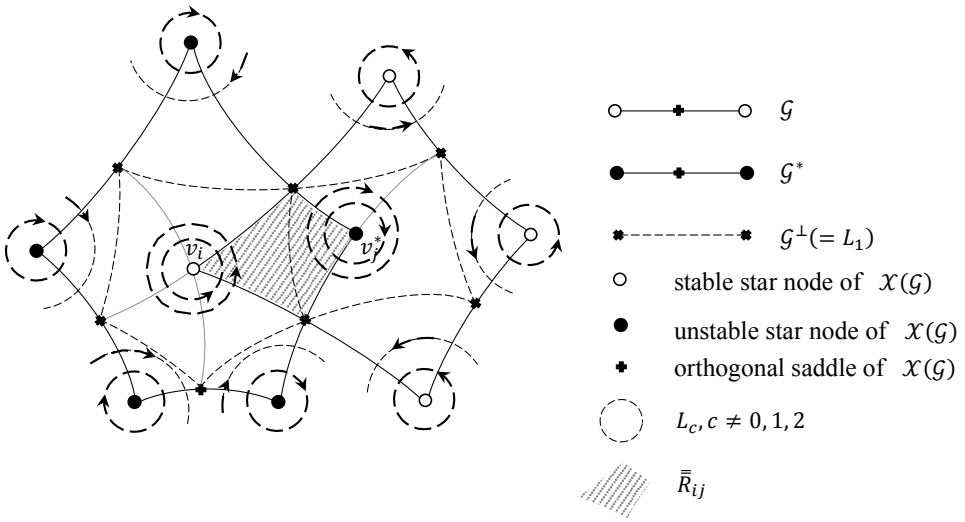

Figure 27: The graphs $\mathcal{G} \wedge \mathcal{G}^*$, $\mathcal{G}^\perp$ and some level sets for h.

We combine this result together with results obtained in the preceding sections as follows:

Theorem 8.3. *Up to conjugacy* ($\sim$) *between flows and equivalency* ($\sim$) *between graphs, the structurally stable Newton flows of r-th order are 1-1 represented by the Newton graphs of order r.*

Proof. Follows from Corollary 7.16 , Lemma 8.1 and Lemma 6.10. □

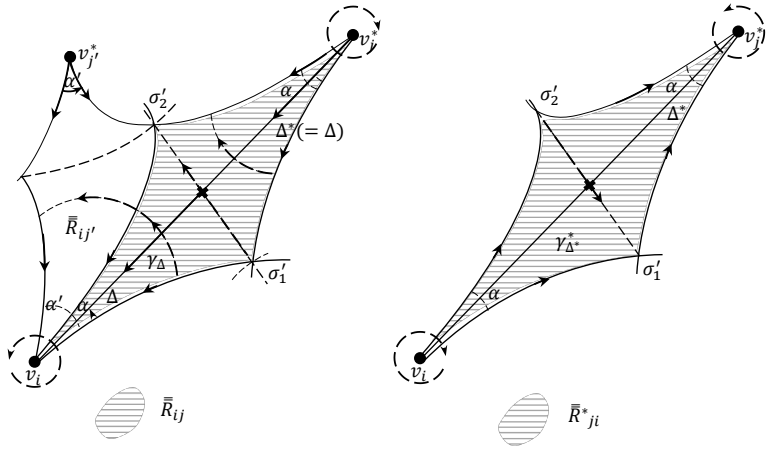

Figure 28: $\overline{\overline{\mathcal{R}}}_{ij}$ and $\overline{\overline{\mathcal{R}}}_{ij}^*$

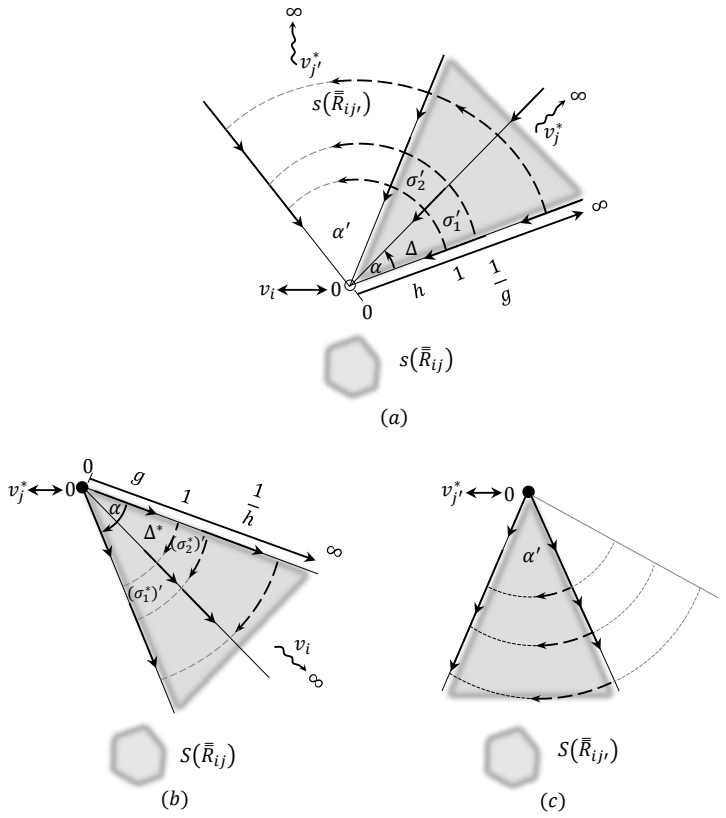

Figure 29: $s(\overline{\overline{\mathcal{R}}}_{ij})$, $S(\overline{\overline{\mathcal{R}}}_{ij})$ and $s(\overline{\overline{\mathcal{R}}}_{ij'})$, $S(\overline{\overline{\mathcal{R}}}_{ij'})$

9 Classification of Newton graphs of order 3

Let $\mathcal{G}(=(\mathcal{G},\Pi))$ be an arbitrary Newton graph of order r, and $\mathcal{G}^*(=(\mathcal{G}^*,\Pi^*))$ a geometrical dual of $\mathcal{G}$. [Thus $\mathcal{G}^*$ is also a Newton graph of order r (cf. Lemma 7.14)]. The vertices and faces of $\mathcal{G}$ are denoted by v_i, respectively by F_{r+i}. The $\mathcal{G}^*$-vertex "located" in F_{r+i} is denoted by v_{r+i}^*, and the $\mathcal{G}^*$-face that "contains" v_i by $F_i^*, i = 1,\cdots,r$. In forthcoming figures, the vertices $\mathcal{G}$ and $\mathcal{G}^*$ will be indicated by their indices in combination with the symbols $\circ$ and $\bullet$ respectively, i.e. $v_i \leftrightarrow \circ_i$, and $v_{r+i}^* \leftrightarrow \bullet_{r+i}$. This induces an indexation of the faces of $\mathcal{G}$ and $\mathcal{G}^*$ as follows: $F_{r+i} \leftrightarrow \bullet_{r+i}$ and $F_i^* \leftrightarrow \circ_i$.

We consider the common refinement $\mathcal{G}\wedge\mathcal{G}^*$ of $\mathcal{G}$ and $\mathcal{G}^*$, and the abstract, directed graph $\mathbb{P}(\mathcal{G})$ underlying $\mathcal{G}\wedge\mathcal{G}^*$. This graph[25] has vertices on three levels (cf. Subsection 7.2):
Level 1: The vertices v_i of $\mathcal{G}$.
Level 2: The "intersections" s_k of the pair (e,e^*) of $\mathcal{G}$- and $\mathcal{G}^*$-edges, $k = 1,\cdots,2r$.
Level 3: The vertices v_{r+i}^* of $\mathcal{G}^*$.

By construction of the graph $\mathcal{G}\wedge\mathcal{G}^*$, each s_k has degree 4 (two connections with vertices

[25]Note that if the Newton graphs $\mathcal{G}$ and $\mathcal{G}'$ are equivalent, then $\mathbb{P}(\mathcal{G}) \sim \mathbb{P}(\mathcal{G}')$. On the other hand equivalency between $\mathbb{P}(\mathcal{G})$ and $\mathbb{P}(\mathcal{G}')$ does not imply $\mathcal{G} \sim \mathcal{G}'$. In fact, as an additional (sufficient) condition, corresponding vertices of $\mathbb{P}(\mathcal{G})$ and $\mathbb{P}(\mathcal{G}')$ should exhibit coherently oriented rotation systems.

on *Level* 1 and two connections with vertices on *Level* 3), whereas the vertices on Level 1 and 3 are not connected. As in Subsection 7.2 we put $\delta_i = \deg(v_i)$ and $\delta_i^* = \deg(v_{r+i}^*)$. We have then:

Lemma 9.1. *The following relatons hold:*

$$1 < \delta_i \leq 2r, 1 < \delta_i^* \leq 2r, \sum_{i=1}^{r} \delta_i = \sum_{i=1}^{r} \delta_i^* = 4r.$$

and moreover,

No s_k is connected by two edges to the same v_i or the same v_{r+i}^*.

Proof. Follows directly from the *E-property*, applied to the multigraphs $\mathcal{G}$ and $\mathcal{G}^*$. □

Recall that $\delta(= \delta(\mathcal{G})) = (\delta_1, \cdots, \delta_r)$ and $\delta^*(= \delta^*(\mathcal{G})) = (\delta_1^*, \cdots, \delta_r^*)$. Also $\delta(\mathcal{G}^*) = \delta^*(\mathcal{G})$ and $\delta^*(\mathcal{G}^*) = \delta(\mathcal{G})$.

From now on, let $\mathcal{G}$ be a 3^{rd} order Newton graph. We adapt the notations: the $\mathcal{G}$-vertices will be denoted by a, b, c, d, e, f, and the corresponding $\mathcal{G}^*$-vertices by $a^*, b^*, c^*, d^*, e^*, f^*$.

Our aim is to give a complete classification (up to equivalency) of all graphs $\mathcal{G}$. We emphasize that, since $r = 3$, the *E-property* already implies that $\mathcal{G}$ is a Newton graph (cf. Lemma 7.17).

We distinguish between the following three possibilities with respect to the boundaries (or Π-walks) of $\mathcal{G}$-faces :

Case 1: The boundary of one of the $\mathcal{G}$-faces, say ∂F_4, has six edges, i.e. $\delta_4^* = 6$.
Case 2: The boundary of one of the $\mathcal{G}$-faces, say ∂F_4, has five edges, i.e. $\delta_4^* = 5$.
Case 3: **Each** boundary of the faces in $\mathcal{G}$ and $\mathcal{G}^*$ has four edges, i.e. $\delta = \delta^* = (4, 4, 4)$.

By Lemma 9.1 the Cases 1, 2 and 3 are mutually exclusive and cover all possibilities. First we should check wether there exist graphs $\mathcal{G}$ that fulfil the conditions in the above cases, and, even so, to what extend $\mathcal{G}$ is determined by these conditions.

Ad Case 1: Because of the *E-property*, and since there are *no loops*, it is necessary for the existence of $\mathcal{G}$ that the Π-walk w_{F_4} of a possible face F_4 fulfils one of the following conditions:

Subcase 1.1 : Traversing w_{F_4} once, each vertex appears precisely twice.
Subcase 1.2 : Traversing w_{F_4} once, there is one vertex (say v_1) appearing three times, one (say v_2) appearing twice, and one (say v_3) showing up only once.

The (*clockwise oriented*)"Π-polygon" for ∂F_4 has six sides, labelled $a, b, \cdots, f$ and six "corner points", labelled by the vertices v_1, v_2, v_3 (repetitions necessary). Identifying points related to the same $\mathcal{G}$-vertex, brings us back to w_{F_4}. Note that the cyclic permutations of the edges in w_{F_4} that are incident with the same vertex are oriented *anti-clockwise* (compare the conventions in Section 7).

In Subcase 1.1 there are precisely two different -up to relabeling- possibilities for w_{F_4} according to the schemes: (see Fig. 30)

$$w_{F_4} : v_1 a v_2 b v_3 c v_1 d v_2 e v_3 f v_1 a v_2 \tag{30}$$

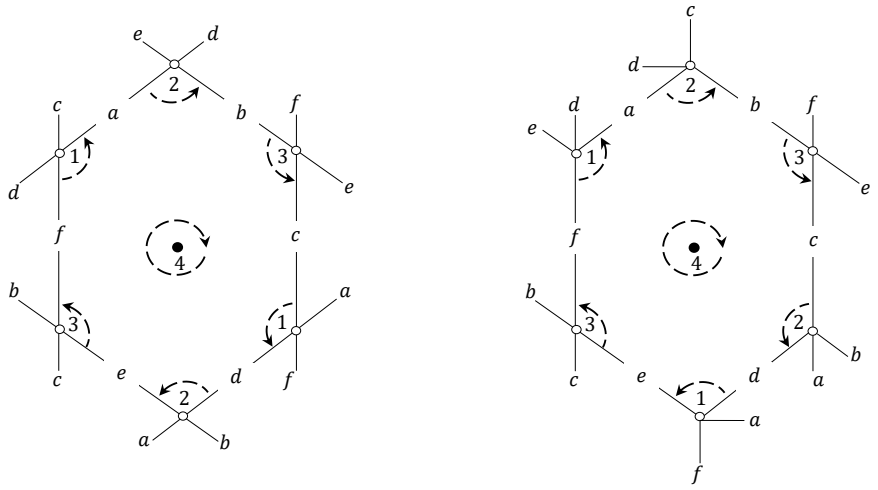

Figure 30: The two possibilities for w_{F_4} in Subcase 1.1.

or

$$w_{F_4} : v_1 a v_2 b v_3 c v_2 d v_1 e v_3 f v_1 a v_2. \tag{31}$$

First, we focus on w_{F_4} given by Scheme (30), see Fig. 30(i). In the (*anti-clockwise*) cyclic permutation of the w_{F_4}-edges, incident with the same vertex, these edges occur in pairs, determining a (positively oriented) sector of F_4. From Subsection 7.2 we know that two F_4-sectors at the same v_i are separated by facial sectors (at v_i) *not* belonging to F_4 (cf. Fig. 30(i)). Since, moreover, the graph we are looking for, admits altogether twelve facial sectors, the cyclic permutation of the edges at v_i are as indicated in Fig. 30(i) and constitute a rotation system that -upto equivalency and relabeling- determines the graph, say $\mathcal{G}$, uniquely.

With the aid of the rotation system in Fig. 30(i) and applying the *face traversal procedure*, as sketched in Subsection 7.1, we find the closed walks $v_2 a v_1 c v_3 e v_2 a v_1$ and $v_2 d v_1 f v_3 b v_2 d v_1$ defining the two other $\mathcal{G}$-faces, say F_5, resp. F_6. (Note that each edge occurs twice in different walks, but with opposite orientation). Glueing together the facial polygons corresponding to F_4, F_5 and F_6, according to equally labeled sides and corner points, gives rise to the plane representations of $\mathcal{G}$ in Fig.31-Scheme (30).

From Fig. 31(i) it follows that the rotation system for $\mathcal{G}^*$ is as depicted in Fig. 32. With the aid of this figure we find, again by the *face traversal procedure*, the following closed subwalks in $\mathcal{G}^*$: $v_4^* a^* v_5^* c^* v_4^* d^* v_6^* f^* v_4^* a^*$, $v_4^* b^* v_6^* d^* v_4^* e^* v_5^* a^* v_4^* b^*$ and $v_4^* f^* v_6^* b^* v_4^* c^* v_5^* e^* v_4^* f^*$, defining the $\mathcal{G}^*$-faces F_1^*, F_2^*, F_3^* respectively. (Note that each edge occurs twice in different walks, but with opposite orientation). Glueing together the facial polygons corresponding to these faces according to equally labeled sides and corner points, yields the plane representations of $\mathcal{G}^*$ in Fig. 31-Scheme (30).

If we start from a Π-walk for F_4, according to the Scheme (31), we find (by the same argumentation as above) plane representations for $\mathcal{G}$ and $\mathcal{G}^*$; see Fig. 31-Scheme (31).

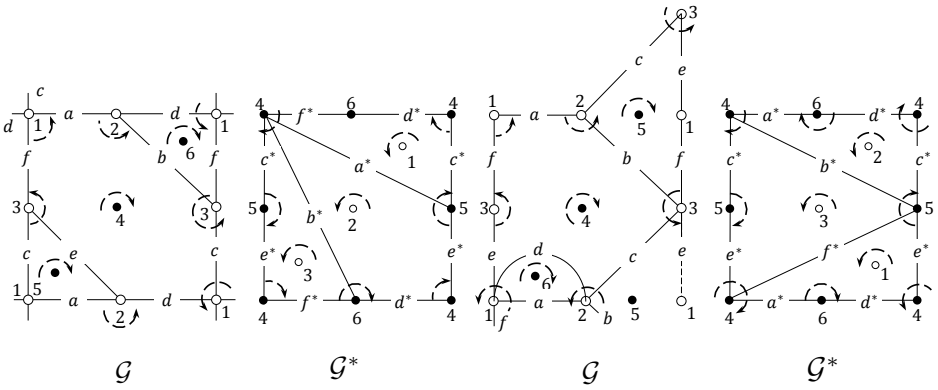

Figure 31: The two possible plane representations for $\mathcal{G}$, $\mathcal{G}^*$ in Subcase 1.1.

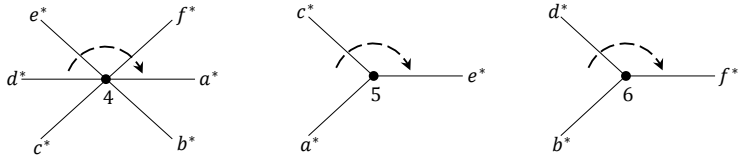

Figure 32: The rotation systems for $\mathcal{G}^*$, according to Scheme (30).

Note that in all graphs in Fig. 31 the anti-clockwise (clockwise) orientation of the cyclic permutations of edges incident with the same vertex induces a clockwise (anti-clockwise) orientation of the faces.

In Subcase 1.2 there is *precisely one* -up to relabeling- possibility for w_{F_4} according to the scheme:

$$w_{F_4} : v_1 a v_2 b v_1 c v_2 d v_1 e v_3 f v_1 a. \tag{32}$$

In this case however, there are *three* pairs of $\mathcal{G}$-edges at v_1 determining (positively measured) sectors of F_4. So, reasoning as in Subcase 1.1, there are two possibilities for the (anti clockwise) cyclic permutations of the $\mathcal{G}$-edges at v_1 (and thus also two different rotation systems; see Fig. 33).

Starting from Fig. 33-(i) and applying the *face traversal procedure*, we find the facial walks $v_1 f v_3 e v_1 b v_2 c v_1 f$ and $v_1 a v_2 d v_1 a$, which together with Scheme (32) define the faces F_5, F_6 and F_4 respectively. Reasoning as in Subcase 1.1, we arrive at the plane realizations of $\mathcal{G}$ and $\mathcal{G}^*$ as depicted in Fig. 34-(i). In the case of Fig. 33-(ii) the facial walks $v_1 d v_2 a v_1 b v_2 c v_1 d$ and $v_1 e v_3 f v_1 e$, together with Scheme (32), define the faces F_5, F_6 and F_4 respectively. Reasoning as in Subcase 1.1, we obtain the plane representations for $\mathcal{G}$ and $\mathcal{G}^*$ as depicted in Fig. 34-(ii).

Note that-in accordance with Lemma 7.5-both graphs $\mathcal{G}$ in Fig. 34 are *self dual*, but-by

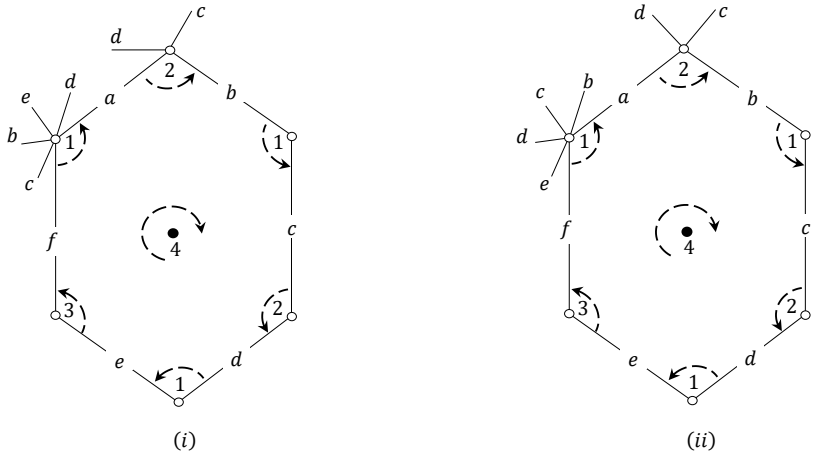

Figure 33: The two possible rotation systems in Subcase 1.2.

inspection of their rotation systems-*not equivalent*.

Ad Case 2: Because the Π-walk of F_4 has no loops and consists of an Euler trail on the five edges of $\mathcal{G}$, there is only one- up to relabeling - possibility for w_{F_4} (see Fig. 35-(i)):

$$w_{F_4} : v_1 a v_3 b v_2 c v_1 d v_2 e v_1 a.$$

In contradistinction with the previous Case 1, now there is one edge, namely f, that is not contained in w_{F_4}. By Lemma 9.1, this edge must connect either v_1 to v_2 ($f : v_1 \leftrightarrow v_2$), or v_1 to v_3 ($f : v_1 \leftrightarrow v_3$), or v_2 to v_3 ($f : v_2 \leftrightarrow v_3$); compare Fig. 35-(ii) where we show the part of $\mathbb{P}(\mathcal{G})$ that is determined by ∂F_4. We focus on the first two sub cases.

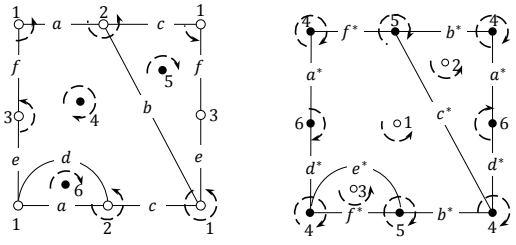

$\mathcal{G}$ $\mathcal{G}^*$

$$\delta(\mathcal{G}) = (6,4,2) = \delta(\mathcal{G}^*)$$

(i)

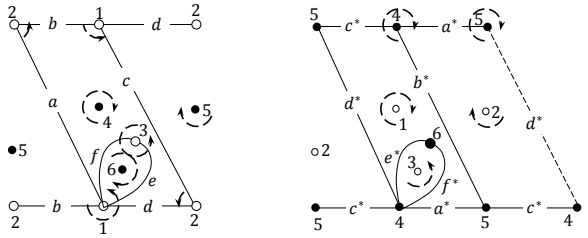

$\mathcal{G}$ $\mathcal{G}^*$

$$\delta(\mathcal{G}) = (6,4,2) = \delta(\mathcal{G}^*)$$

(ii)

Figure 34: The two possible plane representations for $\mathcal{G}$, $\mathcal{G}^*$ in Subcase 1.2.

Taking into account the various positions of f with respect to local sectors of F_4 at v_1 and v_2 (when $f : v_1 \leftrightarrow v_2$), respectively v_1 and v_3 (when $f : v_1 \leftrightarrow v_3$), we find *four* respectively *two* possibilities for the rotation systems; see Fig. 36. The Subcases $f : v_1 \leftrightarrow v_3$ and $f : v_2 \leftrightarrow v_3$ are not basically different[26]. So, we may neglect the case $f : v_2 \leftrightarrow v_3$. Reasoning as in Case 1, the rotation systems in Fig. 36 yield the possible planar representations of $\mathcal{G}$ and $\mathcal{G}^*$; see Fig. 37. Note that- by inspection of their rotation systems -all graphs $\mathcal{G}$ in this figure are different under *orientation preserving equivalencies*, whereas *only* in the cases of Fig. 37(iii) and (iv) these graphs are equal w.r.t. an *orientation reversing equivalency* (apply the relabeling introduced in Footnote 26). Apparently, the graphs $\mathcal{G}$ and $\mathcal{G}^*$ (and thus also $\mathcal{G}^*$ and $\mathcal{G}$) in Fig. 37(i), resp. Fig. 37(v) are equal (under an orientaten preserving equivalency). The graphs $\mathcal{G}$ in Fig. 37 (ii)-(iv),(vi) are *self-dual* (compare Corollary 7.6).
Ad Case 3: Without loss of generality, there are a priori *two* possibilities for the Π-walks of an arbitrary face, say F_4; see Fig. 38(i) and (ii). By Lemma 9.1 and by inspection of the corresponding partial graph $\mathbb{P}(\mathcal{G})$, the first possibility is ruled out. So, we focus on Fig. 38(ii). Recall that two facial sectors at the same vertex v_i are separated by facial sectors (at v_i) *not* belonging to F_4 and that in the actual case we have $\delta = \delta^* = (4,4,4)$. So, we find

[26] Relabeling $v_1 \leftrightarrow v_2$, $a \leftrightarrow b$ and $c \leftrightarrow e$, transforms the two configurations in Fig.36(v) and (vi) into configurations that generate (anti-clockwise oriented) rotation systems describing the case $f : v_2 \leftrightarrow v_3$.

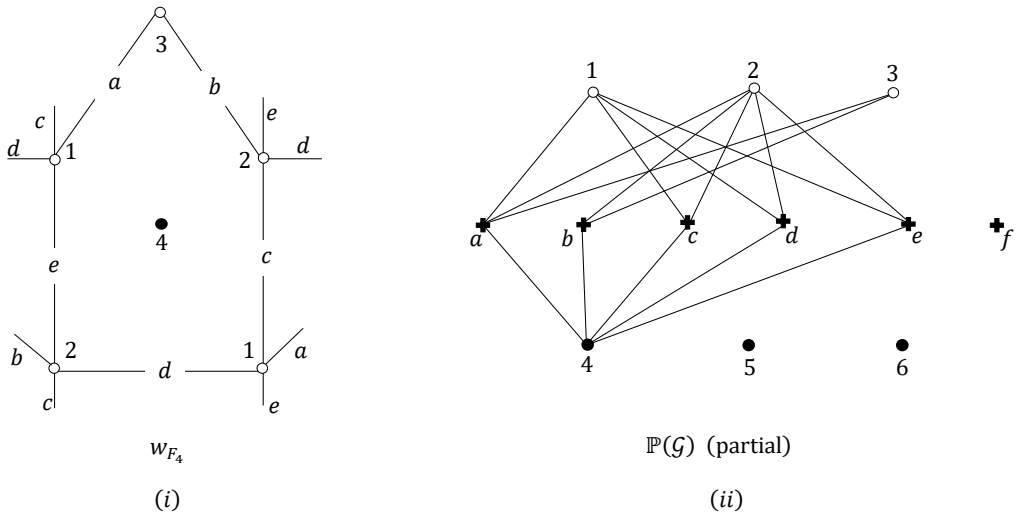

Figure 35: The Π-walk for F_4 in Case 2.

the rotation systems and the distribution of "local facial sectors" as depicted in Fig. 38(ii), where the roles of both e, f and F_5, F_6 may be interchanged. Now, by the face traversal procedure we find:

Apart from relabeling and equivalency, there is only one (self dual) graph possible, Fig. 39.

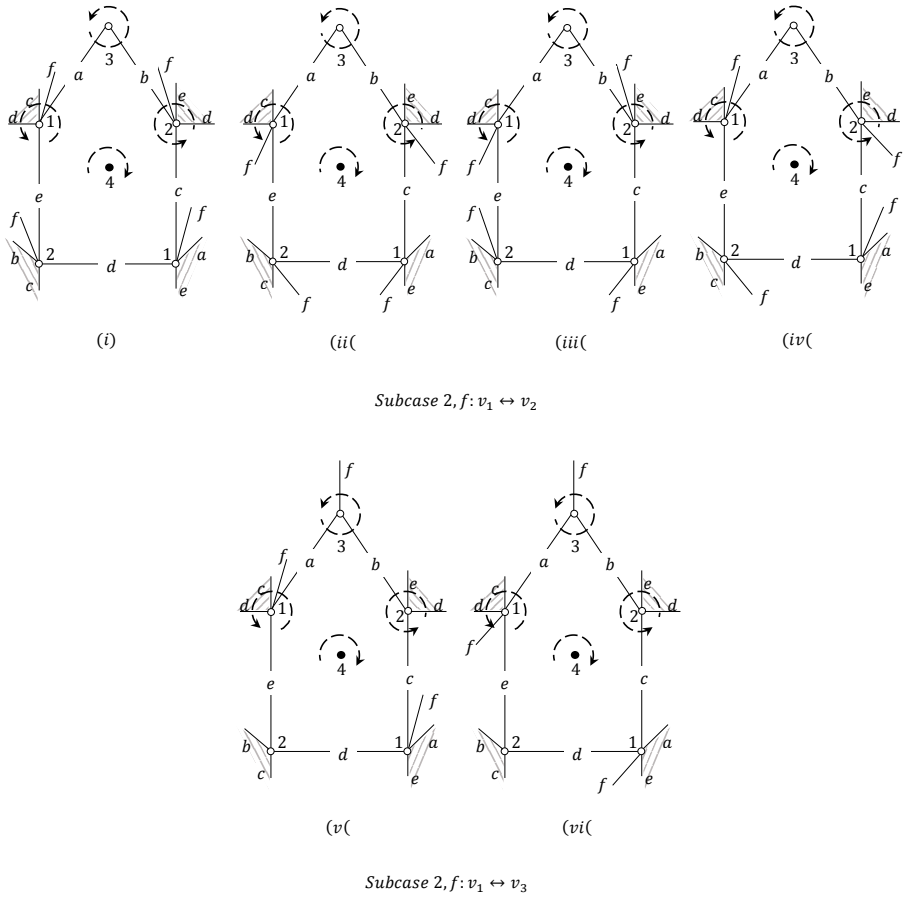

Figure 36: The possible rotation systems for $\mathcal{G}$ in Case 2.

Theorem 8.3, together with the above analysis of the 3^{rd} order Newton graphs yields:

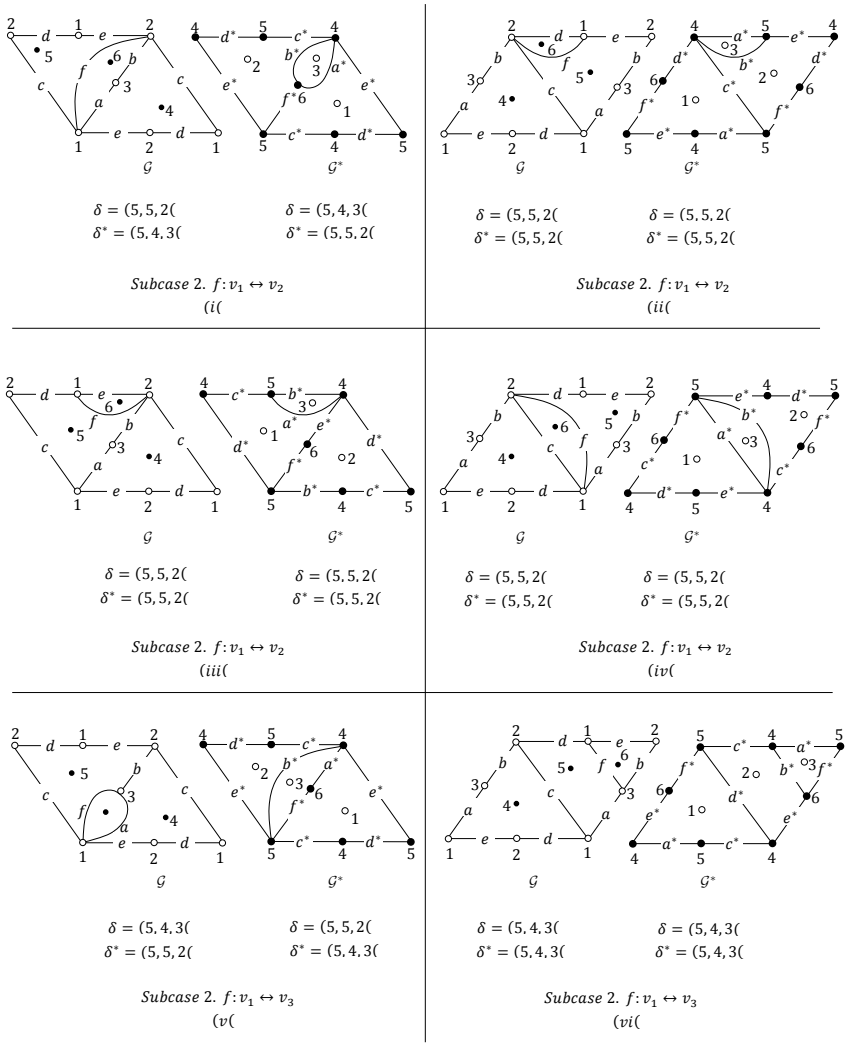

Figure 37: The graphs $\mathcal{G}$ and $\mathcal{G}^*$ in Case 2.

Theorem 9.2. *Apart from conjugacy and duality , there are precisely nine possibilities for the 3^{rd} order structurally stable Elliptic Newton flows. These possibilities are characterized by the Newton graphs in Fig. 40.*

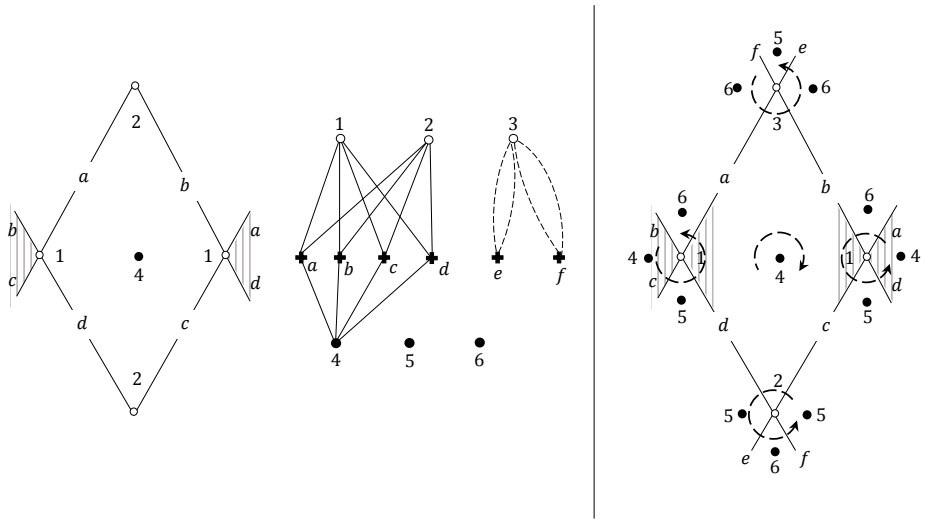

Figure 38: Apriori possibilities for w_{F_4} in Case 3.

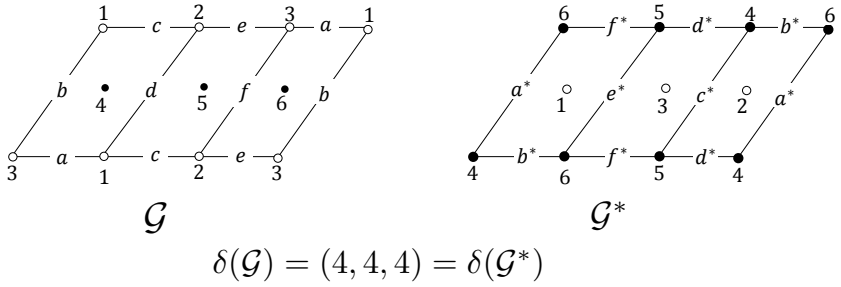

Figure 39: The only possible graphs $\mathcal{G}$ and $\mathcal{G}^*$ in Case 3.

Remark 9.3. *The Case* $r = 2$.
By similar (even easier) arguments as used in the above Case $r = 3$, it can be proved that -up to conjugacy-there is only one (self-dual) possibility for the 2^{nd} order Newton graphs; see Fig.41 (Note that in view of the E-property both facial walks of such graphs have length 4, whereas because of Lemma 7.17 the role of the A-property is not relevant). Together with Theorem 8.3 this yields a proof of Corollary 6.13.

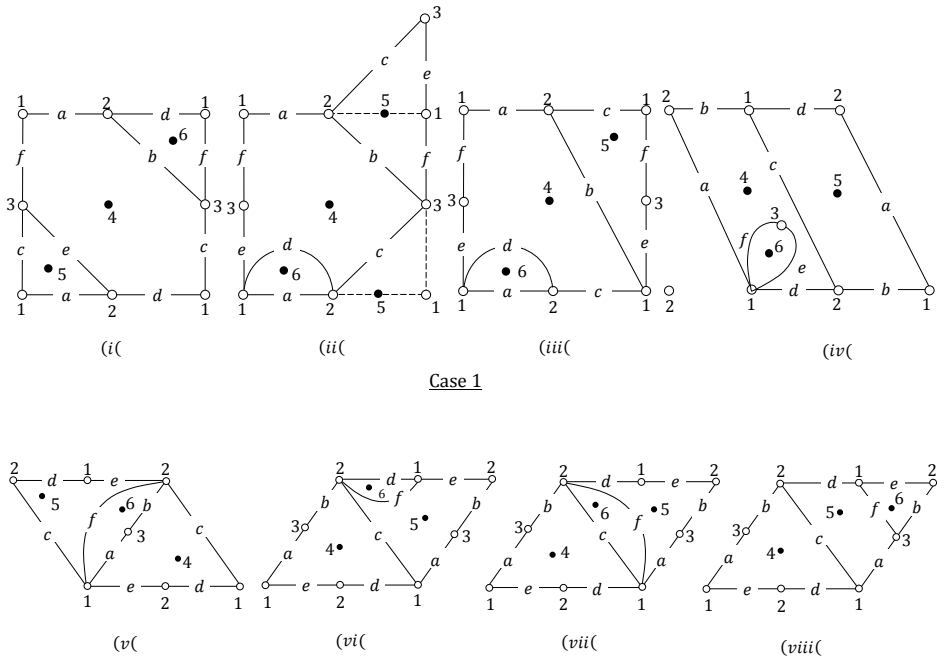

Figure 40: The nine graphs characterizing the flows $\overline{\overline{\mathcal{N}}}(f), f \in \tilde{E}_3$.

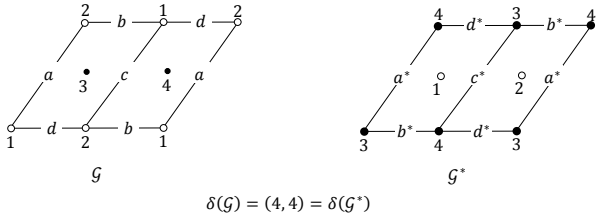

Figure 41: The 2^{nd} order Newton graphs.

10 Pseudo Newton graphs

Throughout this section, let $(\mathcal{G}_r, \Pi)$ be a Newton graph of order r, i.e. a connected multigraph, cellularly embedded in T, with r vertices, $2r$ edges and r faces ($r \geq 2$) that fulfils both the A- and E-property. We adopt the notations as introduced in Section 7, but occasionally write - if no confusion is possible - $\mathcal{G}_r$ instead of $(\mathcal{G}_r, \Pi)$.

Due to the *E-property*, we know that an arbitrary edge of $\mathcal{G}_r$ is contained in precisely two different faces. If we delete such an edge from $\mathcal{G}_r$ and merge the involved faces F_1, F_2 into a new face, say $F_{1,2}$, we obtain a toroidal connected multigraph (again cellularly embedded) with r vertices, $2r-1$ edges and $r-1$ faces: $F_{1,2}$, $F_3, \cdots, F_r$.
If $r = 2$, then this graph has only one face.
If $r > 2$, put $J = \{1, 2\}$, thus $\emptyset \neq J \subsetneq \{1, \cdots, r\}$. Then, we know, by the A-property (cf. Lemma 7.8 (proof)), that $\mathrm{Ext}(\mathcal{G}(J)) \neq \emptyset$. Let v be an exterior vertex of $\mathcal{G}(J)$. If all edges incident with v, are adjacent only to F_1 or F_2, then v must be an interior vertex of $\mathcal{G}(J)$. This is in contradiction with our assumption on v. So, the boundary $\partial F_{1,2}$ contains an edge belonging to another face than F_1 or F_2 , say F_3. Delete this edge and obtain the "merged face" $F_{1,2,3}$.
If $r = 3$, the result is a graph with only *one* face.

If $r > 3$, put $J = \{1, 2, 3\}$. By the same reasoning as used in the case $r = 3$, it can be shown that $\partial F_{1,2,3}$ contains an edge belonging to another face than F_1, F_2 or F_3, say F_4 . And so on. In this way, we obtain - in $r-1$ steps - a connected multigraph, say $\check{\mathcal{G}}_r$, with r vertices, $r+1$ edges and only one face.

Obviously, $\check{\mathcal{G}}_r$ contains vertices of degree ≥ 2. Let us assume that there exists a vertex for $\check{\mathcal{G}}_r$, say v, with $\deg(v)$=1. If we delete this vertex from $\check{\mathcal{G}}_r$, together with the edge incident with v, we obtain a graph with $(r-1)$ vertices, r edges and *one* face. If this graph contains also a vertex of degree 1, we proceed successively. The process stops after L steps, resulting into a (connected, cellularly embedded) multigraph, say $\hat{\mathcal{G}}_\rho$. This graph admits $\rho = r - L$ vertices (each of degree ≥ 2), $\rho + 1$ edges and one face.

Apparently[27] we have: $L < r-1$ and thus $2 \leq \rho \leq r$. In particular:
if $r = 2$, then $\rho = 2$ and $L = 0$.
if $r = 3$, then $\rho = 3$ and $L = 0$, or $\rho = 2$ and $L = 1$; see also Fig.42.

From Remark 9.3 it follows that $\mathcal{G}_2$ is unique (up to equivalency); see also Fig. 41. From the forthcoming Corollary 10.2 it follows that also $\check{\mathcal{G}}_2$ is unique. However, a graph $\check{\mathcal{G}}_r, r > 2$, is not uniquely determined by $\mathcal{G}_r$, as will be clear from Fig. 42, where $\mathcal{G}_3$ is a Newton graph (cf. Section 9, Subcase 1.2 and Fig. 34(i)).

Lemma 10.1. *For the graphs $\hat{\mathcal{G}}_\rho$ we have:*
Either

(a_1) *Two vertices are of degree 3, and all other vertices of degree 2,*

or

(a_2) *One vertex is of degree 4, and all other vertices of degree 2.*

(b) *There is a closed, clockwise oriented facial walk, say w, of length $2(\rho+1)$ such that, traversing w, each vertex v shows up precisely $\deg(v)$ times.*

The walk w is divided into subwalks W_1, $W_2, \cdots$, connecting vertices of degree > 2 that contain (apart from these begin- and endpoints) only-if any- vertices of degree 2.

[27] Assume $L = r - 1$.Then $\hat{\mathcal{G}}_\rho, \rho = 1$, would be a connected subgraph of $\mathcal{G}$, with two edges and one vertex; this contradicts the fact that $\mathcal{G}$ has no loops. Compare the forthcoming Definition 10.5.

(c_1) *If $e_1e_2\cdots e_s$ is a walk of type W_i, then this also holds for its inverse*

$$W_i^{-1} := e_s^{-1}\cdots e_2^{-1}e_1^{-1},$$

where e and e^{-1} stand for the same edge, but with opposite orientation.

(c_2) *W_i and W_i^{-1} are not consecutive in w.*

(c_3) *In Case (a_1), there are precisely 6 subwalks of type W_i, each of them connecting different vertices (of degree 3). In fact w is of the form:*

$$w = W_1W_2W_3W_1^{-1}W_2^{-1}W_3^{-1}.$$

(c_4) *In Case (a_2), there are precisely 4 subwalks of type W_i , each of them being closed and containing at least one vertex of degree 2. In fact w is of the form:*

$$w = W_1W_2W_1^{-1}W_2^{-1}.$$

Proof. ad (a): Each edge of $\hat{\mathcal{G}}_\rho$ contributes precisely twice to the set $\{\deg(v), v \in V(\hat{\mathcal{G}}_\rho)\}$. It follows:

$$\sum_{\text{all } \hat{\mathcal{G}}_\rho\text{-vertices } v} \deg(v) = 2(\rho+1). \tag{33}$$

Put $k_i = \sharp\{\text{vertices of degree } i\}, i = 1, 2, 3, \cdots$. Then (33) yields:

$$2k_2+3k_3+4k_4+5k_5+\cdots = 2(k_2+k_3+k_4+k_5+\cdots+1)(= 2(\rho+1)).$$

Thus, either $k_2 = \rho-2, k_3 = 2$, $k_i = 0$ if $i \neq 2, 3$, or $k_2 = \rho-1$, $k_4 = 1$, $k_i = 0$ if $i \neq 2, 4$.

ad (b): The geometrical dual $(\hat{\mathcal{G}}_\rho)^*$ of $\hat{\mathcal{G}}_\rho$ has only one vertex, say v^*. So, all edges of $(\hat{\mathcal{G}}_\rho)^*$ are loops. Hence, in the *facial* walk w of $\hat{\mathcal{G}}_\rho$ that defines v^*, each edge shows up precisely twice (with opposite orientation). Thus w has length $2(\rho+1)$. Traversing w, each facial sector of $\hat{\mathcal{G}}_\rho$ is encountered once and -at a vertex v- there are $\deg(v)$ many of such sectors.

ad (c): Let e_1ve_2 be a subwalk of w with $\deg(v) = 2$. Both e_1^{-1} and e_2^{-1} occur precisely once in w, and $e_2^{-1}ve_1^{-1}$ is a subwalk of w. This yields statement (c_1). If the subwalk $W = e_1e_2\cdots e_s$ and its inverse are consecutive, then either $e_1^{-1}v_1e_1$, or $e_sv_se_s^{-1}$ are subwalks of the facial walk w of $\hat{\mathcal{G}}_\rho$, where v_1 resp. v_s is the begin-(end)point of e_1 resp. e_s. This is impossible, because e_1, e_1^{-1} and also e_s, e_s^{-1} are the same (up to orientation) and $\hat{\mathcal{G}}_\rho$ has no loops. Hence, the assertion in (c_2) holds. Note that if an edge e occurs in W, then the only subwalk of this type where e (or more precisely e^{-1}) shows up is W^{-1}. From this observation, together with (c_1) and (c_2), it follows that:

- In Case a_1: w is of the form $W_1W_2W_3W_1^{-1}W_2^{-1}W_3^{-1}$; see Fig. 43-a_1. In fact, if one of these subwalks, say W_1, would have equal begin- and endpoint, this vertex is also begin- and endpoint for W_1^{-1}, which is impossible, see (a_1) and (b). This yields (c_3).
- In Case a_2: w is of the form $W_1W_2W_1^{-1}W_2^{-1}$; see Fig. 43-a_2. In fact, the four components are closed (because of (a_2)) subwalks and must contain at least one vertex of degree 2 (since otherwise $\hat{\mathcal{G}}_\rho$ would have a loop).

□

An analysis of its rotation system learns that $\hat{\mathcal{G}}_\rho$ is determined by its facial walk w, and thus also by the subwalks $W_1W_2W_3$ (in Case a_1) or W_1W_2 (in Case a_2). In fact, only the length of the subwalks W_i matters.

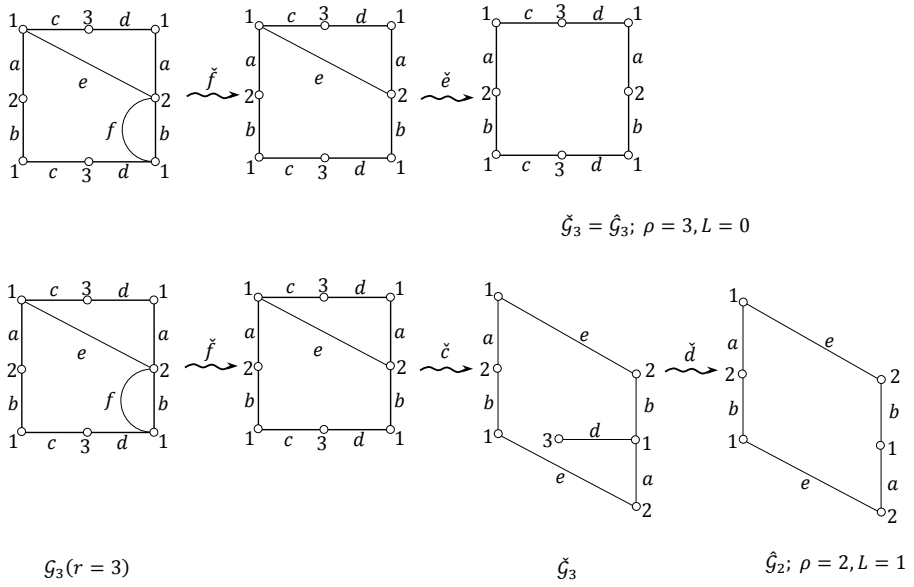

Figure 42: Some graphs $\mathcal{G}_3$, $\check{\mathcal{G}}_r$ and $\hat{\mathcal{G}}_\rho$

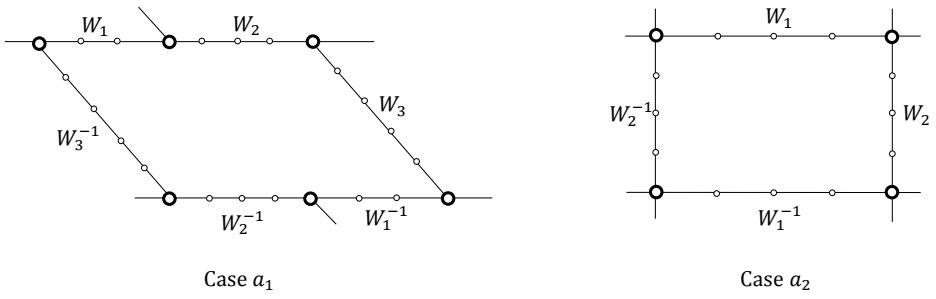

Figure 43: The graphs $\hat{\mathcal{G}}_\rho$

Corollary 10.2. *The graphs $\hat{\mathcal{G}}_2$ and $\hat{\mathcal{G}}_3$ can be described as follows:*

- *By Lemma 10.1 it follows that $\hat{\mathcal{G}}_2$ does not have a vertex of degree 4. So, $\hat{\mathcal{G}}_2$ is of the form as depicted in Fig. 43-a_1, where each subwalk W_i admits only one edge. Hence, there is-up to equivalency- only one possibility for $\hat{\mathcal{G}}_2$. Compare also Fig. 41.*
- *It is easily verified that -in Fig. 44- each graph (on solid and dotted edges) is a Newton graph. In fact, verification of the E-property is sufficient (cf. Lemma 7.17). Hence, in case $\rho = 3$, both alternatives in Lemma 10.1-(a) occur. An analysis of their rotation systems learns that the three graphs with only solid edges in Fig. 44-$(i) - (iii)$ are equivalent, but not equivalent with the graph on solid edges in Fig. 44-(iv). In a*

similar way it can be proved that the graphs in Fig. 44 expose all possibilities(up to equivalency) for $\hat{\mathcal{G}}_3$.

Remark 10.3. *Pseudo Newton graphs*
The graphs such as $\check{\mathcal{G}}_\rho$ and $\hat{\mathcal{G}}_\rho$, obtained from $\mathcal{G}_r$ by deleting edges and vertices in the way prescribed above, are -although derived from Newton graphs- not Newton graphs themselves. Therefore, they will be referred to as to *pseudo Newton graphs*. Replacing (in the inverse order) into $\hat{\mathcal{G}}_\rho$, $\rho = r - L$, the edges and vertices that we have deleted from $\mathcal{G}_r$, we regain subsequently $\check{\mathcal{G}}_r$ and $\mathcal{G}_r$. The following property is obvious:
"Each Newton graph $\mathcal{G}_r$ admits pseudo Newton graphs of the form $\check{\mathcal{G}}.$, $\hat{\mathcal{G}}.$".

Remark 10.4. If we delete from $\hat{\mathcal{G}}_\rho$ an arbitrary edge, the resulting graph remains connected, but the alternating sum of vertices, edges and face equals +1. Thus one obtains a graph that is not cellularly embedded.

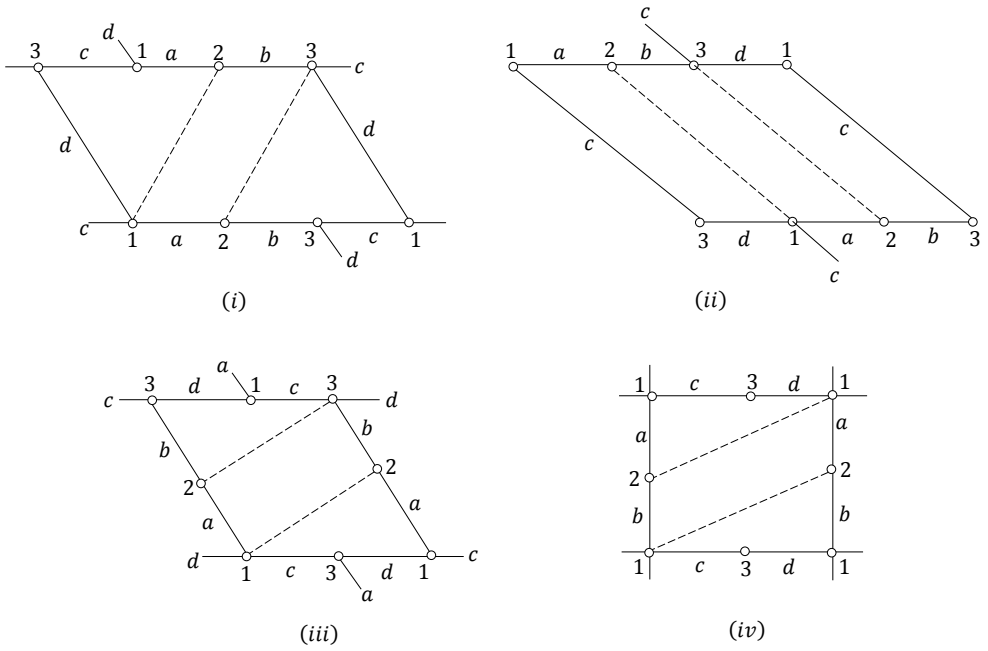

Figure 44: All possible graphs $\hat{\mathcal{G}}_3$

Definition 10.5. A *Nuclear Newton graph* is a cellularly embedded graph in T with one vertex and two edges.

Apparently a Nuclear Newton graph is connected and admits one face and two loops. In particular such a graph has a trivial rotation system. Hence, all nuclear Newton graphs are topologically equivalent and -exposing the same structure as the Pseudo Newton graphs $\hat{\mathcal{G}}_\rho$- will be denoted by $\hat{\mathcal{G}}_1$. Note that a Nuclear Newton graph fulfils the *A-property* (but certainly not the *E-property*). Consequently, a graph of the type $\hat{\mathcal{G}}_1$ is neither a Newton graph, nor equivalent with a graph $\mathcal{G}(f), f \in \check{E}_r$. Nevertheless, Nuclear Newton graphs will play an important role because, in a certain sense, they "generate" all structurally stable Newton flows. This will be explained in Section 12.

11 The nuclear elliptic Newton flow

Throughout this section, let f be an elliptic function of order $r \geq 2$ with -viewed to as to a function on $T = T(\Lambda(\omega_1, \omega_2))$ - only one zero and one pole, both of order r. Our aim is to derive the result on the corresponding (so-called nuclear) Newton flow that was already announced in Remark 5.8.

When studying -up to conjugacy- the nuclear flow $\overline{\overline{\mathcal{N}}}(f)$, we may assume (cf. Theorem 4.6) that $\omega_1 = 1, \omega_2 (= \tau) = i$, thus $\Lambda = \Lambda_{1,i}$. In particular, the period pair $(\omega_1, \omega_2) = (1, i)$ is reduced. Adopting the notations as used in Section 4 and in the proof of Lemma 5.7, we represent $[f]$ (and thus $\overline{\overline{\mathcal{N}}}(f)$), by the Λ-classes $[\mathbf{a_1}], [\mathbf{b_1}]$, where $\mathbf{a_1}$ resp. $\mathbf{b_1}$ stands for the zero, resp. pole, for f, situated in the period parallelogram $P (= P_{1,i})$. Due to (15), (16) we have:

$$\mathbf{b_1} = \mathbf{a_1} + \frac{\lambda_0}{r}, \quad \mathbf{b_1}' = \mathbf{b_1} - \lambda_0.$$

We may assume that $\mathbf{a_1}, \mathbf{b_1}$ are not on the boundary ∂P of P. Since the period pair $(1, i) (= (\omega_1, \omega_2))$ is reduced, the images under f of the P-sides γ_1 and γ_2 are closed Jordan curves (cf. Fig. 11 and use the explicit formula for λ^0 as presented in Section 5). From this, we find that the winding numbers $\eta(f(\gamma_1))$ and $\eta(f(\gamma_2))$ can -a priori- only take the values -1, 0 or +1. The combination $(\eta(f(\gamma_1)), \eta(f(\gamma_2))) = (0, 0)$ is impossible (because $\mathbf{a_1} \neq \mathbf{b_1}$). The remaining combinations lead, for each value of $r = 2, 3, \cdots$, to eight different values for $\mathbf{b_1}$ each of which giving rise, together with $\mathbf{a_1}$, to eight pairs of classes mod Λ that fulfil (9), determining flows in $N_r(\Lambda)$, cf. Fig. 45. Since any two pairs of these classes are related by a unimodular transformation on the periods of Λ, possibly in combination with a transition of the type $\Lambda \to \Lambda^\alpha = \alpha\Lambda$, the corresponding flows are equivalent (cf. the proofs of Lemmas 3.1 and 4.3) and will be denoted by $\overline{\overline{\mathcal{N}}}(f|_{\mathbf{a_1}})$. So, we may focus on one specific pair, say $\mathbf{a_1}, \mathbf{b_1} = \mathbf{a_1} + \frac{1+i}{r}$, and thus $\mathbf{b_1}' = \mathbf{b_1} - (1 + i)$.

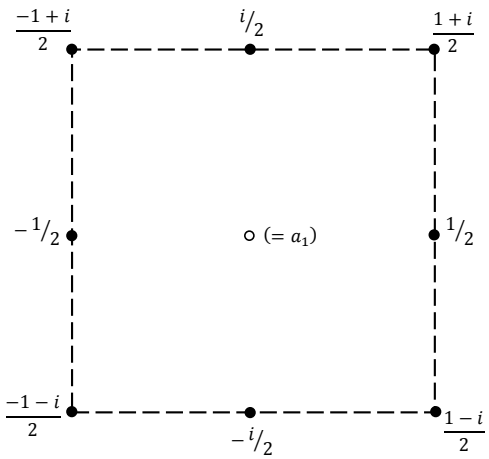

Figure 45: Eight pairs $(\mathbf{a_1}, \mathbf{b_1})$ determining the same nuclear flows; $\mathbf{a_1} = 0$, $r = 2$.

Now, let z_0 be arbitrary in P. The translation $z \mapsto z + z_0 - \mathbf{a_1}$ turns $\overline{\overline{\mathcal{N}}}(f|_{\mathbf{a_1}})$ into an equivalent flow, with only one attractor (z_0) and one repellor: *the* nuclear flow $\overline{\overline{\mathcal{N}}}(f|_{z_0})$ on T. It follows:

Lemma 11.1. *All nuclear elliptic Newton flows of the same order are mutually conjugate.*

So, in order to study the phase portraits of these flows, it is enough to select an arbitrary $\mathbf{a}$ in P and some $\mathbf{b}$ (related to $\mathbf{a}$ by (9)). We choose $\mathbf{a} = 0$ and $\mathbf{b} = \frac{1+i}{r}$, thus $\mathbf{b}' = \frac{1+i}{r} - (1+i)$ and rename $f|_{\mathbf{a}}$ as f . With this choice, the saddles for $\overline{\overline{\mathcal{N}}}(f)$ correspond (cf. Section 5) to the zeros for:

$$
\begin{aligned}
&-\frac{d}{dz}[\log \sigma^r(z-\mathbf{a})/\sigma^{r-1}(z-\mathbf{b})\sigma(z-\mathbf{b}')] \\
&= -r\zeta(z) + (r-1)\zeta(z-\frac{1+i}{r}) + \zeta(z-\frac{1+i}{r}+1+i)
\end{aligned}
$$

(Note that this is an elliptic function with in P two *simple* poles, namely: $0, \frac{1+i}{r}$, thus also two zeros in P). Apart from the periodicity w.r.t. the square P, the phase portrait of $\overline{\mathcal{N}}(f)$, is also symmetric under reflection in the line l through 0 and $1+i$. So, there are two possibilities for the position of these two saddles in P: (cf. Fig. 46)

1. situated on the the line l;
2. not on l, but symmetric w.r.t. to this line; in particular they are different (thus simple) and will be denoted by σ_1, σ_2.

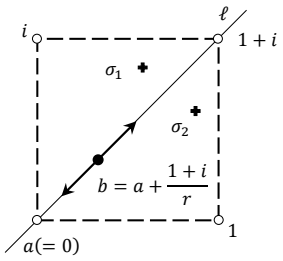

Figure 46: Zero ($\circ$) , pole ($\bullet$) and critical points ($+$) for f in $P(= P_{1,i})$

A careful analysis of how the zeros (sinks) and poles (sources) for f contribute separately to the velocity field of the steady stream corresponding to the flow $\overline{\mathcal{N}}(f)$, learns that the first possibility does not occur. So, we may assume that only the possibility as depicted in Fig. 46 holds. In the sequel, we use the following facts concerning $\overline{\mathcal{N}}(f)$:

(I) periodicity with respect to 1 and i;

(II) invariancy under reflection in the line l;

(III) at a zero (pole) for f -both of order r- each value of $\arg(f)$ appears r times on *equally distributed* incoming (outgoing) $\overline{\mathcal{N}}(f)$-trajectories (cf. the comment on Fig. 2).

From (II), it follows that l is build up of trajectories connecting the zeros and poles for f on l (cf. Fig. 46). In particular, the l-segments, determined by 0 and $\frac{1+i}{r}$, and by $\frac{1+i}{r}$, and $(1+i)$ are $\overline{\mathcal{N}}(f)$-trajectories, connecting the pole $\frac{1+i}{r}$ with the zeros 0 and $(1+i)$. By (5), we may arrange the argument function arg on $\mathbb{C}$ such, that on the l-segment between $\frac{1+i}{r}$ and $1+i$, we have $\arg(f) = 0$, and thus -by (III)- $\arg(f) = \pi$ on the l-segment between 0 and $\frac{1+i}{r}$. A moment of reflection learns that at least one $\overline{\mathcal{N}}(f)$-tracjetory, say Γ_1 , leaving from the pole $\frac{1+i}{r}$ tends to a $\overline{\mathcal{N}}(f)$-saddle, say s_1. Then -by (II)- the image of Γ_1 under the reflection in l, say Γ_1', connects $\frac{1+i}{r}$ to a saddle $s_2 (\neq s_1 \bmod \Lambda)$. Now, from (I) and (II)

it follows that s_1 and s_2 are situated in P. So, we may assume that $s_1 = \sigma_1$, $s_2 = \sigma_2$. In particular there are no saddle connections. Again by (I), (II) it is easily seen that -in the situation of Fig. 47- the unstable $\overline{\mathcal{N}}(f)$-manifold through σ_1, connects the zeros i and $1+i$, whereas the unstable manifold through σ_2 connects 1 with $1+i$. Altogether, this results into a fairly complete impression of the phase portrait of $\overline{\mathcal{N}}(f)$, and thus of $\overline{\overline{\mathcal{N}}}(f)$:

Corollary 11.2. *The phase portrait of a nuclear Newton flow of order r is-up to topological equivalency as depicted in Fig. 47. In particular, there are two simple saddles, and no saddle connections.*

Compare Lemma 5.7 and in particular Remark 5.8.

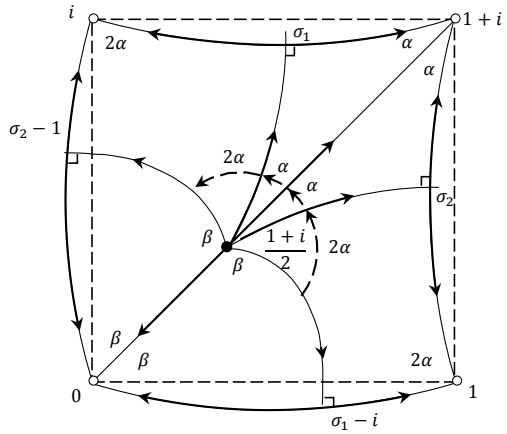

Figure 47: Phase portrait of nuclear Newton flow ($P = P_{1,i}$)

Remark 11.3. : (*Canonical form of the phase portrait of the nuclear Newton flow*).
Due to the fundamental property (5), and using (III), it is possible to derive explicit expressions (in terms of the order r) for the angles α and β in Fig. 47. We find:

$$\alpha = \frac{1}{4r}, \quad \beta = \frac{2r-3}{4r} \tag{34}$$

This enables us to present pictures -up to conjugacy- of $\overline{\overline{\mathcal{N}}}(f), r = 2, 3, 4, \cdots$ (cf. Fig. 48). These pictures are realistic, if $\Lambda = \Lambda_{1,i}, \mathbf{a} = 0, \mathbf{b} = \frac{1+i}{r}$. Note that if $r=2$, the phase portrait of $\overline{\overline{\mathcal{N}}}(f)$ is equivalent to $\overline{\overline{\mathcal{N}}}(\wp)$, in the *lemniscate* case , where $\wp = \wp|_\Lambda$ and $\Lambda = \Lambda_{1,i}$ (cf. [1]).

Fig.48 suggests that nuclear Newton flows of different order are conjugate (which -from a *steady stream* point of view- is rather plausible). In order to give a formal proof, we need one more definition:

Let f be -as before- an elliptic function of order r with on T only one zero and only one pole (and thus two simple critical points). Then:

Definition 11.4. $\mathcal{H}(f)$ is the graph on T with as vertex, edges and face respectively:

(i) the zero for f on T (as an attractor for $\overline{\overline{\mathcal{N}}}(f)$),

(ii) the unstable manifolds for $\overline{\overline{\mathcal{N}}}(f)$ at the critical points for f on T (as $\overline{\overline{\mathcal{N}}}(f)$-saddles),

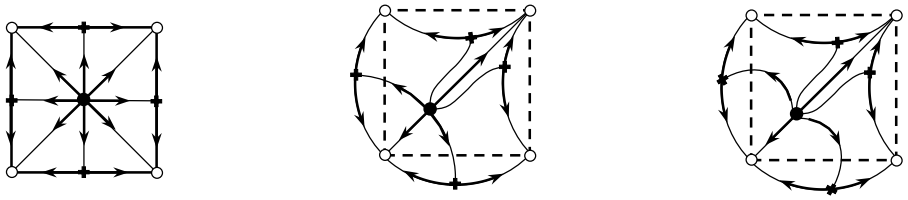

Figure 48: The canonical nuclear Newton flows; $r = 2, 3, 4$.

(iii) the basin of repulsion for $\overline{\overline{\mathcal{N}}}(f)$ of the pole for f on T (as a repellor for $\overline{\overline{\mathcal{N}}}(f)$).

$\mathcal{H}(f)$ is a *pseudo graph* (loops and multiple edges permitted) and will be referred to as the *nuclear Newton graph* for the nuclear flow $\overline{\overline{\mathcal{N}}}(f)$. By Lemma 11.1, different functions f (of the same order r) give rise to equivalent graphs $\mathcal{H}(f)$. Thus, we may speak of *the* pseudo Newton graph for *the* nuclear flow of order r, denoted by $\mathcal{H}_r$. So, $\mathcal{H}(f) \sim \mathcal{H}(\frac{1}{f}) \sim \mathcal{H}_r$. In accordance with Sections 6 and 7, we oriented $\mathcal{H}_r$ clockwise, and thus $\mathcal{H}_r^*$ anti-clockwise. The common refinement $\mathcal{H}_r \wedge \mathcal{H}_r^*$ ($\sim \mathcal{H}(f) \wedge \mathcal{H}(f)^*$) is defined in the same way as $\mathcal{G}_r \wedge \mathcal{G}_r^*$ ($\sim \mathcal{G}(f) \wedge \mathcal{G}(f)^*$). In view of (34) the conditions A_1–A_3 in Definition 7.7 do also hold for $\mathcal{H}_r$. In particular, the graph $\mathcal{H}_r$ is of the same type as the nuclear Newton graph $\hat{\mathcal{G}}_1$, compare the comment on Definition 10.5.

If $[a]$ and $[b]$ are the classes mod Λ that represent respectively the zero and pole for f on T (and a, b are chosen in P), we introduce:

$$\Psi_a(z) = \sqrt{\sum_{\omega \in \Lambda} |z - a - \omega|^{-(4r-4)}}; \quad \Psi_b(z) = \sqrt{\sum_{\omega \in \Lambda} |z - b - \omega|^{-(4r-4)}}, \tag{35}$$

where the summation takes place over all points in lattice Λ.

We define the planar flow $\underline{\mathcal{N}}(f)$ by:

$$\frac{dz}{dt} = -\Psi_a(z)\Psi_b(z)(1 + |f(z)|^4)^{-1}\overline{f'(z)}f(z) \tag{36}$$

Lemma 11.5. *The flow $\underline{\mathcal{N}}(f)$ is smooth on $\mathbb{C}$ and exhibits the same phase portrait as $\overline{\mathcal{N}}(f)$. In particular, there are no saddle connections. However, its attractors (at zeros for f) and its repellors (at the poles for f) are all generic, i.e. of the hyperbolic type.*

Proof. Since $r \geq 2$ (thus $4r - 4 \geq 4$) , series of the type as under the square root in (35) are uniform convergent in each compact subset of $\mathbb{C} \backslash (\Lambda_{\omega_1 - a, \omega_2 - a} \cup \Lambda_{\omega_1 - b, \omega_2 - b})$ From this, together with the smoothness of $\overline{\mathcal{N}}(f)$ on $\mathbb{C}$, it follows that $\underline{\mathcal{N}}(f)$ is smooth outside the union of $\Lambda_{\omega_1 - a, \omega_2 - a}$ and $\Lambda_{\omega_1 - b, \omega_2 - b}$. Special attention should be paid to the lattice points. Here the smoothness of $\underline{\mathcal{N}}(f)$ as well as the genericity of its attractors and repellors follows by a careful (but straightforward) analysis of the local behaviour of this vector field around these points, as well as the fact that these points are either a zero, or a pole of order r for f. Since outside their equilibria $\underline{\mathcal{N}}(f)$ and $\overline{\mathcal{N}}(f)$ are equal -up to a strictly positive factor- their portraits coincide. □

Theorem 11.6. *All flows $\underline{\mathcal{N}}(f)$ are mutually conjugate.*

Proof. By Lemma 11.5, a flow $\underline{\mathcal{N}}(f)$ of any order is structurally stable as a C^1-vector field on T (cf.[32]). So, we may consider the distinguished graph of such a flow. Such a graph is defined as the abstract, directed graph underlying $\mathcal{H}(f) \wedge \mathcal{H}(\frac{1}{f})$ ($\sim \mathcal{H}_r \wedge \mathcal{H}_r^*$), together with its four canonical regions (distinguished sets of Type 1); compare also Section 6. Application of (22) yields the assertion (cf. [33]). □

From Lemmata 11.1, 11.5 and Theorem 11.6 it follows:

Corollary 11.7. *Any two nuclear Newton flows (of arbitrary order) are conjugate.*

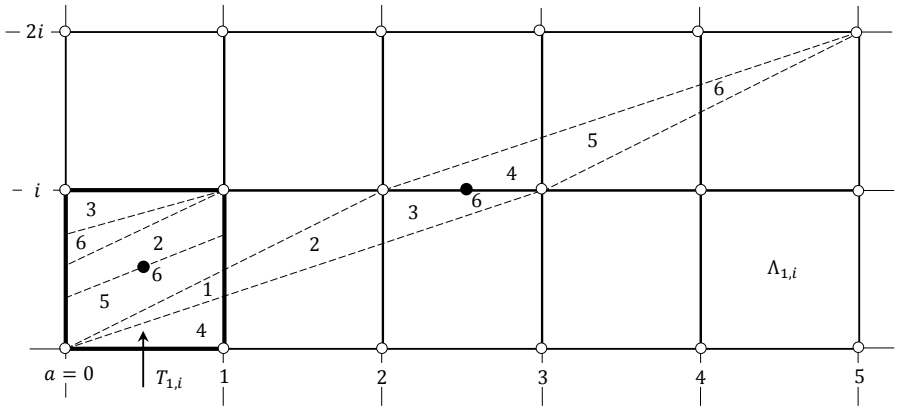

Figure 49: The nuclear Newton graph $\mathcal{H}(\wp_{3+i,2+i})$ on the torus $T(= T_{1,i})$.

We end up with a comment on the nuclear Newton graph $\mathcal{H}(f_{\omega_1,\omega_2})$, where the pair (ω_1, ω_2) is related to $(1, i)$ by the unimodular transformation

$$M = \begin{pmatrix} p_1 & q_1 \\ p_2 & q_2 \end{pmatrix}, \;\; p_1 q_2 - p_2 q_1 = +1.$$

The above condition implies that (p_1, p_2) and (q_1, q_2) are co-prime, and

$$\omega_1 = p_1 + p_2 i, \;\; \omega_2 = q_1 + q_2 i.$$

Our aim is to describe $\mathcal{H}(f_{\omega_1,\omega_2})$ as a graph on the canonical torus $T(= T_{1,i})$. In view of Lemma 3.1, the two edges of $\mathcal{H}(f_{\omega_1,\omega_2})$ are closed Jordan curves on T , corresponding to the unstable manifolds of $\underline{\mathcal{N}}(f_{\omega_1,\omega_2})$) at the two critical points for f that are situated in the period parallelogram P_{ω_1,ω_2}. These unstable manifolds connect a with $a + p_1 + p_2 i$, and $a + q_1 + q_2 i$ respectively. Hence, one of the $\mathcal{H}(f_{\omega_1,\omega_2})$-edges wraps p_1-times around T in the ω_1-direction and p_2-times around T in the ω_2-direction, whereas the other edge wraps q_1-times around this torus in the ω_1-direction respectively q_2-times in the ω_2-direction. See also Fig. 49, where we have chosen for f the Weierstrass $\wp$-function (lemniscate case), i.e. $r = 2$, $a = 0$ and $\omega_1 = 3 + i, \omega_2 = 2 + i$. Compare also Fig. 48, case $r = 2$.

12 Representation of pseudo Newton graphs

In this section we discuss the connection between pseudo Newton graphs and Newton flows. In order not to blow up the size of this study, we focus - after a short introduction - on the

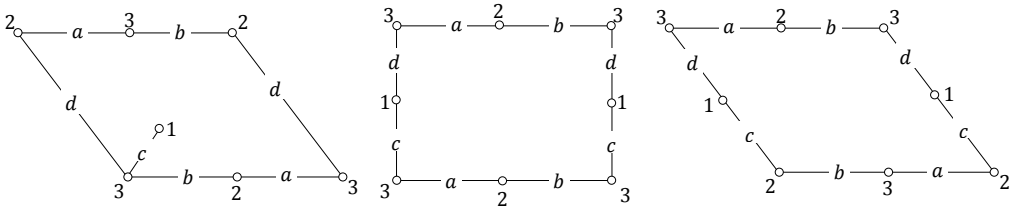

Figure 50: The three different graphs $\check{\mathcal{G}}_3$.

Cases $r = 2$ and 3. Note however, that even from these simplest cases the main idea of our approach becomes already clear.

We consider functions $f \in E_r$ with r *simple* zeros and *one* pole of order r. (Such functions exist in view of (9) and (16)). The set of all these functions is denoted by $\underline{E}_r$ and will be endowed with the relative topology induced by the topology τ_0 on E_r. In view of Lemma 5.7 (case $A = r, B = 1$) a sufficiently, but arbitrarily small neighborhood in $\underline{E}_r$ of f contains a function, say g, with r *simple* zeros, $(r + 1)$ *simple* critical points and only one pole (of order r). Reasoning as in the the proof of Theorem 5.6 (density part of Assertion 1) we even may assume that the corresponding flow $\overline{\overline{\mathcal{N}}}(g)$ does not exhibit saddle connections. Hence, the set $\underline{E}_r^0$, of all such functions g is open and dense in $\underline{E}_r$.

From now on, let g be in $\underline{E}_r^0$. Then, the graph on T with as vertices the r zeros for g, as edges the $r + 1$ unstable manifolds for $\overline{\overline{\mathcal{N}}}(g)$) at the critical points for g, and as only face the basin of repulsion for $\overline{\overline{\mathcal{N}}}(g)$ at the pole for g, is well-defined. This (connected!) graph will be denoted by $\check{\mathcal{G}}(g)$.

By means of a suitably chosen damping factor, we may view the flows $\overline{\overline{\mathcal{N}}}(g)$, $g \in \underline{E}_r^0$, to as to structural stable (compare the proofs of Lemma 11.5 and Theorem 11.6). We consider the distinguished graph of $\overline{\overline{\mathcal{N}}}(g)$. Since there is only one pole for g (i.e., a repellor for $\overline{\overline{\mathcal{N}}}(g)$), all distinguished sets (of either Type1 or Type 3) are centered at this repellor. From this, it is easily derived that $\check{\mathcal{G}}(g)$ is cellularly embedded (compare the proof of Lemma 6.9). Each edge of the dual $\check{\mathcal{G}}^*(g)$ is a loop (because g has only one pole). So, each unstable manifold of $\overline{\overline{\mathcal{N}}}(g)$ appears twice as an edge in the facial walk w_g for the face of $\check{\mathcal{G}}(g)$, be it with opposite orientations. So, altogether, this facial walk admits $2(r + 1)$ edges. Note that the distinguished sets of Type 3 correspond only to $\check{\mathcal{G}}(g)$-vertices (i.e., zeros for g) of degree 1, whereas all other vertices give rise to sets of Type 1.

Lemma 12.1. *For each $g \in \underline{E}_r^0$, the graph $\check{\mathcal{G}}(g)$ is of type $\check{\mathcal{G}}_r$.*

Proof. (only for $r = 2, 3$)
First we note that, due to the construction in Section 10, there is only one possibility for $\check{\mathcal{G}}_2 = \hat{\mathcal{G}}_2$ (see Fig. 43 a_1, where $\delta_1 = \delta_2 = 3, L = 0$ and the subwalks W_i admit only one edge). For $\check{\mathcal{G}}_3$ there are three possibilities (see Fig. 50, where the values of δ_i discriminate between these types).
$\underline{r = 2}$: The facial walk w_g admits *six* edges and *two* vertices (repetition necessary). If one of these vertices has degree 1, *four* of the edges in w_g must be incident with the other vertex. This is impossible since w_g has no loops (because the zeros for g are simple). So, each vertex

has degree $\geqslant 2$. Now, the assertion follows as in the proof of Lemma 10.1 (compare also Corollary 10.2).
$\underline{r=3}$: The facial walk w_g admits *eight* edges and *three* vertices (repetition necessary).

- If all vertices are of degree $\geqslant 2$, then $\check{\mathcal{G}}(g)$ is of the types as depicted in Fig. 50-(b), (c) $[\check{\mathcal{G}}(g) = \check{\mathcal{G}}_3 = \hat{\mathcal{G}}_3]$; compare the proof of Lemma 10.1 and Fig. 44.
- If *only one* of these vertices, say v, has degree 1, we distinguish between two subcases:
  - (i) Deleting v together with the edge, incident with v, results into a new graph with only one face and a facial walk admitting *three* edges and *two* vertices of degree $\geqslant 2$ (repetition necessary). By Corollary 10.2 it follows that the latter graph equals $\hat{\mathcal{G}}_2$, and thus the original graph $\check{\mathcal{G}}(g)$ is as depicted in Fig. 50-(a).
  - (ii) Deleting v, together with the edge incident with v, results into a new graph with a vertex of degree 1. If we delete also this vertex together with the adjacent edge, we obtain a new graph with only one face and a facial walk admitting *two* edges and *one* vertex (of degree $\geqslant 2$). Since all zeros for g are simple this is not possible.
- If (at least) *two* of these vertices have degree 1, the same argument as used in Subcase (ii) leads to a contradiction.

□

Also the converse of Lemma 12.1 is true:

Lemma 12.2. *Each graph of the type $\check{\mathcal{G}}_r$, can be represented as a graph $\check{\mathcal{G}}(g)$ with g in $\underline{\underline{E}}{}^0_r$.*

Proof. (only for $r = 2, 3$)
$\underline{r=2}$: A direct consequence of the existence of flows $\overline{\overline{\mathcal{N}}}(g)$, $g \in \underline{\underline{E}}{}^0_r$, and Lemma 12.1.
$\underline{r=3}$: Consider the 3^{rd} order nuclear Newton flow $\overline{\overline{\mathcal{N}}}(f)$ as introduced in Section 11 (cf. Fig. 47 and 48-(b)). The idea is:

To split off from the 3^{rd} order zero for f a simple zero (v_1) "Step 1", and thereupon, to split up the remaining double zero ($v_1^{'}$) into two simple ones (v_2, v_3) "Step 2", in such a way that by an appropriate strategy, the resulting functions give rise to Newton flows with associated graphs, determining each of the three possible types $\check{\mathcal{G}}_3$ in Fig. 50 .
Ad Step 1 : We perturb the original function f into an elliptic function g with one simple (v_1) and one double ($v_1^{'}$) zero (close to each other), and one third order pole w, fulfilling Relation (15) and (16) (thus close to the pole of f). The original flow $\overline{\overline{\mathcal{N}}}(f)$ perturbs into a flow $\overline{\overline{\mathcal{N}}}(g)$ with v_1 and $v_1^{'}$ as attractors and w_1 as repellor. When v_1 tends to $v_1^{'}$, the perturbed function g will tend to f, and thus the perturbed flow $\overline{\overline{\mathcal{N}}}(g)$ to $\overline{\overline{\mathcal{N}}}(f)$, cf. Lemma 5.1. In particular, when the splitted zeros are sufficiently close to each other and the circle C_1 that encloses an open disk D_1 with center $v_1^{'}$, is chosen sufficiently small, C_1 is a global boundary (cf.[21]) for the perturbed flow $\overline{\overline{\mathcal{N}}}(g)$. It follows that, apart from the equilibria v_1 and $v_1^{'}$ (both of Poincaré index 1) the flow $\overline{\overline{\mathcal{N}}}(g)$ exhibits on D_1 one other equilibrium (with index -1): a simple saddle c (compare Section 1 and [15]). From this, it follows (cf. Relation (5)) that the phase portrait of $\overline{\overline{\mathcal{N}}}(g)$ around v_1 and $v_1^{'}$ is as sketched in Fig. 51-(a). On the (compact!) complement $T \backslash D_1$ this flow has one repellor (w_1) and two saddles. The repellor may be considered as hyperbolic (compare Lemma 11.5), whereas the saddles are distinct and thus simple (because $\overline{\overline{\mathcal{N}}}(f)$ has two simple saddles, say σ_1, σ_2, depending continuously on v_1 and $v_1^{'}$). Hence, the restriction of $\overline{\overline{\mathcal{N}}}(g)$ to $T \backslash D_1$ is ε-structurally stable (cf. [32]). So, we may conclude that, if v_1 (chosen sufficiently close to $v_1^{'}$) turns around $v_1^{'}$, the phase portraits outside D_1 of the perturbed flows undergo a change that is negligible in the sense

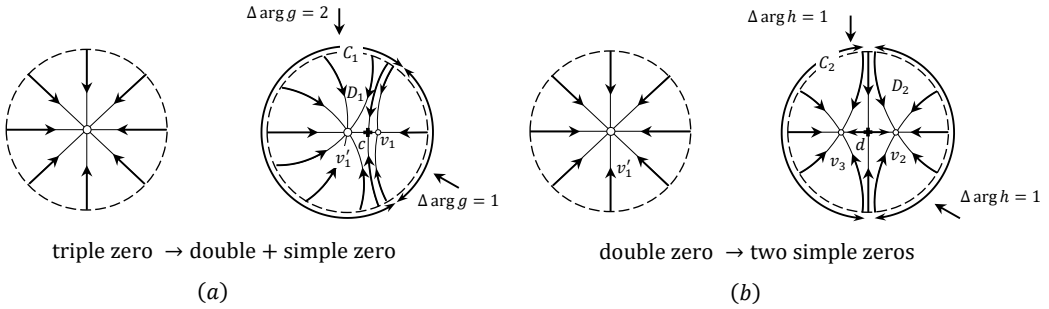

Figure 51: Splitting zeros

of the C^1-topology. Therefore, we denote the equilibria of $\overline{\overline{\mathcal{N}}}(g)$ on $T\backslash D_1$ by w, σ_1, σ_2 (i.e., without reference to v_1). We move v_1 around a small circle, centered at $v_1^{'}$ and focus on two positions (I, II) of v_1, specified by the choice of the angle α at $v_1^{'}$ together with the corresponding arc $\gamma(\approx \frac{2\alpha}{3})$ in C_1. In fact, we choose $\alpha = \frac{1}{8}$ (position I), or $\alpha = \frac{3}{8}$ (position II). See Fig. 52, where we sketched some trajectories of the phase portraits of $\overline{\overline{\mathcal{N}}}(g)$ on D_1. (Note that $\gamma \approx \frac{2}{3}\alpha$ because $v_1^{'}$ is a double zero, and w_1 a triple pole for g). Compare also Fig. 47 and formula (34) for $r = 3$. Similarly, the (approximate) values of the angles at v_1 and $v_1^{'}$ as well as the values of the arcs of C_1, associated with these angles can be explained. See Fig. 52.

Ad Step 2 : We proceed as in Step 1. Splitting $v_1^{'}$ into v_2 and v_3 (sufficiently close to each other) yields a perturbed elliptic function h, and thus a perturbed flow $\overline{\overline{\mathcal{N}}}(h)$. Consider a circle C_2, centered at the mid-point of v_2 and v_3, that encloses an open disk D_2 containing these points. If we choose C_2 sufficiently small, it is a global boundary of $\overline{\overline{\mathcal{N}}}(h)$. Reasoning as in Step 1, we find out that $\overline{\overline{\mathcal{N}}}(h)$ has on D_2 two simple attractors (v_2 , v_3) and one simple saddle: d (close to the mid point of v_2 and v_3; compare Fig. 51-(b)). Moreover, as for $\overline{\overline{\mathcal{N}}}(g)$ in Step 1, the flow $\overline{\overline{\mathcal{N}}}(h)$ is ε-structurally stable outside D_2. So, we may conclude that, if v_2 and v_3 turn (in diametrical position) around their mid-point, the phase portraits outside D_2 of the perturbed flows undergo a change that is negligible in the sense of C^1-topology. Therefore, we denote the equilibria of $\overline{\overline{\mathcal{N}}}(h)$ on $T\backslash D_2$ by v_1, w_1, c, σ_1, and σ_2 (i.e., without reference to v_2 and v_3).

Finally, for v_1 in the position of Fig. 52-(I) we choose the pair (v_2,v_3) as in Fig. 53-I; and for v_1 in the position of Fig. 52-(II), we distinguish between two possibilities: Fig. 53-IIa or Fig. 53-IIb. Note that, with these choices of v_1, v_2, v_3 each of the obtained functions has three simple zeros and one triple pole. Moreover, the four saddles are simple and not connected, whereas the three zeros are simple as well. So the graph of the associated Newton flow is well defined and has only one face, four edges and three vertices. Recall that the various values of $\delta_i(= \delta(v_i))$ discriminate between the three possibilities for the graphs of type $\check{\mathcal{G}}_3$). Now inspection of Fig. 53 yields the assertion. □

Up till now, we paid attention to pseudo Newton graphs with only one face (i.e., of type $\check{\mathcal{G}}.$ or $\hat{\mathcal{G}}.$). If $r = 2$, these are the only possibillities.
If $r = 3$, there are also pseudo Newton graphs (denoted by $\underline{\mathcal{G}}$) with two faces and angles summing up to 2 or 1. When the boundaries of any pair of the original $\mathcal{G}_3$-faces have a subwalk in common, these walks have length 1 or 2. (Use the A-property and compare Fig.

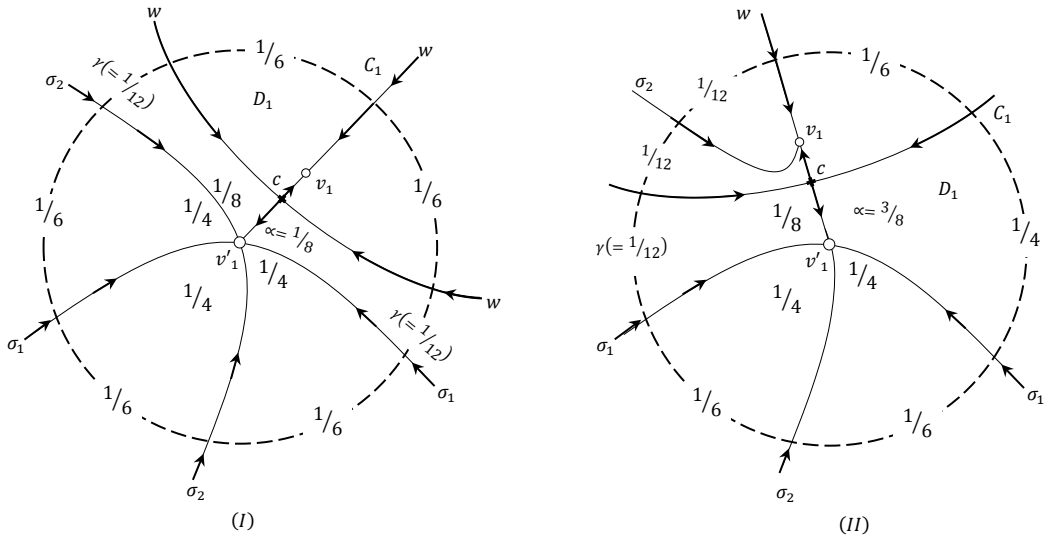

Figure 52: Two phase portraits for $\overline{\overline{\mathcal{N}}}(g))$ on D_1

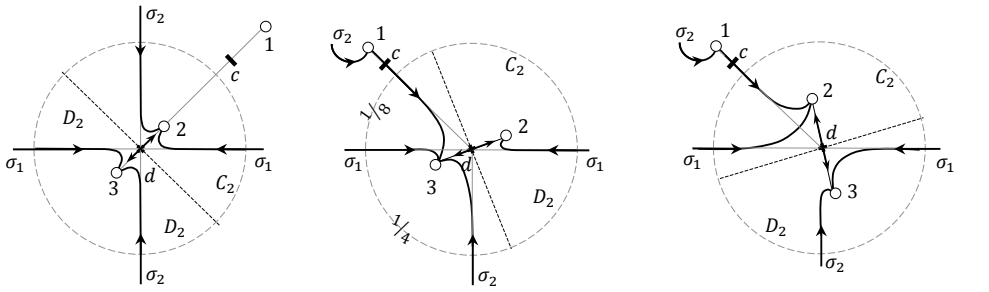

Figure 53: Three phase portraits for $\overline{\overline{\mathcal{N}}}(h))$ on D_2

40). So, when two $\mathcal{G}_3$-faces are merged, the resulting $\underline{\mathcal{G}}$-face admits *either* only vertices of degree $\geqslant 2$ *or* one vertex of degree 1. From now on, we focus on the Newton graphs as exposured in Fig. 40 (i),(iv) [since all other Newton graphs (in this figure) can be dealt with in the same way, there is no loss of generality]. Then the two $\underline{\mathcal{G}}$-faces under consideration are F_7 (:= $F_{4,5}$) and F_6; see Fig. 54 (in comparison with Fig. 40 (i),(iv)).

We consider the common refinement $\underline{\mathcal{G}} \wedge \underline{\mathcal{G}}^*$ of $\underline{\mathcal{G}}$ and its dual $\underline{\mathcal{G}}^*$. Either all distinguished sets are of Type 1, or there is precisely one distinguished set of Type 3.[28] Argueing as in Subsection 7.2, we claim that $\underline{\mathcal{G}} \wedge \underline{\mathcal{G}}^*$ determines a structurally stable torodial flow, say $\mathcal{X}(\underline{\mathcal{G}})$, with as equilibria: stable and unstable proper nodes (corresponding to the $\underline{\mathcal{G}}$- resp. $\underline{\mathcal{G}}^*$-vertices) and orthogonal saddles (corresponding to the pairs (e, e^*) of $\underline{\mathcal{G}}$- and $\underline{\mathcal{G}}^*$-edges). Now, we proceed as in Section 8 and assure - by the aid of local redrawings -that at the $\underline{\mathcal{G}}$- and $\underline{\mathcal{G}}^*$-vertices of a distinguished set in F_6 the angles are equal, whereas in case of F_7 the angle at the $\underline{\mathcal{G}}^*$-vertex equals half the angle at the $\underline{\mathcal{G}}$-vertex, see Fig. 54. By Theorem B in [35] we find - as in Section 8 - a self indexing function h on T, such that

$$\mathrm{grad}_R(h) = \mathcal{X}(\underline{\mathcal{G}}),$$

where $R(\cdot)$ is a Riemannian metric on T, that coincides on neighborhoods of the $\mathcal{X}(\underline{\mathcal{G}})$-equilibria with the standard metric. As in Section 8, we introduce a flow $\mathrm{grad}_R^{\perp}(h)$, which is R-orthogonal to $\mathcal{X}(\underline{\mathcal{G}})$ and has centers (resp. orthogonal saddles) at the nodes (resp. the saddles) of $\mathcal{X}(\underline{\mathcal{G}})$. The associated graph $\underline{\mathcal{G}}^{\perp}$ on the saddles of $\mathrm{grad}_R^{\perp}(h)$ is connected and cellularly embedded. Because of the occurrence of a Type 3-distinguished set, $\underline{\mathcal{G}}^*$ may admit a loop. Moreover, there are *ten* ($= 4r - 2; r = 3$) open canonical regions for $\mathcal{X}(\underline{\mathcal{G}})$ and also for the dual $\mathcal{X}(\underline{\mathcal{G}}^*)$ ($=-\mathcal{X}(\underline{\mathcal{G}})$), with various appearances : $\overline{\overline{\mathcal{R}}}_{i6}(\cdot,\cdot)$, $\overline{\overline{\mathcal{R}}}_{i7}(\cdot,\cdot)$, $\overline{\overline{\mathcal{R}}}_{37}(\cdot,\cdot)$ resp. $\overline{\overline{\mathcal{R}}}^*_{6i}$, $\overline{\overline{\mathcal{R}}}^*_{7i}$, $\overline{\overline{\mathcal{R}}}^*_{73}$, compare Fig. 54, 55. Here - and in the sequel - we restrict ourselves to the two special cases in Fig.54 (that are representative for all other possibilities). Note that equally labelled regions, like $\overline{\overline{\mathcal{R}}}_{i6}$ and $\overline{\overline{\mathcal{R}}}^*_{6i}$, coincide as point sets.

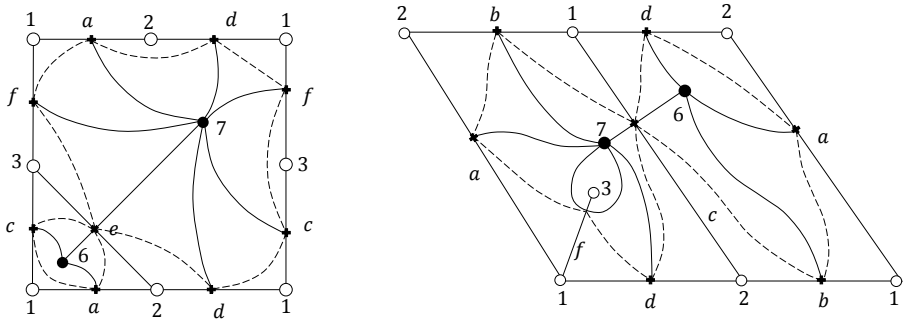

Figure 54: The graphs $\underline{\mathcal{G}}$ (—), $\underline{\mathcal{G}}^*$ (- - -) and $\underline{\mathcal{G}}^{\perp}$ ($\cdots$).

With aid of the function h and the analogue function g (w.r.t. $\mathcal{X}(\underline{\mathcal{G}}^*)$), the R-orthonormal net of $\mathcal{X}(\underline{\mathcal{G}})$- and $\mathrm{grad}_R^{\perp}(h)$-trajectories on $\mathcal{X}(\underline{\mathcal{G}})$- regions is mapped (homeomorpically and respecting orientations) onto the polar net of sectors in the $u+iv$-plane, resp. $U+iV$-plane, spanned by an angle α resp. $-\alpha$ (in case $j = 6$), or $-\frac{1}{2}\alpha$(in case $j = 7$) at 0 [:=stable node v_i, resp. unstable node v_6^* or v_7^*].

[28]The E-property holds not always for F_7: Only if there is a $\underline{\mathcal{G}}$-vertex of degree 1, the dual $\underline{\mathcal{G}}^*$ admits a *contractible* loop (corresponding with the edge adjacent to this vertex); all other $\underline{\mathcal{G}}^*$-loops- if there are any- are *non-contractible*.

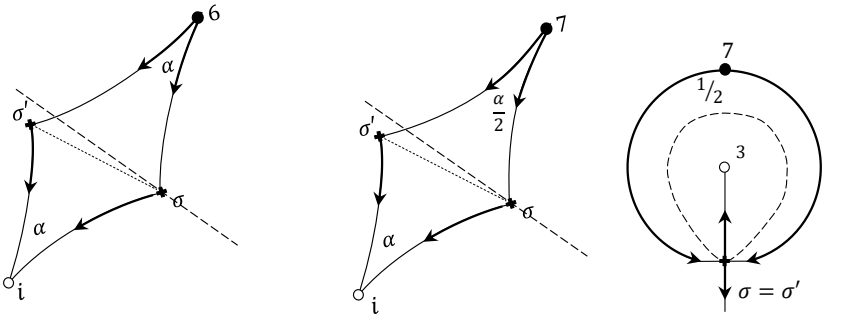

$\mathcal{R}_{i6}(=\mathcal{R}^*_{6i}), i=1,2,3,\ 0<\alpha<1$ $\mathcal{R}_{i7}(=\mathcal{R}^*_{7i}), i=1,2,3,\ 0<\alpha<1$ $\mathcal{R}_{37}(=\mathcal{R}^*_{73}), i=3,\ \alpha=1$

Figure 55: The various appearances of the canonical regions of $\mathcal{X}(\underline{\mathcal{G}})$.

These sectors are denoted by $s_{i,j}$, and $S_{i,j}$ $j=6,7$. See Fig. 56 in comparison with Fig. 55. Next, we consider the reduced torus $\check{T}=T\backslash\{\underline{\mathcal{G}}\wedge\underline{\mathcal{G}}^*\text{-vertices}\}$ with as atlas

$$\{F^*_{v_i}\backslash v_i, F_{v^*_j}\backslash v^*_j \mid i=1,2,3, j=6,7\}.$$

This atlas provides $\check{T}$ with a complex analytic structure, exhibiting coordinate transfomations between $\overline{\overline{\mathcal{R}}}_{ij}$ as a subset of $F^*_{v_i}\backslash v_i$ and $\overline{\overline{\mathcal{R}}}_{ij}$ as a subset of $F_{v^*_j}\backslash v^*_j$, induced by the analytic bijections:

$s_{i,j}\leftrightarrow S_{i,j}:\ u{+}iv\leftrightarrow U{+}iV=(u{+}iv)^{-1},$ if $j=6,$ and $u{+}iv\leftrightarrow U{+}iV=(u{+}iv)^{-\frac{1}{2}},$ if $j=7.$

If we pull back $\overline{\overline{\mathcal{N}}}(u+iv)$ $(=-(u+iv))$, $\overline{\overline{\mathcal{N}}}^{\perp}(u+iv)$ $(=-i(u+iv))$ on $s_{i,j}$ and $\overline{\overline{\mathcal{N}}}U+iV)$ $(=-(U+iV))$, $\overline{\overline{\mathcal{N}}}^{\perp}(U+iV)$ $(=-i(U+iV))$ on $S_{i,j}$, to $\overline{\overline{\mathcal{R}}}_{ij}$,we obtain analytic vector fields (functions) on $\overline{\overline{\mathcal{R}}}_{ij}$. By glueing together all these functions along the trajectories in the common boundaries of the canonical regions of $\mathcal{X}(\underline{\mathcal{G}})$, we find a complex analytic function on $\check{T}$, and by continuous extension a meromorphic function, say f, on T with poles of order 1 and 2, corresponding to the faces F_6 and F_7 respectively, with three simple zeros that correspond to the $\underline{\mathcal{G}}$-vertices, and with five $(=2r-1; r=3)$ simple critical points. The net of $\mathcal{X}(\underline{\mathcal{G}})$- and $\mathrm{grad}^{\perp}_R(h)$-trajectories is just the net of $\overline{\overline{\mathcal{N}}}(f)$- and $\overline{\overline{\mathcal{N}}}^{\perp}(f)$-trajectories, i.e. a steady stream with one source of strength 2, one source of strength 1 , three sinks of strength 1, and five simple stagnation points.

More generally, we claim:

Conjecture: (Compare Remark 10.3)

Let r and r' be integers such that: $2\leqslant r, 1<r'<r$, and let $\underline{\mathcal{G}}_{r,r'}$ be a Pseudo Newton graph with r vertices, one face with angles summing up to r', and $r-r'$ faces with angles summing up to 1. Then, the graph $\underline{\mathcal{G}}_{r,r'}$, represents a meromorphic function on T with r simple zeros, $r-r'+1$ poles (one of order r', the others of order 1) and $2r-r'$ simple critical points Also: graph $\underline{\mathcal{G}}_{r,r'}$ determines a steady stream on T with r sinks of strength 1, $r-r'+1$ sources (one of strength r', the others of strength 1) and $2r-r'$ simple stagnation points. Moreover, using techniques as exhibited in Case $r=3$, the nuclear Newton flow of order r generates - by splitting up (bifurcating) degenerate zeros/poles and constructing pseudo Newton graphs- all structurally stable Newton flows of order r.

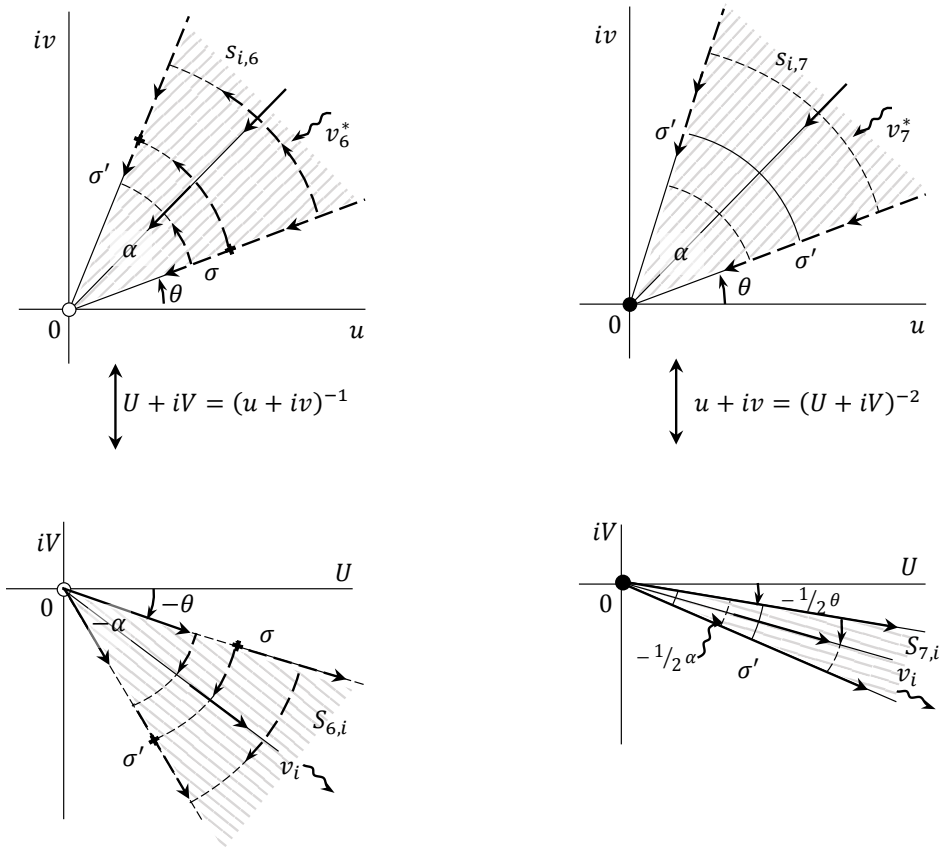

Figure 56: The sectors $s_{i,j}$ and $S_{i,j}$.

13 Final remarks

13.1 Rational versus elliptic Newton flows.

Our study is inspired by the analogy between rational and elliptic functions. We raised the question whether, and -if yes - to what extent, this analogy persists in terms of the corresponding Newton flows (on resp. the Riemann sphere S^2 and the torus T). An affirmative answer to this question is given by comparing the *characterization, genericity, classification and representation aspects* of rational Newton flows (see Theorem 2.1) with their counterparts as described in Theorem 5.6 (1)-(2), Theorem 6.11 and Theorem 8.3.

More in particular, the above analogy becomes manifest when we look at the special case of *balanced rational* Newton flows of order $r \geqslant 1$. By these, we mean structurally stable flows of the form $\overline{\overline{\mathcal{N}}}(\frac{p_n}{q_m})$, with p_n, q_m two co-prime polynomials of degrees respectively $n, m, |n-m| \leqslant 1, r = \max\{n, m\}$. Such flows admit $2r$ star nodes (r stable and r unstable) together with $2r-2$ orthogonal saddles. [Note that at $z = \infty$ (north pole) there is an unstable node if $n = m+1$, a stable node if $m = n+1$, and a saddle if $m = n$]. Due to the duality property (5), the transition $\frac{p_n}{q_m} \leftrightarrow \frac{q_m}{p_n}$ causes the reverse of orientations of the trajectories of $\overline{\overline{\mathcal{N}}}(\frac{p_n}{q_m})$ and $\overline{\overline{\mathcal{N}}}(\frac{q_m}{p_n})$. So, these flows are conjugate and without loss of generality, we assume $n \geqslant m$. Now, the sphere graph $G(\frac{p_n}{q_m})$ for $\overline{\overline{\mathcal{N}}}(\frac{p_n}{q_m})$ can be defined (in strict analogy with Definition 6.1) as a connected, cellularly embedded multigraph on r vertices, $2r-2$ edges and r faces; apparently, also: $G(\frac{q_m}{p_n}) = G^*(\frac{p_n}{q_m})$ holds. As in the elliptic case, it can be proved that $G(\frac{p_n}{q_m})$ fulfils both the E- and the A-property. (However, in this special case it is found that the later property already implies the first one). Subsequently, it is shown that any cellularly embedded multigraph in S^2 with r vertices, $2r-2$ edges and r faces, admits the A-property iff certain (Hall) inequalities are satisfied. Altogether, this leads to a concept of Newton graph that is formally the same as the concept of Newton graph in Definition 7.13. In particular, classification and representation results, similar to Theorem 6.11 and Theorem 8.3, are derived (cf. [23], [24]).

We conclude that there is a striking analogy between the sets of balanced Newton flows and elliptic Newton flows, both of order $r, r \geqslant 2$. (Note that an elliptic Newton flow of order 1 is not defined, whereas a balanced Newton flow of order 1 is just the north-south flow (cf. Fig. 7 and 8, with $n = 1$).

Finally, we note that - as in the elliptic case - for lower values of r a list of all possible (up to conjugacy) balanced Newton flows, represented by their graphs, is available. For example, see Fig. 57, where the pictures of the graphs $G_r(\frac{p_n}{q_m})$ and $G_r^*(\frac{p_n}{q_m})$, $r = 2,\ 3$, suggest that the conditions A1, A2, A3, in Definition 7.7 are indeed fulfilled. The proof that these graphs are the only possibilities, based on the Representation Theorem for rational Newton graphs (compare [23] and arguments as used in Section 9), is omitted.

13.2 Complexity aspects

We indicate the existence of a "good" (i.e., polynomial) algorithm deciding whether a given cellularly embedded torodial graph $\mathcal{G}_r$ is a Newton graph or not. To this aim, we check both the E- and A-property.

E-property: Use that the graphs (facial walks) ∂F_j are Eulerian iff all vertices have even degree.
A-property: Let B be a finite bipartite graph with bipartition (X, Y), and denote for any subset S in X the neighbour set in Y by $N(S)$. We consider the so called Strong Hall

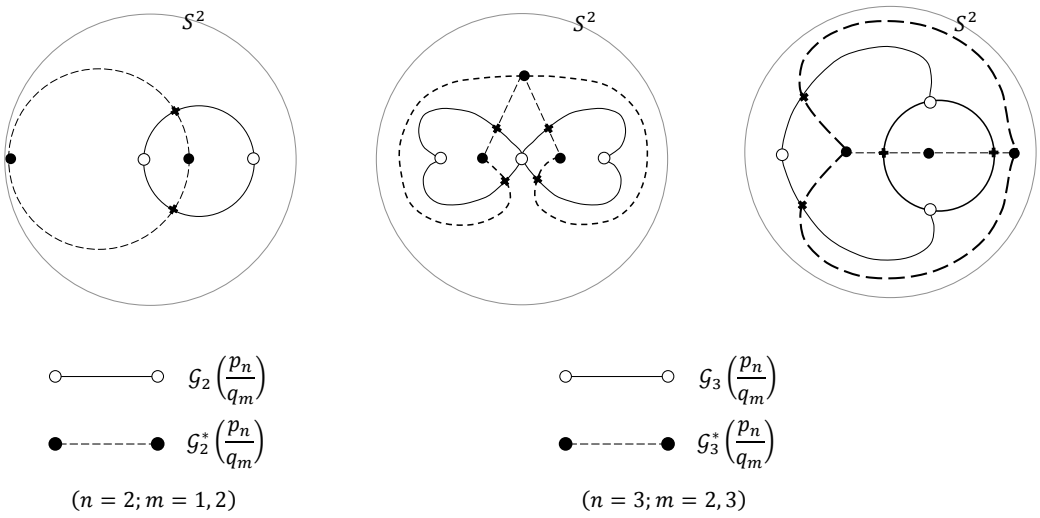

Figure 57: The different graphs for balanced rational Newton flows of order $r = 2, 3$.

Property (cf. [12]):

$$|S| < |N(S)|, \text{ for all nonempty } S \subset X. \tag{37}$$

For each *bipartite* graph, obtained from (B, X, Y) by adding one vertex (p) to X and one edge which joins p to an Y-vertex, we also consider the Hall property (cf. [11]):

$$|\check{S}| \leqslant |N(\check{S})|, \text{ for all subsets } \check{S} \text{ of } X \cup \{p\}. \tag{38}$$

It is easily shown that (37) and (38) are equivalent, and thus: Because the verification of (38) is possible in polynomial time (cf. [11]), this is also true for (37). Now, we select an arbitrary $\mathcal{G}_r$-face F_j, say F_r , and specify (B, X, Y) by $X = \{F_1, \cdots, F_{r-1}\}$. $Y = V(\mathcal{G}_r)$, where adjacency is defined by inclusion. The inequalities in the right hand side of Lemma 7.11 take the form (37) for all non-empty J in $\{1, \cdots, r-1\}$, and considering all possible choices for F_j, we are done.

References

[1] Abramowitz, A., Stegun, I.A. (eds): *Handbook of Mathematical Functions. Dover Publ. Inc. (1965).* .

[2] Andranov, A.A., Leontovich, E.A., Gordon, I.I., and Maier, A.G.: *Theory of bifurcations of dynamical systems on a plane. John Wiley, New York 1973.*

[3] Braes, D.: *Über die Einzugbereiche der Nullstellen von Polynomen beim Newton Verfahren. Numer. Math.* 29, pp. 123-132 (1977).

[4] Branin, F.H.: *A widely convergent method for finding multiple solutions of simultaneous non linear equations. IBM J.Res. Develop.* pp. 133-148 (1974).

[5] Brug, van den Ch.: *Newton flows voor Jacobi functies. Doctoral thesis. Universiteit Twente, Enschede, The Netherlands (1993). [in Dutch].*

[6] Chandrasekharan, K.: *Elliptic Functions. Grundlehren der mathematischen Wissenschaften, Springer Verlag (1985).*

[7] Diener, I.: *On the global convergence of path-following methods to determine all solutions to a system of nonlinear equations. Math. Prog.* 36, pp 340-353 (1887).

[8] Gomulka, J.: *Remarks on Branins method for solving non linear equations. In: Towards global optimization, L.C.W. Dixon and G.P. Szeg (eds.), North Holland Publ. Co. (1975).*

[9] Helminck, G.F., Kamphof, F.H., Streng, M., Twilt, F.: *The qualitative behaviour of Newton flows for Weierstrass $\wp$-function. Complex Variables,* Vol. 47, No.10, pp. 867-880. (2002).

[10] Twilt, F.; Helminck, G.F.; Snuverink, M.; Van den Burg, L.: *Newton flows for elliptic functions: a pilot study*, Optimization 57 (2008), no. 1, 113–134.

[11] Bondy, J.A. and Murty, U.S.R.: *Graph Theory with Applications*, Macmillan & Co, London, 1976[2].

[12] Coleman, T.F., Edenbrandt, A. and Gilbert, J.R.: *Predicting Fill for Sparse Orthogonal Factorization. Jour. Assoc. Comp. Machinery*, Vol.33, No 3, July 1986. pp. 517-532.

[13] Giblin, P.J.: *Graphs, surfaces and homology*, John Wiley and Sons (1977).

[14] Gunning R.C. *Theory of Riemann surfaces. Princeton University Press (1976)* .

[15] Guillemin, V., Pollack, A. :*Differential Topology*, Prentice hall Inc. (1974).

[16] Harary, F.: *Graph theory*, Addison-Wesley Publ. Co. Inc. (1969).

[17] Hartman, P. *Ordinary Differential Equations*, Birkhäuser (1982).

[18] Hirsch, M.W.: *Differential Topology. Springer Verlag (1976)* .

[19] Hirsch, M.W., Smale, S.: *Algorithms for solving f(x)=0. Comm. Pure Appl. Math.,* 32, pp. 281-312 (1979).

[20] Hirsch, M.W., Smale, S.: *Differential equations, dynamical systems and linear algebra. Acad. Press, New York, (1974)* .

[21] Jongen, H.Th., Jonker, P., Twilt, F.: *Non linear Optimization in $\mathbb{R}^n$: MorseTheory, Chebyshev Approximation, Transversality, Flows, Parametric Aspects. Kluwer Ac. Publ., Dordrecht, Boston (2000)* .

[22] Jongen, H.Th., Jonker, P., Twilt, F.: *The continuous Newton method for meromorphic functions. In: Geometric Approaches to Differential Equations (R. Martini, ed), Lect. Notes in Math., Vol. 810, , pp. 181-239. Springer Verlag(1980)* .

[23] Jongen, H.Th., Jonker, P., Twilt, F.: *The Continuous, desingularized Newton method for meromorphic functions. Acta Applicandae Mathematicae* 13, Nos. 1 and 2, pp. 81-121 (1988) .

[24] Jongen, H.Th., Jonker, P., Twilt, F.: *On the classification of plane graphs representing structurally stable Rational Newton flows. Journal of Combinatorial Theory,* Series B, Vol. 51, No.2, pp. 256-270 (1991) .

[25] Jongen, H.Th., Jonker, P., Twilt, F.: *The Newton Method for Meromorphic Functions. Acta Mathematicae,* Vol. 13, Nos. 1 &2 (1988).

[26] Mangasarian, O.I.: *Nonlinear programming*, McGraw-Hill Book Co. (1969).

[27] Markushevich, A.I.: *Theory of Functions of a Complex Variable, Vol. II, Prentice Hall (1965)* .

[28] Markushevich, A.I.: *Theory of Functions of a Complex Variable, Vol. III, Prentice Hall (1967)* .

[29] Meier, H-G.: *Diskrete und kontinuierliche Newton-Systeme im Komplexen. Ph.D. thesis, RWTH Aachen (1991)* .

[30] Mirsky, L. *Transversal theory: an account of some aspects of combinatorial mathematics New York: Academic Press (1971)* .

[31] Mohar, B.;Thomassen, C. : *Graphs on surfaces*. John Hopkins Studies in the Mathematical Sciences. John Hopkins University Press, Baltimore, MD, 2001.

[32] Peixoto, M.M.: *Structural stability on two-dimensional manifolds. Topology,* 1, pp. 101-120 (1962).

[33] Peixoto, M.M.: *On the classification of flows on 2-manifolds. In:Dynamical Systems, M.M. Peixoto, ed., pp. 389-419, Acad. Press, NewYork (1973)* .

[34] Smale, S.: *On the efficiency of algorithms in analysis. Bull. Am. Math. Soc.,* 13-2, pp. 87-121 (1985).

[35] Smale, S.: *On Gradient Dynamical Systems. Ann. of Math.*, Second Series, Vol. 74, No. 1 (1961), pp. 199-206.

[36] Twilt, F.: *Newton flows for meromorphic functions. Ph.D. thesis, University of Twente, Enschede, The Netherlands (1981)* .